



University of  
Stavanger

**Faculty of Science and Technology**

## **MASTER'S THESIS**

Study program/ Specialization: Konstruksjoner & Materialer / Offshore kontruksjoner	Spring semester, 2015  <u>Open</u> / Restricted access
Writer: Geir Tuntland Hauge	..... (Writer's signature)
Faculty supervisor: S.A.S.C Siriwardane  External supervisor(s):	
Thesis title: Effects of localized corrosion on welded steel joints	
Credits (ECTS): 30	
Key words: Fatigue test, corrosion, welded joint, strain-life curve, cyclic plasticity	Pages: 116  + enclosure: 8  Stavanger, ..... Date/year

# Preface

This is the final project of my master's degree in Civil and Structural engineering at the University of Stavanger. It was written during the spring semester of 2015.

I would like to express my sincere gratitude to associate professor S.A.S.C Sudath Chaminda Siriwardane for his continuous academic and moral support. In times when it looked the darkest, and the panic set in he was a great source to seek some inspiration.

Gratitude to Rosenberg Worley Parsons AS for their willingness to assist with the fabrication of the specimens, and supplying the materials needed.

# Abstract

With steel structures placed in ever increasing depths in the oil industry, inspection of the structures are increasingly more challenging. Loss of coating on a weld exposes the weld to a corrosive environment, where the lack of cathodic protection will result in harmful corrosion on the weld. Localized corrosion like pitting corrosion results in small pits which acts as cracks in the surface. Corrosion in combination with low cycle fatigue can result in catastrophic failure of a structure prior to the designed fatigue life of the structure.

This paper is based on the assumption that corrosion has an effect on the fatigue life of a welded steel joint. To investigate this assumption further an experiment was designed. The experiment was designed to check if localized corrosion had an effect on the fatigue life of a welded steel joint when subjected to loads in the plastic range. In cooperation with Worley Parson Rosenberg AS 15 steel members were prepared. Two different corrosive environments were chosen. The specimens were subjected to low cycle fatigue tests on three different stress levels. Specimen surface and fracture surface were investigated using a scanning electron microscope.

The results of the fatigue testing initially showed that the specimens that were subjected to corrosion failed at lower cycles than the non-corroded specimens. This was disproven by the four corroded specimens that were tested later. Though the fatigue test was inconclusive with regards to number of cycles to failure, the investigation of corroded surface with the scanning electron microscope showed promising results with regards to pitting corrosion. The pictures obtained from the microscope showed over 20 individual pits formed over a period of four weeks. This shows the rapid formation and initiation of pits in the surface, and it is reasonable to state that the effects of this type of corrosion will play a significant role to estimated fatigue life on a welded steel joint.

# Introduction

## 1.1 Motivation

Steel structures exposed to aggressive environmental conditions are subjected to loss of coating and loss of material due to corrosion. This results in a continued reduction in the structural steel members used in the structure. As this reduction continues other structural properties are reduced, including effective cross sectional area, moment or inertia, torsional and warping constants. Some of these does not change linearly with a change in member thickness. Cross sectional governed properties like stress and strain cause less resistance than planned, and may cause the overall stiffness of the structure to be changed. Localized forms of corrosion like pitting corrosion represents cracks in the material surface, and combined with cyclic loading this can cause a significant reduction in the fatigue life. By the loss of cross sectional area a joint is more vulnerable to local buckling. Guidelines in how to address and assess these predicaments are not commonly available. The objective of this thesis will be to study the effect of corrosion on welded steel joints, and its effect on the fatigue life of welded steel joints.

## 1.2 Limitations

It is necessary to limit the scope of this thesis. This is mostly due to limitations of available testing equipment at the University of Stavanger. The thesis will limit itself to consider acquired number of cycles to failure in the fatigue test, low cycle fatigue and the visual impact of corrosion. There are today several guidance manuals for how to conduct a low cycle fatigue test. ISO 12106 *Metallic materials - fatigue testing - axial-strain-controlled method* is chosen as guidance for this thesis. This will be supplemented with equations, coefficients and exponents from DNV RPC-208 (Veritas, 2013).

### **1.3 Method**

The thesis will be split into three separate parts. In the first part the theory behind corrosion, fatigue and corrosion-fatigue will be described. The following part will describe ISO 12106 *Metallic materials - fatigue testing - axial-strain-controlled method*, and how the test shall be conducted.

The last part will show the practical and theoretical approach to the results. It will utilize the principals behind corrosion and fatigue described in the theory part to conduct and assess the results. The test specimens will only be subjected to corrosion for six weeks due to the time available. The results from the testing will either show that there is an influence of corrosion after only six weeks or not.

Any unforeseen problems, mistakes or other obstacles will be discussed in the interpretation of the results.

# Abbreviations

LCF – Low cycle fatigue

ULCF – Ultra-low cycle fatigue

HCF – High cycle fatigue

LCCF – Low cycle corrosion fatigue

Plastic range – Load on the material in which the response is permanent elongation

Elastic range – load on the material in which the response is no permanent elongation

ULS - Ultimate Limit State

ALS - Accidental Limit State

HAZ – Heat Affected Zone

DNV – Det Norske Veritas

NS – Norsk Standard

## Table of contents

Preface .....	1
Abstract .....	2
Introduction .....	3
1.1 Motivation .....	3
1.2 Limitations.....	3
1.3 Method.....	4
Abbreviations .....	5
Table of contents .....	6
List of figures .....	9
List of tables .....	11
2 Literature review .....	12
2.1 Corrosion .....	12
2.1.1 Types of corrosion(Fontana & Greene, 1978; Greene, 1967).....	14
2.1.2 Stress corrosion cracking .....	16
2.1.3 Basic wet corrosion cell .....	20
2.1.4 Redox reaction.....	22
2.1.5 Pitting corrosion (N. International, 2015c) .....	25
2.1.6 Mechanism of pitting corrosion .....	27
2.1.7 Differential-Aeration corrosion (Trethewey & Chamberlain, 1995) .....	27
2.2 Fatigue .....	32
2.2.1 Methods for testing LCF and ULCF .....	40
2.3 The Goodman relation(University, 2011) .....	42
2.3.1 Fracture Mechanics .....	43
3 Corrosion fatigue .....	44
3.1 Low cycle corrosion fatigue (LCCF).....	44
3.2 Why investigate LCCF on welded joints.....	44

4	Design of test .....	46
4.1	Hysteresis loop .....	47
4.2	Fatigue testing.....	48
4.2.1	Hysteresis loop .....	49
4.2.2	Machine .....	50
4.2.3	Load cell .....	50
4.2.4	Gripping of specimen .....	51
4.2.5	Alignment check .....	51
4.2.6	Strain measurements .....	51
4.2.7	Checking and verification .....	52
4.3	Specimens .....	52
4.3.1	Geometry .....	53
4.3.2	Flat products of thickness less than 5 mm.....	53
4.4	Preparation of specimens .....	55
4.4.1	General .....	55
4.4.2	Surface condition of specimen .....	56
4.4.3	Dimensional check .....	56
4.4.4	Procedure.....	57
4.4.5	Test machine control .....	57
4.4.6	Mounting of the specimen.....	57
4.4.7	Cycle shape – Strain rate or frequency of cycling .....	57
4.5	Start of test.....	58
4.5.1	Preliminary measurements .....	58
4.5.2	Number of specimens .....	58
4.5.3	Data recording .....	58
4.5.4	Data acquisition.....	59
4.5.5	Failure criteria .....	59



4.5.6	End of test.....	60
5	Preparation of test specimens.....	61
6	Fatigue test .....	67
6.1	Background for fatigue test .....	67
6.1.1	Material .....	68
6.1.2	Test machine .....	69
6.1.3	Code guidelines for cyclic loading .....	72
6.2	Surface conditions of corroded specimens .....	79
6.3	Fatigue test of specimens.....	84
6.4	Investigation of fracture.....	89
7	Interpretation of results .....	94
8	Probability.....	110
9	Discussion .....	112
10	Conclusion.....	114
10.1	Recommendations for future work .....	114
	References .....	115
	Appendix A .....	117
	Appendix B .....	118
	Appendix C .....	121

# List of figures

Figure 2-1 Illustration of anodic stress corrosion cracking (Anderson, 2005).....	17
Figure 2-2 Polarization diagram, illustrating the zones that tend to favour stress corrosion cracking (Anderson, 2005).....	17
Figure 2-3 Pourbaix diagram for iron in water (Anderson, 2005) .....	18
Figure 2-4 Illustration of a redox reaction (Garnham, 2006).....	22
Figure 2-5 Simple explanation of the meaning behind the word redox .....	24
Figure 2-6 Illustration of pit formations (N. International, 2015a).....	26
Figure 2-7 Illustration of pit formations (N. International, 2015a).....	26
Figure 2-8 The mechanism of pitting because of differential aeration beneath a water droplet (Trethewey & Chamberlain, 1995) .....	27
Figure 2-9 General corrosion over the whole of the wetted metal surface depletes the oxygen levels in the adjacent electrolyte (Trethewey & Chamberlain, 1995).....	28
Figure 2-10 Illustration of endurance limit and corrosion affected steel (ETBX, 2001-2008) 32	
Figure 2-11 Stress concentration due to a hole (Center, 2015).....	34
Figure 2-12 S-N curve representing methods to determine number of cycles to failure [Appendix B] (University, 2015) .....	35
Figure 2-13 Void nucleation, growth and coalescence in ductile metals: a) inclusions in the matrix, b) void nucleation, c) void growth, d) strain localization between voids, e) necking between voids and f) void coalescence and fracture (Anderson, 2005).....	37
Figure 2-14 A smooth specimen (EPIInc, 2012).....	40
Figure 2-15 Illustration of relation of equation 2-30 (Center, 2015) .....	41
Figure 2-16 Illustration of strain (Center, 2015) .....	41
Figure 2-17 Illustration of void nucleation, growth, coalescence and fracture (Weck, Wilkinson, Maire, Toda, & Embury, 2015).....	43
Figure 4-1 Illustration of a typical hysteresis loop (Jiang & Zhang, 2008) .....	49
Figure 4-2 Illustration of grips (I. standard, 2003).....	54
Figure 5-1 & Figure 5-2 Pre weld steel plates .....	61
Figure 5-3 & Figure 5-4 Post weld plates .....	62
Figure 5-5, Figure 5-6 & Figure 5-7pre and post cut of welded plates.....	63
Figure 5-8 & Figure 5-9 Grinding of weld.....	64
Figure 5-10 & Figure 5-11 Cutting of specimens .....	65
Figure 5-12, Figure 5-13 & Figure 5-14 Pre milled specimen and milling of specimen .....	66

Figure 6-1 Illustration of test machine dimensions .....	69
Figure 6-2 Machine specifications .....	69
Figure 6-3 & Figure 6-4 Test machine's grips .....	70
Figure 6-5 Specimen placed in machine's grips .....	71
Figure 6-6 Table A-1 detail category of non-welded details (Veritas, 2014) .....	73
Figure 6-7 Table A-5 Detail category welded parts (Veritas, 2014).....	73
Figure 6-8 Calculated values from DNV sea water and close to sea air .....	78
Figure 6-9 Surface of sea water corroded specimen .....	79
Figure 6-10 Surface of sea water corroded specimens, milling marks .....	80
Figure 6-11 Higher magnification of longest milling marks.....	81
Figure 6-12 Higher magnification of shortest milling marks.....	81
Figure 6-13 Pitting corrosion .....	82
Figure 6-14 Higher magnification and measurement of pitting corrosion.....	83
Figure 6-15 Testing of specimen, pre necking .....	84
Figure 6-16 Necking of specimen .....	85
Figure 6-17 Fracture of specimen .....	86
Figure 6-18 Obtained number of cycles to failure of sea water corroded specimens .....	88
Figure 6-19 Obtained number of cycles to failure of close to sea air corroded specimens.....	88
Figure 6-20 Fracture surface .....	89
Figure 6-21 Two distinct areas of fracture .....	90
Figure 6-22 Two distinct areas of fracture .....	90
Figure 6-23 Upper right corner, ductile fracture .....	91
Figure 6-24 Spherical inclusion which nucleated a microvoid .....	92
Figure 6-25 Overall inspection of ductile fracture .....	93
Figure 7-1 Obtained number of cycles to failure of all test specimens.....	95
Figure 7-2 Hysteresis loop for specimen 1 .....	97
Figure 7-3 Hysteresis loop for specimen 4.....	98
Figure 7-4 Hysteresis loop for specimen 6.....	99
Figure 7-5 Hysteresis loop for specimen 7.....	100
Figure 7-6 Hysteresis loop for specimen 16.....	101
Figure 7-7 Hysteresis loop for specimen 5.....	102
Figure 7-8 Hysteresis loop for specimen 3.....	103
Figure 7-9 Hysteresis loop for specimen 8.....	104
Figure 7-10 Hysteresis loop for specimen 10.....	105

Figure 7-11 Displaced specimen after weld .....	108
Figure 7-12 Illustration of residual stresses in specimens.....	109

## List of tables

Table 6-1 Chemical composition of low carbon steel .....	68
Table 6-2 Low cycle fatigue test – fatigue life.....	75
Table 6-3 Ramberg-osgood relation.....	75
Table 6-4 Stress/strain values for test .....	76
Table 6-5 Parameters for Eq. 6-2 .....	76
Table 6-6 Results from Ramberg-Osgood implemented in Eq.6-2.....	77
Table 6-7 Estimated number of cycles to failure on sea water corroded specimens from DNV .....	78
Table 6-8 Obtained number of cycles to failure from fatigue test .....	87
Table 7-1 Smallest cross sectional area of the specimens.....	94
Table 7-2 Overview of number of cycles to failure from all specimens .....	95
Table 7-3 Results from fatigue test specimen 1 .....	97
Table 7-4 Results from fatigue test specimen 4 .....	98
Table 7-5 Results from fatigue test specimen 6 .....	99
Table 7-6 Results from fatigue test specimen 7 .....	100
Table 7-7 Results from fatigue test specimen 16 .....	101
Table 7-8 Results from fatigue test specimen 5 .....	102
Table 7-9 Results from fatigue test specimen 3 .....	103
Table 7-10 Results from fatigue test specimen 8 .....	104
Table 7-11 Results from fatigue test specimen 10 .....	105
Table 7-12 Number of cycles to failure from test done on the highest stress levels.....	106
Table 7-13 Number of cycles to failure from extra specimens .....	106

# 2 Literature review

## 2.1 Corrosion

Interest in material deterioration and how to prevent it has been of interest since mankind was first able to apply nature's resources to our needs. It was early noticed that the materials changed, they seemed to change in properties and structure. Something around the applied resource made it deteriorate. There are reports about material deterioration as far back as 412 B.C. The document, written on papyrus, described measures to mitigate the problems of bacterial and animal attacks using arsenic and sulphur mixed with Chian oil. New recipes to control these, and new problems, was made through the centuries. When steel was first used to construct ships, a new problem was riced. One started to notice another type of decay, namely rust (Doctors, 2015)

Due to the applicability of steel both on land and sea, the interest in the subject of corrosion has been high for many years. There has been so much research, in all types and forms, that the information is vast. Especially in engineering this problem has been of great importance. The prevention of wastage of metals has become a concern, maybe the greatest except for the wastage of human life. Hoover has described it well:

*"It is only through the elimination of waste and the increase in our national efficiency that we can hope to lower the cost of living, on the one hand, and raise our standards of living, on the other. The elimination of waste is a total asset. It has no liabilities". (Speller, 1935)*

In 2002, the U.S Federal Highway Administration released a 2-year study of the direct cost of metallic corrosion in nearly every U.S industry sector (International, 2002). The study showed that approximately 3.1 % (276 billion dollars, \$) of the nation's Gross Domestic Product (GDP) goes to cover some form of corrosion. The study spans from 1999 to 2001, and the aim of the study was to provide cost estimates and identify national strategies to minimize the impact of corrosion. The study contains detailed strategies regarding cost by each industry sector and preventive corrosion control strategies that, if implemented, could save billions of dollars per year.

This shows the severity of the impact corrosion has. When a study of this magnitude is undertaken, it clearly shows the seriousness of corrosion damage to both structures and economy.

Corrosion has shown to be especially prone to bridges, and is regarded as one of the main causes of bridge accidents. The build-up of oxide can accumulate such a volume that it can push apart the bridge modules. This is what happened to the Mianus Bridge in 1983 (Board, 2015) in the state of Connecticut in the U.S. Some years earlier there had been maintenance on the surface, and as a result of this, storm drains were blocked. This caused accumulation of water, which again resulted in a gathering of rust. This expanded till there were no more room for it to expand, were the result was a displacement of a hangar and pin assemblies. The entire bridge module came loose, and fell 100 feet down in to the river. Three people were killed and three injured.

### **2.1.1 Types of corrosion(Fontana & Greene, 1978; Greene, 1967)**

#### Uniform corrosion – attack corrosion

Is the most common form of corrosion. Characteristic traits of uniform corrosion is corrosion products across the entire exposed surface caused by a electrochemical or chemical reaction. The effects of this is a deterioration of the product, causing it to get thinner and eventually fail. Has the biggest effect on the wastage of metal on a basis of tonnage. Though corrosion is not desirable in any way, this type of corrosion has a bigger concern due to economy compared to the more aggressive types of corrosion.

#### Galvanic corrosion

Is when an electrochemical process happens between two dissimilar metals. The least noble metal usually takes the role as an anode, and therefore loses electrons, which again causes a layer of oxide to form on this metal. The metals have to be in an electrolyte for this to happen, which means that a conducting solution has to be present. The more noble metal usually does not show signs of corrosion. It is this principal that is used on outboard motors on boats. A lump of zinc is attached close to the part of the motor that is submerged, this is called a sacrifice anode. The term galvanic corrosion is usually reserved for the process between two dissimilar metals.

#### Crevice corrosion

This type of corrosion often happens in confined spaces, where a solution is trapped. One can think of seals like a nut on a bolt. A stagnant solution can be trapped in the interface between the material and the nut. It cannot escape, and corrosion initiates. This causes crevices to form, and is very localized making it a very serious type of corrosion,

#### Pitting corrosion

Is an extremely localized form of corrosion. Pits, as the name indicates, form rather quickly in the material, and can be the reason to catastrophic failure. The pits can be isolated or be so close together that they look like a rough surface. The pits can be small or large in diameter, usually small. The pit may be described as a cavity or hole with the surface diameter about the same or less than the depth. Hard to detect and, even in laboratory tests. Failures due to pitting corrosion often happens extremely sudden.

### Intergranular corrosion

Is when the boundaries of crystallites in a material is more susceptible to corrosion than its insides. Could be caused by impurities in a material normally resistant to corrosion. Like iron particles in aluminium.

### Selective leaching

Is a process where galvanic corrosion on a micro scale is used to remove certain metals in an alloy. The least noble metal will be removed from the alloy.

### Erosion corrosion

Is a type of corrosion where there is a corrosive fluid running over the metal. The rate of corrosion may be controlled by the speed of the fluid. It can either be increased or decreased.

### Stress-corrosion cracking

Is thoroughly explained in the next chapter.



### 2.1.2 Stress corrosion cracking

The term stress corrosion cracking is often substituted with corrosion fatigue when it comes to tensile forces on a body that is subjected to pitting corrosion. The description of stress corrosion cracking is directly from p. 525 – 527 (Anderson, 2005)

Stress corrosion cracking (SCC) refers to crack propagation due to an anodic reaction at the crack tip. The crack propagates because the material at the crack tip is consumed by the corrosion reaction. In many cases, SCC occurs when there is little visible evidence of general corrosion on the metal surface, and is commonly associated with metals that exhibit substantial passivity.

In order for the crack to propagate by this mechanism, the corrosion rate at the crack tip must be much greater than the corrosion rate at the walls of the crack. If the crack faces and crack tip corrode at similar rates, the crack will blunt. Under conditions that are favourable to SCC, a passive film (usually an oxide) forms on the crack walls. This protective layer suppresses the corrosion reaction on the crack faces. High stresses at the crack tip cause the protective film to rupture locally, which exposes the metal surface to the electrolyte, resulting in crack propagation due to anodic dissolution.

Because of the need for a passive layer to form on the crack faces, conditions that favour SCC often do not favour general corrosion. Stress corrosion cracking tends to occur in the transition between active and passive behaviour, as well as the transition between passive and transpassive behaviour. SCC susceptibility coincides with susceptibility to corrosion pitting. Corrosion pits often act as a nucleation sites for SCC due to local stress concentration and occluded chemistry effects.

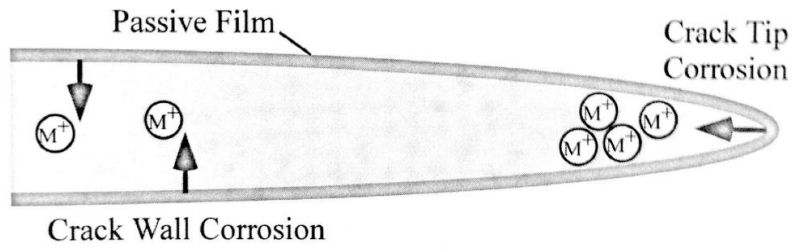


Figure 2-1 Illustration of anodic stress corrosion cracking (Anderson, 2005)

Figure 2-1 shows a simple illustration of anodic stress corrosion cracking. The crack-tip corrosion rate must be much greater than the corrosion rate at the crack walls. Such a condition requires that a passive film form on the crack walls.

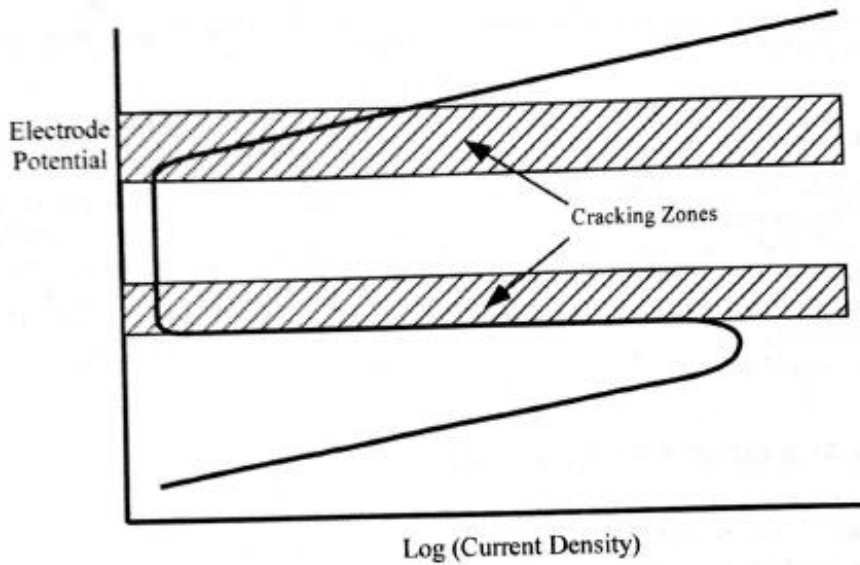


Figure 2-2 Polarization diagram, illustrating the zones that tend to favour stress corrosion cracking (Anderson, 2005)

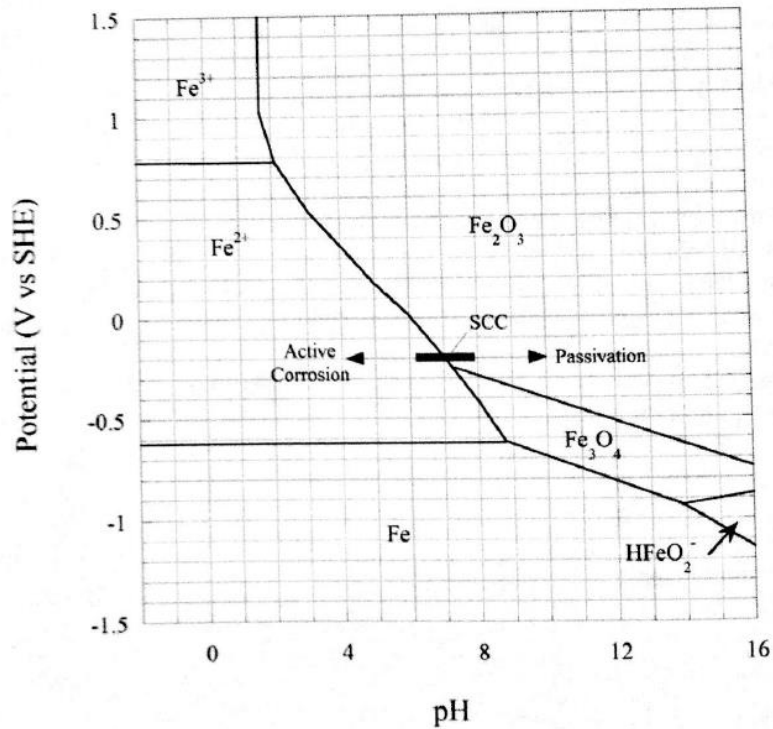


Figure 2-3 Pourbaix diagram for iron in water (Anderson, 2005)

Figure 2-3 shows the Pourbaix diagram for iron in water. (I.e. acidic conditions). SHE stands for standard hydrogen electrode. The optimal pH for stress corrosion cracking is 7 for a potential of 0.2 V vs. SHE. T.L Anderson, *Fracture Mechanics; Fundamentals and Applications* (Boca Raton, FL: Taylor and Francis Group, 2005), p.526.

In this active region, iron will oxidize to  $Fe^{2+}$  or  $Fe^{3+}$ . Consider a potential of -0.2 V and a pH ranging from 4 to 10, as indicated in figure 2-3. At the upper end of this range, the oxide is stable and the iron surface passivates. The low end of this region is an area of active corrosion. The optimal pH for SCC in this case is 7. At higher pH levels, the oxide film becomes stable, and the corrosion rate is very slow due to passivation. At lower pH levels, a passive film does not form, and general corrosion occurs instead of SCC.

Ongoing research is aimed at developing predictive models that enable the crack tip environment to be inferred from the bulk environment, and significant successes have been recorded over the past two decades. T.L Anderson, *Fracture Mechanics; Fundamentals and Applications* (Anderson, 2005) p.527.

In the case of this thesis, the passive film is brought to a minimum on purpose with regards to the thesis main focus, namely the effects of localized corrosion on welded joints. Our specimens are partially coated with corrosion retarding paint, but the area around the weld and joining steel plates are left open, and are therefore susceptible to corrosion. The film is reduced in the machining of the specimens, but a passive film will form nevertheless as the corrosion product (rust/oxide) in itself is a passive film.

### 2.1.3 Basic wet corrosion cell

The description of a basic wet corrosion cell is directly from p. 75-77 (Trethewey & Chamberlain, 1995)

Corrosion science involves a study of **electrodics**, electrochemical process which take place at **electrodes**. An electrode is essentially the boundary between a solid phase (metal) and a liquid phase (aqueous environment) and these processes take place across the phase boundary. They involve effects of both mass and charge; mass is usually transferred (in both directions) between the solid metal and the liquid environment, whilst charge is exchanged between atoms and ions. It is commonly thought of *atoms* in solid metals, but *ions* in **electrolyte**, in solid films of surface oxide, or in corrosion products.

Electrolyte is an electrically conducting solution. Very pure water is not normally considered to be an electrolyte; the conductivity of typical commercial deionised water is about 1-10 mS  $m^{-1}$ . Under most practical conditions, however, an aqueous environment will have a sufficient conductivity to act as an electrolyte. Soft tap water has conductivity typically about 10--20 mS  $m^{-1}$ , compared with a value for 3.5% sodium chloride solution of 5.3 S  $m^{-1}$ . Note that electrons as isolated particles never cross the interface; all charge is carried in electrolytes in the form of ions.

It is usually possible to identify different regions of a corroding metal/electrolyte interface at which the electrodic processes occur. If the reactions are net anodic (electron-producing) that part of the interface is called an **anode**. If they are net cathodic (electron-consuming) that part of the interface is called a **cathode**.

For a basic wet corrosion cell four essential components can be identified: **anode**, **cathode**, **electrolyte** and **connections**.

The part of a metal/electrolyte interface which behaves as an **anode** usually corrodes by loss of electrons from electrically neutral metal atoms in the solid state, forming discrete ions. These ions often enter the solution, but they may also react with other species at the interface to form insoluble solid corrosion products which usually accrue on the metal surface. This is a common anode reaction in neutral alkaline environments and may block further metal dissolution, retarding the corrosion and resulting in passivation.

The corrosion reaction of a metal M is usually expressed by the simplified equation:



in which the number of electrons taken from each atom is governed by the valence of the metal.  $z = 1, 2$  or  $3$  (commonly)

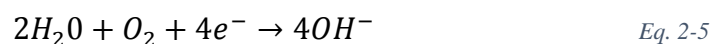
The cathode is an essential complement to the anode because it consumes the electrons generated by the anode. A cathode does not normally corrode, although it may suffer damage under certain conditions. To determine the process occurring at cathodes, one look for possible electron-consuming (reduction) reactions. To do this one look at the reverse of equation (1.0).



This equation is commonly referred to as a replating reaction. Two other important reduction reactions may also occur at the cathode: a two-step process in which hydrogen gas is formed:



and a process that consumes dissolved oxygen and generates hydroxyl ions:



Hydrogen ions,  $H^+$ , are always present in water, to a greater or lesser extent, and therefore their reduction, represented by equations (1.2) and (1.3), is always possible. The reaction varies with pH and is more likely with low pH, meaning the hydrogen ion ( $H^+$ ) is rich in the solution. The second reduction reaction equation (1.4), is dependent upon the level of dissolved oxygen ( $O_2$ ) in solution. Although in well-aerated solutions this is typically about 5-10 parts per million (ppm) and seems rather small, nevertheless, this amount is quite sufficient for this process to be important.

The anode and cathode require an electrical connection for a current to flow in the corrosion cell. There is no need for a physical connection when the anode and cathode are part of the same metal.

The removal of any of the four components of the simple wet corrosion cell will stop the corrosion reaction.

#### 2.1.4 Redox reaction

Redox is short for reduction and oxidation. A redox reaction is all chemical reactions where the atoms have their oxidation state changed.

**Oxidation:** Loss of electrons, increase in oxidation state

**Reduction:** Gain of electrons, decrease in oxidation state

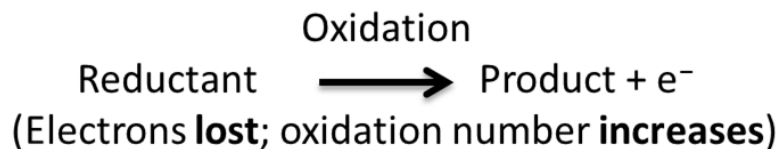
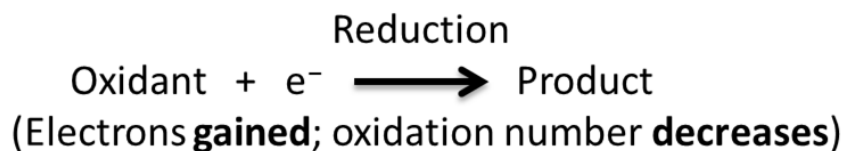
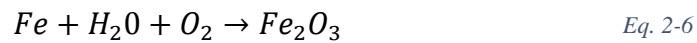


*Figure 2-4 Illustration of a redox reaction (Garnham, 2006)*

Redox reactions in this thesis revolves around the common name for corrosion, namely rust. When our steel members are exposed to a corrosive environment, in this case sea water and air adjacent to sea water, a transfer of electrons occur. Oxygen dissolves in water, creating ions. These ions have a valence, meaning they have room for electrons. The iron atom (Fe) have

extra ions to give away. From figure 3.1 the conclusion here will be that the Fe oxidizes and the ions formed from oxygen dissolving reduces.

iron + water + air = rust



Iron in the presence of moisture( $H_2O$ ) will lose electrons, becoming a positively charged ion in water.

oxidation reaction: Iron is oxidized (losing  $e^-$ )

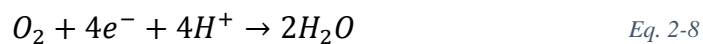


(s): solid

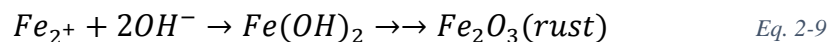
(aq): aqueous

Those electrons are then used to reduce the oxygen dissolved in the water ( $H^+$  and  $OH^-$ )

Reduction reaction: Oxygen is reduced (gains  $e^-$ )



Those  $Fe_{2+}$  ions react with the  $OH^-$  ions in water to produce iron hydroxide, which will dry in several steps to produce rust:



The redox reaction requires water, which explains why a moist environment speeds up the rusting process. Rusting can occur in dry climates, but it tends to happen much more slowly due to the relatively low humidity in the air. (John Wiley & Sons Publishers, Inc, 2002)

As later shown by the rapid corrosion that happens when the members have been soaked in sea water. The  $Na^+$  and the  $Cl^-$  speed up the process. These ions are not in themselves a part of



the reaction, but they have valences that help transfer the electrons from the iron (Fe) to the  $H^+$  and  $OH^-$  ions.

## "OIL RIG"

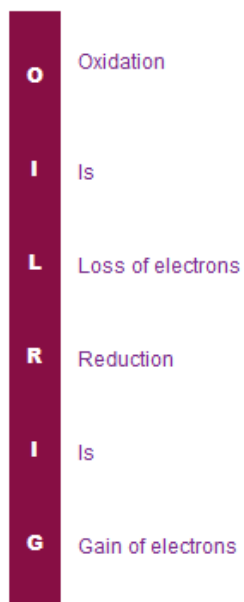


*Figure 2-5 Simple explanation of the meaning behind the word redox*

The term reduction can be confusing with regards to redox reaction. This figure gives an overview so that it is easier to have control of the terms.

### 2.1.5 Pitting corrosion (N. International, 2015c)

Pitting corrosion is a localized form of corrosion by which cavities or "holes" are produced in the material usually at an angle of 90 degrees to the surface. Pitting is considered to be more dangerous than uniform corrosion damage because it is more difficult to detect, predict and design against. Corrosion products often cover the pits. A small, narrow pit with minimal overall metal loss can lead to the failure of an entire engineering system. Pitting corrosion, which, for example, is almost a common denominator of all types of localized corrosion attack, may assume different shapes. Pitting corrosion can produce pits with their mouth open (uncovered) or covered with a semi-permeable membrane of corrosion products. Pits can be either hemispherical or cup-shaped

Pitting is initiated by:

- a. Localized chemical or mechanical damage to the protective oxide film; water chemistry factors which can cause breakdown of a passive film are acidity, low dissolved oxygen concentrations (which tend to render a protective oxide film less stable) and high concentrations of chloride (as in seawater)
- b. Localized damage to, or poor application of, a protective coating
- c. The presence of non-uniformities in the metal structure of the component, e.g. non-metallic inclusions.

Theoretically, a local cell that leads to the initiation of a pit can be caused by an abnormal anodic site surrounded by normal surface which acts as a cathode, or by the presence of an abnormal cathodic site surrounded by a normal surface in which a pit will have disappeared due to corrosion.

Apart from the localized loss of thickness, corrosion pits can also be harmful by acting as stress risers. Fatigue and [stress corrosion cracking](#) may initiate at the base of corrosion pits. One pit in a large system can be enough to produce the catastrophic failure of that system.

Some definitions:

Pitting: corrosion of a metal surface, confined to a point or small area that takes the form of cavities. \*

Pitting factor: ratio of the depth of the deepest pit resulting from corrosion divided by the average penetration as calculated from weight loss. \*

### Some types of pitting corrosion

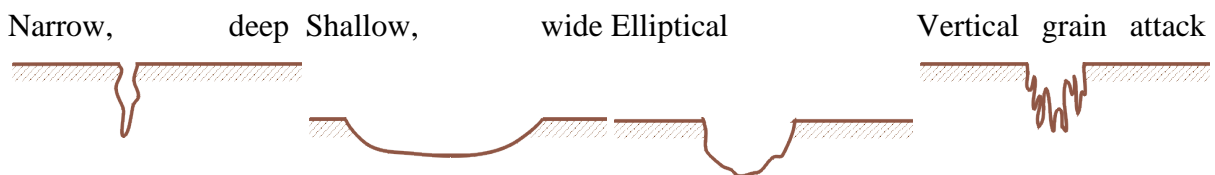


Figure 2-6 Illustration of pit formations (N. International, 2015a)

### Sideway Pits

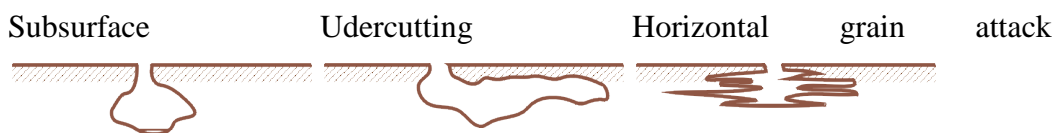


Figure 2-7 Illustration of pit formations (N. International, 2015a)

### 2.1.6 Mechanism of pitting corrosion

The mechanism of pitting corrosion is directly, p. 169-171 (Trethewey & Chamberlain, 1995)

The mechanism of pitting of carbon steel was first described by Evans U R 1961 *The corrosion and oxidation of metals*, Edward Arnold, London, p.127. This work was for a long time represented as a significant advance in the understanding of pitting. It is later on understood that the features are classified better as differential-aeration corrosion.

### 2.1.7 Differential-Aeration corrosion (Trethewey & Chamberlain, 1995)

When a member of carbon steel with a smooth surface is exposed to water (rain, sea water, etc), it will after a few days *rust* rapidly. The *rust* occurs as hard deposits, scabs or tubercles. This happens in localized areas where water droplets have remained the longest. If the *rust* is removed with a steel brush, the surface area will be found to be pitted in the areas previously covered by corrosion products. At this stage the term *italics* is used since *rust* is commonly understood as the brown corrosion product formed on corroded iron or steel surfaces. This corrosion product is actually a mixture of chemical species and has a more precise definition.

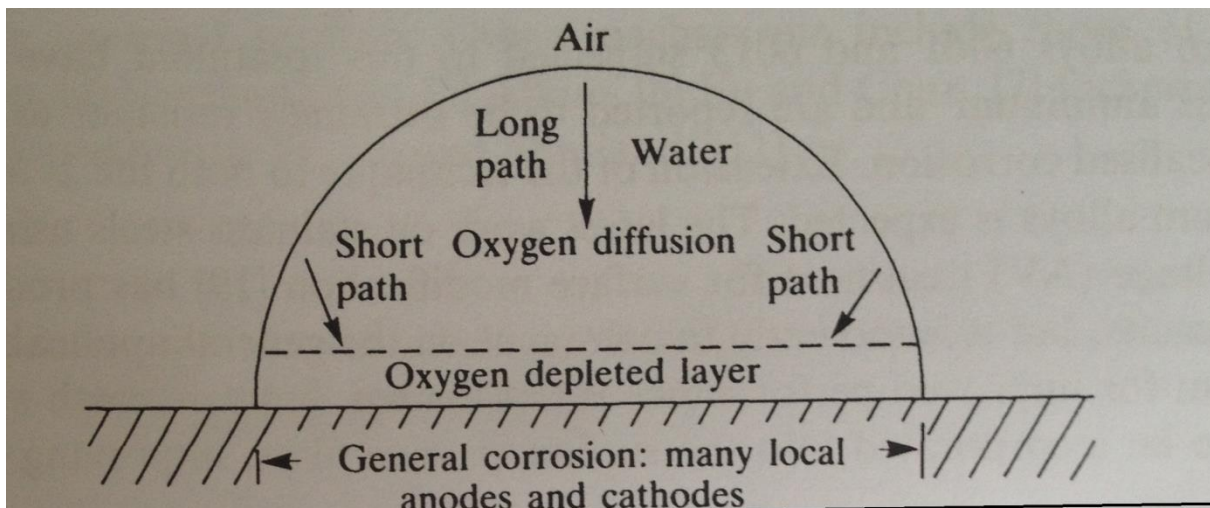


Figure 2-8 The mechanism of pitting because of differential aeration beneath a water droplet (Trethewey & Chamberlain, 1995)

Figure 2-8 shows that the initiation of a pit is preceded by general corrosion over the whole of the wetted surface. This is probably as a result of simple grain boundary

effects. Consumption of oxygen by the normal cathode reaction in neutral solution causes an oxygen concentration gradient within the electrolyte.

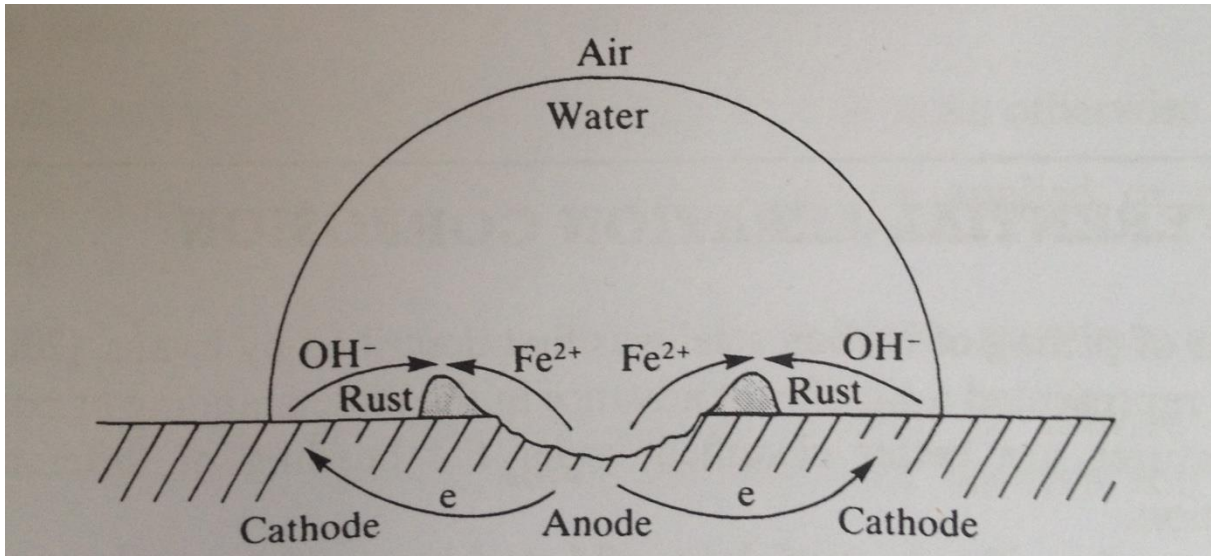


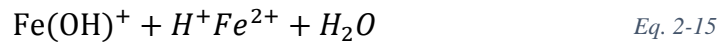
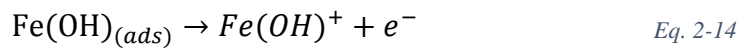
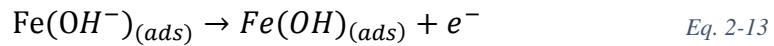
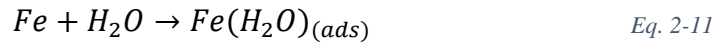
Figure 2-9 General corrosion over the whole of the wetted metal surface depletes the oxygen levels in the adjacent electrolyte (Trethewey & Chamberlain, 1995)

The wetted area adjacent to the air/electrolyte interface receives more oxygen by diffusion than the area at the centre of the drop, which is at a greater distance from the oxygen supply. This concentration gradient anodically polarizes the central region, which actively dissolves:



The hydroxyl ions that is generated in the cathode region diffuses inwards and react with the iron ions diffusing outwards, causing the deposition of insoluble corrosion product around the depression or pit. This retards the diffusion of oxygen, accelerates the anodic process in the centre of the drop and causes the reaction to be autocatalytic which is shown in Fig 2-9.

Equation (3.4.1) is very simplified, the actual steps are as follows:

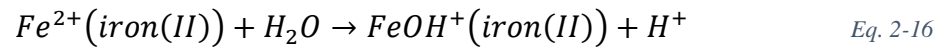


The expression *ads* represents *adsorbed* and implies that reaction occurs in the solid phase at the solid/liquid interface. The summation of the five equations above leads directly to equation (3.5.1).

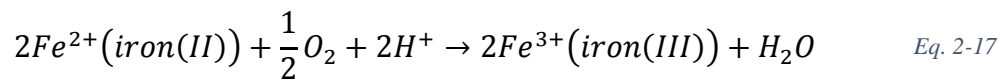
Iron has two valency states. Iron can lose two or three electrons. This is called iron(II) and iron(III). These ions form in aqueous solutions, and here numerous iron ions can exist. The oxidation state can be disguised by reaction with negative hydroxyl ions.

The aforementioned Evans explanation has been extended by Wranglen G 1985 *An introduction to corrosion and protection of metals, Chapman and Hall, London, p.24* and well summarized by Shreir L L 1994 *Localized Corrosion. In Corrosion*, edited by L L Shreir, R A Jarman and G T Burstein, Butterworth-Heinemann, Oxford, pp. 1:181-3. to better explain pit formation on carbon steel.

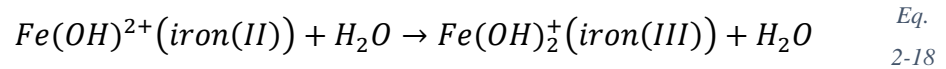
What happens first is a hydrolysis reaction occurs, here the acidity is increased.



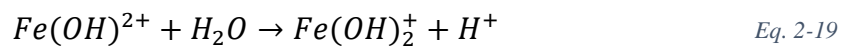
The formation of iron (III) ions is an oxidation reaction facilitated by the presence of oxygen. Even when the iron is combined in the  $Fe(OH)^+$  ion, it can be oxidized to the iron (III) state:



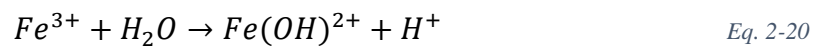
or



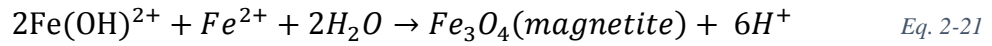
More hydrolysis reactions are possible, in which the solution is further acidified:



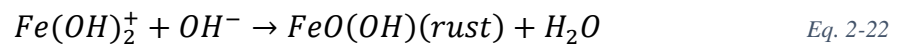
and



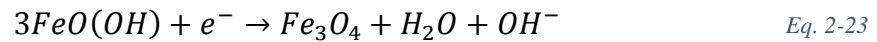
All iron ions in equations (3.4.10 and 3.4.11) are iron (III) ions. The two major corrosion products, magnetite and rust, are respectively denoted by the formula  $Fe_3O_4$  and  $FeO(OH)$ , and they are formed from the complex ionic species:



and



Rust is now a specific chemical species. At cathodic sites outside the pit, along with the usual oxygen reduction reaction, ( $2H_2O + O_2 + 4e^- \rightarrow 4OH^-$ ), the rust is now reduced to magnetite:



A layer of corrosion products grow over the pit and its immediate surroundings, forming a scab or tubercle and isolating the environment within the pit from the bulk electrolyte. It is reckoned that the autocatalytic process is assisted by an increased concentration of chloride ions within the pit.



## 2.2 Fatigue

Fatigue is known as exhaustion of a material. During loads below its ultimate strength or yield strength. With oscillations both in high and low frequencies causes cracks to initiate within the material. Fatigue is divided into high cycle fatigue (HCF), low cycle fatigue (LCF) and ultra-low cycle fatigue (ULCF) with the last two in the plastic/inelastic range of the material. Fatigue is caused by a stress concentration which again causes strain on the part one is investigating. With small loads in HCF testing the material reaches the so-called endurance limit, which implies that with a constant applied stress the material will endure this indefinitely. This is however not the case when corrosion is present. The usual S-N curve shows this endurance limit with a straight line, but the S-N curve for corrosion the line will permanently have a decline, meaning it will cross the x-axis giving a number of cycles to failure for any stress level.

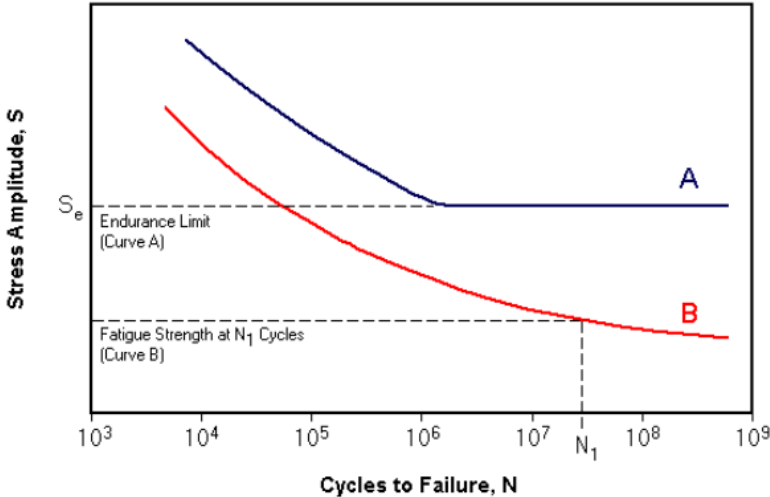


Figure 2-10 Illustration of endurance limit and corrosion affected steel (ETBX, 2001-2008)

Line A representing the endurance limit.

Line B representing fatigue testing of corroded specimens.

What is stress? (Center, 2015)

Stress is measured in Pascals (Pa), and is a representation of force divided by the specimens cross sectional area. Stress is an internal distribution of the forces applied to a specimen, and balances the force and load applied to it. Usually stress is divided into *engineering* and *true* stress. *Engineering* stress uses the known data for the given situation, meaning the original cross section, the original length etc. *True* stress uses instantaneous values, meaning what the value is for the cross section, length etc. at any given point in for example a tensile test. It can be both uniformly and non-uniformly distributed. This depends on the way the force or load is applied to it. If a specimen is uniform and is pulled from both ends, the stress will be uniformly distributed along the cross sectional area. On the other hand, if there is drilled a hole somewhere on the cross section the stress will no longer be uniform. There will now be a discontinuity in the material of the specimen. The hole represents a reduction in the cross section, which will cause the material to be weaker at this location. Stress is derived from the following equation:

$$\sigma = \frac{F}{A_0} \quad \text{Eq. 2-24}$$

$\sigma$  is the stress

F is the force applied to a body/specimen

$A_0$  is the original cross sectional area

What is strain? (Center, 2015)

Is the reaction a material has on stress applied to it. Stress can be elastic and inelastic. Elastic strain means that the elongation that happens during the load cycle has no permanent effect on the material in terms of elongation. Inelastic strain is the opposite. The stress on the material is so high that a permanent elongation takes place. Like in stress, strain can be divided into *engineering* strain and *true* strain, and the meaning is the same for strain as it is in stress. Both types of strain is dimensionless, but usually mm/mm or m/m is used in the metric system. The strain concentration is not necessarily uniform.

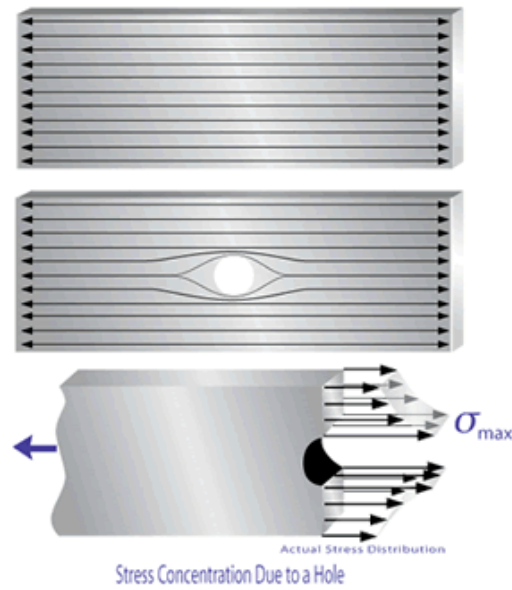


Figure 2-11 Stress concentration due to a hole (Center, 2015)

Let us consider the same hole that was mentioned in the stress description, and place this hole at the centre of the specimen. This represents a discontinuity in the cross section. There is now a smaller cross section, and the strain will not be uniformly distributed on a uniform area. Material has been removed from the cross section meaning that no load can be carried. The strain then has to be redistributed over the remaining material. The strain concentration will now be along the hole's outer perimeter, because of the uneven distribution of load due to the discontinuity of the material.

$$\text{Strain} = \frac{\text{elongation}}{\text{original length}} = \frac{\Delta L}{L_0} \quad \text{Eq. 2-25}$$

Miner's [Appendix B] (University, 2015) rule is one of the most widely used models for determining failure due to fatigue in a system. It is a cumulative model where if there is  $k$  different stress levels and the average number of cycles to failure in  $i$ th stress,  $S_i$ , is  $n_i$ , then the fraction  $C$  is;

$$\sum_{i=1}^k \frac{n_i}{N_i} = C \quad \text{Eq. 2-26}$$

Where:

$n_i$  is the number of cycles accumulated at stress  $S_i$

$C$  is the fraction of life consumed by exposure to the cycles at the different stress levels. In general, when the damage fraction reaches 1, failure occurs.

If we consider an S-N curve from the material we want to consider we can use the Miner's rule to determine the number of cycles (N) to failure.

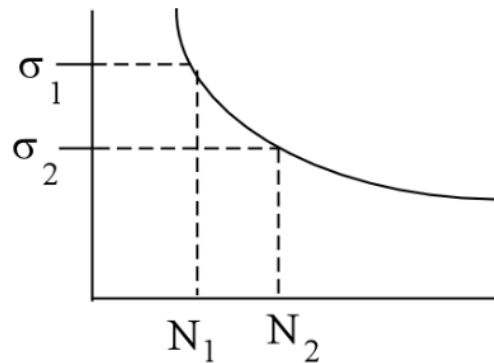


Figure 2-12 S-N curve representing methods to determine number of cycles to failure [Appendix B] (University, 2015)

A test specimen can tolerate a certain amount of damage, C. If that specimen experience damages  $C_i$  ( $i = 1, \dots, N$ ) from N sources, then it can be expected that the specimen will fail if;

$$\sum_{i=1}^N C_i = C \quad \text{Eq. 2-27}$$

or, equivalently

$$\sum_{i=1}^N \frac{C_i}{C} = 1 \quad \text{Eq. 2-28}$$

defines failure, where  $C_i/C$  is the fractional damage received from the  $i$ th source.

Low Cycle Fatigue is usually characterized by the Coffin-Manson equation:

$$\frac{\Delta \varepsilon_p}{2} = \varepsilon'_f (2N)^c \quad \text{Eq. 2-29}$$

$\frac{\Delta \varepsilon_p}{2}$  is the plastic strain amplitude

$\varepsilon'_f$  the fatigue ductility constant

$2N$  Number of reversals to failure (  $N = \text{cycles}$ )

$c$  the fatigue ductility exponent (  $-0.5, -0.7$ )

According to Morrow , the relationship between strain amplitude  $\frac{\Delta \varepsilon}{2}$ , and the permanent fatigue life,  $N_f$  can be written as

$$\frac{\Delta \varepsilon}{2} = \frac{\Delta \varepsilon^{el}}{2} + \frac{\Delta \varepsilon^{pl}}{2} = \frac{\sigma'_f}{E} (2N_f)^b + \varepsilon'_f (2N_f)^c \quad \text{Eq. 2-30}$$

$N_f$  is the number of cycles to failure. This covers the fatigue life with regards to both elastic and plastic strain. This equation will be the chosen equation when estimating the fatigue life of the specimens that will be subjected to fatigue test. The abbreviation of this formula will be explained in chapter 6.1.3.

The term fatigue was first used by Jean-Victor Poncelet (Vervoort & Wurmman, 2015 ). The idea on the other hand was described earlier by Wilhelm Albert (Vervoort & Wurmman, 2015 ). He had noticed that chains used to hoist ore from a mine was failing below its capacity. This was the first study and reporting of fatigue behaviour. He constructed a machine that was able to repeatedly load the chain, and he discovered that the failure was not associated with a sudden overload of the material, but rather dependent upon load and number of cycles in which the material was loaded with. This introduced a whole new area in engineering, and has given origins to a lot of research on the subject. It is clear that fatigue behaviour consists of inclusions in the matrix, void nucleation, void growth, necking between voids and void coalescence which leads to fracture in the material.

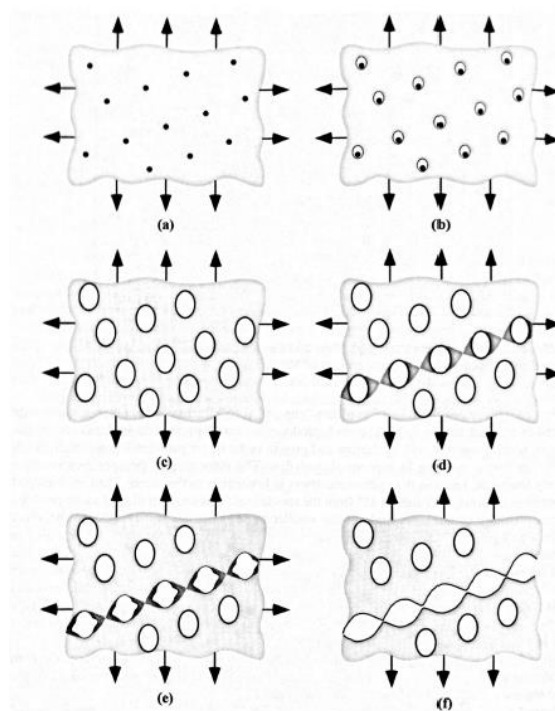


Figure 2-13 Void nucleation, growth and coalescence in ductile metals: a) inclusions in the matrix, b) void nucleation, c) void growth, d) strain localization between voids, e) necking between voids and f) void coalescence and fracture (Anderson, 2005)

In the engineering discipline three methods has been used for fatigue life estimation, and it is optional which one is used. These are the stress-life method, strain-life method and linear elastic fracture mechanics. The important thing that is considered in choosing which method is to be used, is what the dominant factor for this test is. It is meant by this that in LCF and ULCF, strain is the recommended factor and the strain concentration/accumulation is the cause of failure. For HCF stress is more applicable since the force is not in the plastic range, and

therefore stress will give a better answer to these types of predicaments or problems. Which means that stress accumulation is the cause of failure. The common definition of HCF is that the number of cycles to failure is more than  $10^4$  cycles. Which in return defines LCF as below  $10^4$ , usually below  $10^3$ . ULCF is more recent and though there is research done on this subject, relevant information towards the purpose of study for this thesis was hard to find. There is different definitions of how many cycles of failure is needed to call it ULCF, but the general notice is 10 – 20 cycles.

Fatigue research is vast, though the problems can be understood, a precise model for estimation is hard to establish. There can be found practical methods and probabilistic methods in this area. The fatigue problem in itself is serious, but it can also be combined with other effects on materials like in this thesis; corrosion. Dong, Y and Frangopol, D.M, 2015 (Dong & Frangopol, 2015) presented a probabilistic approach to optimum inspection and repair plans for ship structures considering corrosion and fatigue. Amongst their findings they concluded with that effects of corrosion is larger than that associated with fatigue cracking, but that the fatigue cracking acts as the main factor for risk assessment close to the end of the service life when considering both corrosion and fatigue

Big loads in the plastic area of the metal cause big deformations to a structure, and often the structure fails, or is being rendered useless. Probably the most famous accident in HCF, who also gave a breeding ground to fatigue research, is the Versailles train crash (Smith, 2007) It showed that one of the locomotives axels failed due to metal fatigue. It was discovered that the axel broke due to stress concentration, where the crack continued to grow with the repeated loading. Fatigue problems come into play during frequent loading, like cars over bridges and air plane wings during flight. LCF and ULCF appears often in extreme conditions like earthquakes, collisions, big waves on offshore steel jacket, oscillation on a crane boom when lifting heavy loads etc. The structure's material comes to the Ultimate Limit State (ULS) and Accidental Limit State (ALS). With a safety factor implemented on these structures, repairs should be able to be done. But in the offshore industry the equipment and structures are placed in corrosive environments. A breach in the jacket legs coating may give conditions for corrosion to start on the materials used. This breach can happen from foreign objects drifting on the currents, animals rubbing against it, small collisions with service boats etc. From the corrosion forms listed above, the most critical one in this environment is pitting corrosion. This localized form of corrosion can penetrate into the metal quite rapidly, and during extreme loads the

material can be so damaged that failure of the entire jacket leg can happen. Probably one of the most famous accidents in Norwegian history is the accident on the Alexander Kielland platform (Moan, 2010). A later investigation showed that one of the six bracings had failed due to repeated loading. It showed that it was a 6 mm fillet weld which joined a non-load-bearing flange plate to this bracing. The poor profile of the fillet weld contributed to a reduction in its fatigue strength. This caused the rig to capsize, killing 123 people. So threat to human life is present. So the objective of this thesis will be to check the effects of localized corrosion on steel joints in the plastic strain range with regards to Low Fatigue Cycle (LFC) and Ultra Low Fatigue Cycle (ULFC).



### 2.2.1 Methods for testing LCF and ULCF

LCF and ULCF use strain-life method as opposed to HCF which use stress-life method. Often the same type of specimen is used for any of the tests. One usually use a smooth specimen, shown in figure 2-14. The specimen has a tapered form towards the centre of the specimen, which causes the stress/strain concentration to form at the smallest cross sectional area.



Figure 2-14 A smooth specimen (EPIInc, 2012)

The smooth bar specimen is very versatile, it can be used for all the types of fatigue methods one tests for, whether it be bending, tension or other types of fatigue testing. The specimen represents a discontinuity in the material. The principal used when obtaining the stress on a specimen is the equation below:

$$\sigma = \frac{F}{A_0} \quad \text{Eq. 2-31}$$

Where  $\sigma$  is stress in megapascals (MPa)

F is the force in Newtons (N)

$A_0$  is the original cross sectional area of the specimen ( $mm^2$ )

The stress concentration will be accumulated in the part of the specimen where the cross section is smallest. This means that this part of the specimen has least capacity to withstand the forces applied to it.

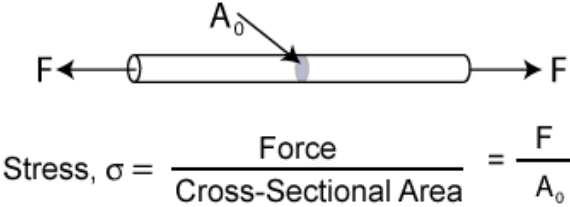


Figure 2-15 Illustration of relation of equation 2-30 (Center, 2015)

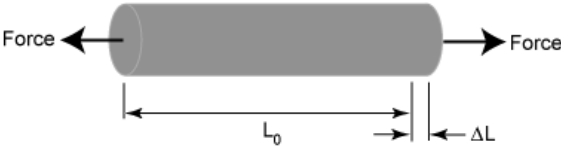


Figure 2-16 Illustration of strain (Center, 2015)

### 2.3 The Goodman relation(University, 2011)

The use of mean stress in the DNV standards refers to a stress ratio of zero ( $R = \frac{\sigma_{max}}{\sigma_{min}} = -1$ ).

This is due to that the tension and compression force is opposite equal, meaning tension = - compression. The mean stress is calculated by following equations:

$$\sigma_m = \frac{\sigma_{max} + \sigma_{min}}{2} \quad \text{Eq. 2-32}$$

$$\sigma_a = \frac{\sigma_{max} - \sigma_{min}}{2} \quad \text{Eq. 2-33}$$

The Goodman relation is used to rewrite the stress when the load case produces a stress ratio value not equal to negative one. The equation is presented as:

$$\sigma_a = \sigma_f * \left(1 - \frac{\sigma_m}{\sigma_y}\right) \quad \text{Eq. 2-34}$$

Where;

$\sigma_a$  is the alternating stress

$\sigma_f$  is the true fracture stress

$\sigma_m$  is the mean stress value

$\sigma_y$  is the material's ultimate tensile strength

In laboratory experiments the alternating stress and the mean stress value will, in most cases, be recorded by the test equipment (i.e. test machine software). To compare achieved results from a test to DNV standards it is often the fatigue limit for completely reversed loading that is needed to be calculated. A rewrite of the equation is then needed. The rewrite presents a conservative approach for alternating stress when dividing mean stress with the yield strength of the material. In short, one divides the alternating stress on the remaining capacity of the material.

$$\sigma_{a,m=0} = \frac{\sigma_a}{\left(1 - \frac{\sigma_m}{\sigma_y}\right)} \quad \text{Eq. 2-35}$$

### 2.3.1 Fracture Mechanics

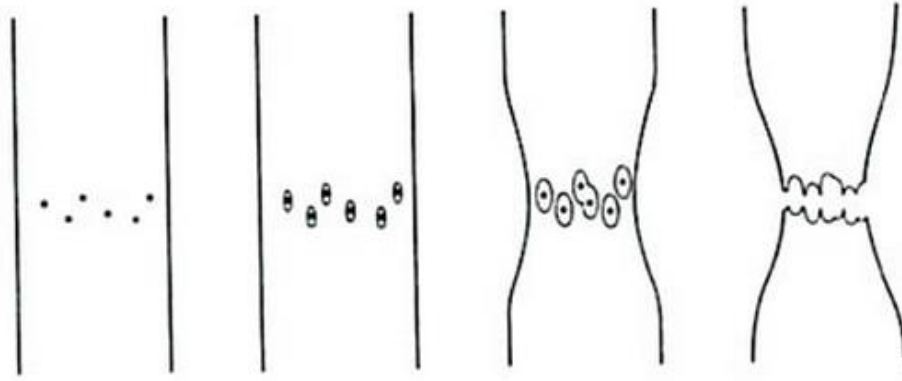


Figure 2-17 Illustration of void nucleation, growth, coalescence and fracture (Weck, Wilkinson, Maire, Toda, & Embury, 2015)

This picture shows the same principle course of actions described in the previous passage. Small cracks nucleates in the material due to the cyclic loading. This means that the loading causes small deformations to accumulate within the material. The material cannot recover, so the initiated cracks grow, until the cracks have grown so big that it coalesces with each other and finally causes the material to fracture. For a ductile fracture to happen the material has to let dislocations happen. A dislocation allows the material to slide, which again gives origins to plastic behaviour. If the material does not let dislocations to happen, one will experience a brittle fracture.

*“Fracture mechanics often plays a role in life prediction of components that are subject to time-dependent crack growth mechanisms such as fatigue or stress corrosion cracking”*(Anderson, 2005)

In linear elastic fracture mechanics (LEFM) the parameter stress-intensity factor correlates to the rate of cracking. If the fracture toughness is known the critical crack size for failure can be calculated. As stated in T.L Anderson (Anderson, 2005) the crack growth rate in metals can be described by the empirical relation:

$$\frac{da}{dN} = C(\Delta K)^m \quad \text{Eq. 2-36}$$

Where  $da/dN$  is the crack growth per cycle

$\Delta K$  is the stress-intensity range and  $C$  and  $m$  are material constants.

## 3 Corrosion fatigue

Chapter 2.1 and 2.2 describes individually what corrosion and fatigue is. This chapter will focus on the combination of corrosion and fatigue, and discuss the potential danger of the combination. As mentioned in chapter 2.2 there is different definitions in which LCF and HCF is defined. Usually HCF is defined as  $10^4$  cycles, which again defines LCF as below  $10^4$ . This boundary is set as  $10^5$  in NORSOK (Anijs, 2013). But  $10^4$  is mostly used. It can also be defined as  $10^3$ . No matter which way one wishes to define it, the difference is often the load case of which a body is subjected. Refer chapter 2.2 where there is defined three assessment methods for fatigue. LCF is governed by the strain life method, which use the strain applied to a body to assess the fatigue life.

### 3.1 Low cycle corrosion fatigue (LCCF)

As stated in chapter 2.1.2, corrosion fatigue where pitting corrosion is the dominant factor the term corrosion fatigue is substituted with stress corrosion cracking. This is due to that the formation of pits, can be seen as equal to formation of cracks. The difference between just crack growth and pitting corrosion is that with pitting corrosion initiated the crack growth will not be governed by the cyclic loading alone. The mechanism of stress corrosion cracking and the formation of pitting corrosion is described in chapter 2.1.2 and 2.1.5, and will therefore not be described further in this chapter.

### 3.2 Why investigate LCCF on welded joints

The impact of corrosion on a load bearing structure can significantly reduce the estimated fatigue life. Steel is the most common material used in the off shore industry and is in itself a reactive material, meaning it can easily transfer electrons. A weld is regarded as the weakest point in a steel structure, and it is therefore normal to inspect the penetration of the weld to assure that it is fully penetrated. Typical methods to check this is X-ray, magnetic particle inspection or ultrasound. The methods check the uniformity and penetration of the weld.

Usually the inspector checks if there are any cracks in the weld. (NORSOK, 2010) has requirements to welds placed at certain depths. Usually the inspection class is defined by the depths in which the weld will be placed in. The inspection class is determined from how complex it is to inspect it once it is taken into use (i.e. which depth it is placed in). As mentioned above a breach in the coating can happen from factors that cannot be controlled. If the coating covering a weld is breached the weld will immediately be subjected to a corrosive environment. In addition to the cyclic loading that the weld is subjected to on a regular basis, the effects of corrosion will reduce the fatigue life based on the significance of the corrosion attack. Pitting corrosion will be the most significant attack with regards to corrosion.

Therefore a LCF test will be conducted on specimens representing a welded joint that has been subjected to corrosion. It is desirable to investigate two different corrosive environments, namely sea water and air close to the sea. Air close to the sea will have a relatively high humidity and will also contain  $H^+$  and  $Cl^-$  ions. This will increase the acidity in the electrolyte formed on the specimens from the humidity and rain.

## 4 Design of test

The tests will be done in accordance with ISO 12106 *Metallic materials - fatigue testing - axial-strain-controlled method*, but it is taken into account limitations, and availability of the equipment at the University of Stavanger.

The testing of specimens in this thesis will be tension-tension due to the limitations on testing machine "Zwick Z020", and therefore not all of ISO 12106 points can be accounted for. The test will seek to fulfill the ISO 12106 requirements as far as it is reasonably practicable for the given testing method.

ISO 12106 use the following terms and definitions.

**stress**  $\sigma = \frac{F}{A}$

Engineering stress is not applicable due to the fact that the test will be in the plastic range.

### **gauge length**

Length between extensometer measurement points.

### **strain**

$$\varepsilon = \int_{L_0}^L \frac{dL}{L}$$

Where  $L$  is the instantaneous length of the gauge section.

Engineering strain is not applicable due to the fact that the test will be in the plastic range.

$$\varepsilon > 0,01 \quad 10\%$$

**cycle**

Smallest segment of the strain-time function that is repeated periodically.

**maximum**

Greatest algebraic value of a variable within one cycle.

**minimum**

least algebraic value of a variable within one cycle.

**mean**

One-half of the algebraic sum of the maximum and minimum values of a variable

**range**

Algebraic difference between the maximum and minimum values of a variable

**amplitude**

Half the range of a variable

**fatigue life**

$N_f$

Number N of cycles that have to be applied to achieve failure.

**4.1 Hysteresis loop**

Closed curve of the stress-strain response during one cycle.



## 4.2 Fatigue testing

### symbols

$E$  - modulus of elasticity, in gigapascals (GPa)

$E_T$  - modulus for unloading following a peak tensile stress, in gigapascals (GPa)

$N_f$  - number of cycles to failure

$t_f$  - time to failure ( $=N_f$  cycles), in seconds (s)

$\sigma$  - true stress, in megapascals (MPa)

$\varepsilon$  - true strain

$\Delta$  - range of a parameter

$R_{r0,2}$  - proof stress

Rz - mean surface roughness, in micrometers ( $\mu\text{m}$ )

$R_\sigma$  - stress ratio ( $=\sigma_{min}/\sigma_{max}$ )

$R_\varepsilon$  - strain ratio ( $=\varepsilon_{min}/\varepsilon_{max}$ )

$\dot{\varepsilon}$  - strain rate, in seconds to the power of minus one ( $S^{-1}$ )

### 4.2.1 Hysteresis loop

A hysteresis loop is a graphical projections of stress vs. strain. Usually this loop shows tension and compression, as this is the most usual way to test fatigue. For the test in this thesis a better representation of a hysteresis loop is shown in fig 3.1. Fig 3.1 shows that for each cycle in the plastic strain region gives a permanent elongation to the material. This is represented on the x-axis where one can see that as the cycles increase the start of each cycle has an off-set of the elongation that accumulated in the previous cycles. This is a time-based dependent system of a system's out-put and past inputs.

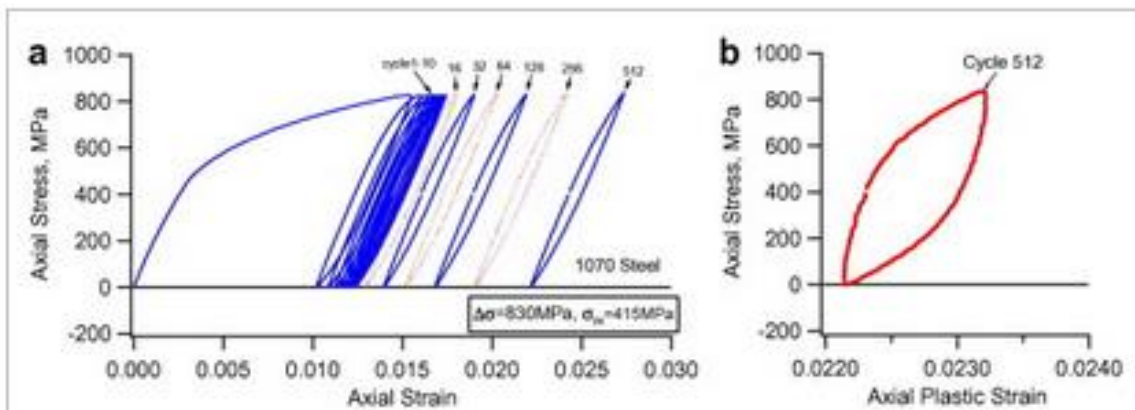


Figure 4-1 Illustration of a typical hysteresis loop (Jiang & Zhang, 2008)

ISO 12106 *Metallic materials - fatigue testing - axial-strain-controlled method*, has criteria's to machines being used for low cycle fatigue testing.

#### **4.2.2 Machine**

Point 5.1.1 in ISO 12106.

The standard referrers to tension-compression test, but since this test will be tension-tension the same guidelines will be applied but with exclusions where it is not applicable. The most important aspect in general is that the machine is designed for a smooth start up with no backlash when passing through zero. The machine should also have great lateral rigidity when the crosshead is in the operation position and accurate alignment between the test space references.

The complete machine loading system (including load cell, grips and specimen) shall have great lateral rigidity and be capable of controlling strain and measuring force when applying the recommended wave cycle. It may be hydraulic or electromechanical.

#### **4.2.3 Load cell**

Point 5.1.2

Load cell for this test shall be designed for tension-tension, and not tension-compression as stated in this point in the ISO. Main concern is that its capacity shall be suitable for the forces applied during the test.

The indicated force as recorded at the output from the computer in an automated system shall be within the specified permissible variation from the actual force. The load cell capacity shall be sufficient to cover the range of forces measured during a test to an accuracy better than 1% of the reading.

This test is not governed by temperature, and will be tested in room temperature in the laboratory at the University of Stavanger.

#### **4.2.4 Gripping of specimen**

##### Point 5.1.3

The gripping device shall transmit the cyclic forces to the specimen without backlash along its longitudinal axis. The distance between the grips shall be small to avoid any tendency of the specimen to buckle. Buckling is not relevant for this test, so this will be excluded. The geometric qualities of the device shall ensure correct alignment in order to meet the requirements specified in 5.1.4; it is therefore necessary to limit the number of components of which these gripping devices are composed and reduce the number of mechanical interfaces to a minimum.

The gripping device shall ensure that the way in which the specimen is mounted is reproducible. It shall have surfaces ensuring alignment of the specimen and surfaces allowing transmission of tensile and compressive forces without backlash throughout the duration of the test.

#### **4.2.5 Alignment check**

##### Point 5.1.4

The alignment shall be checked before each series of tests and any time a change is made to the load train. This section of ISO describes bending which is irrelevant to the test for this thesis.

#### **4.2.6 Strain measurements**

The strain shall be measured from the specimen using an axial extensometer.

The extensometer used shall be suitable for measuring dynamic strain over long periods during which there shall be minimal drift, slippage and instrument hysteresis. It shall measure directly the axial strain on the gauge section of the specimen.

The strain-measuring system, including the extensometer and its associated electronics, shall be accurate to within 1% of the range of strain applied.

The geometry of the contact zones and the pressure exerted by the extensometer on the specimen shall be such that they prevent slippage of the extensometer but do not damage to the specimen.

#### **4.2.7 Checking and verification**

The test machine and its control and measurement systems shall be checked regularly.

Specifically:

Each transducer and its associated electronics shall always be checked as a unit:

- the force-measuring system(s) shall be verified in accordance with the relevant ISO or national standard.
- the strain-measuring system(s) shall be verified in accordance with the relevant ISO or national standard

It is good practice before each series of tests to check the gauge length of the extensometer, the load cell and the extensometer calibration using a shunt resistor or another suitable method.

### **4.3 Specimens**

### **4.3.1 Geometry**

The gauge portion of the specimen in a low-cycle fatigue test represents a volume element of the material under study, which implies that the geometry of the specimen shall not affect the use of the results.

This geometry shall fulfill the following conditions:

- provide a uniform cylindrical gauge portion. This is not relevant for our specimens
- minimize the risk of buckling in compression to avoid failure initiation at the transition radius. Compression will not be a factor, but will be taken into account in the theoretical rewriting of tension-tension to tension-compression.
- provide a uniform strain distribution over the whole gauge portion.
- allow the extensometer to measure the strain without interference or slippage.

### **4.3.2 Flat products of thickness less than 5 mm**

The correct alignment of the specimen shall be carefully checked with a trial specimen for:

- parallelism and alignment of grips;
- alignment of specimen with the loading axis

This verification shall be carried out using a specimen, with a geometry similar as possible to that of the test specimen, instrumented with strain gauges on the two faces.

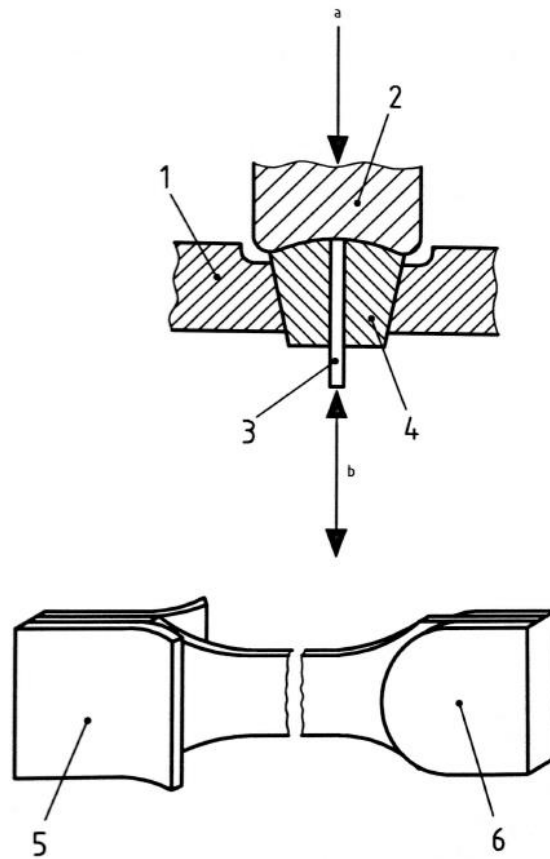


Figure 4-2 Illustration of grips (I. standard, 2003)

**Figure 6 - Gripping scheme for flat-sheet specimen p.13 ISO 12106**

**Key**

- 1. body of fixture
- 2. conical clamp
- 3. sheet specimen
- 4. conical chuck
- 5. bent end tabs to prevent grip indentation in gripping area (may be held in place by epoxy)
- 6. rounded end tabs

a clamping force

b cyclic load

## 4.4 Preparation of specimens

General guidelines from ISO 12106 are used to fabricate the specimens. Some reservations are necessary with regards to availability and limitations both at Rosenberg's location and the equipment at the University of Stavanger, but it will be sought to follow these guidelines to the best measure as possible. Also as the author's experience with fabrication is limited some errors is to be expected.

From ISO 12106 - *Metallic materials - Fatigue testing - Axial-strain-controlled method*.

### 4.4.1 General

In any low-cycle fatigue test programme designed to characterize the intrinsic properties of a material, it is important to observe the following recommendations in the preparation of specimens. A deviation from these recommendations is possible if the test programme aims to determine the influence of a specific factor (surface treatment, oxidation, etc) that is incompatible with these recommendations. In all cases, any deviation shall be noted in the test report.

#### **Machining procedure**

The machining procedure selected may produce residual stresses on the specimen surface likely to affect the test results. These stresses may be induced by heat gradients at the machining stage or they may be associated with deformation of the material or micro structural alterations. Their influence is less marked in tests at elevated temperatures because they are partially or totally relaxed once the temperature is maintained. However, they should be reduced by using an appropriate final machining procedure, especially prior to final polishing stage. For harder materials, grinding rather than tool operation (turning or milling) may be preferred.

- Grinding: from 0,1 mm of the final diameter at a rate of o more than 0,005 mm/pass
- Polishing: remove the final 0,025 mm with papers of decreasing grit size. It is recommended that the final direction of polishing be along the specimen axis.

NOTE 1 - Alteration in the microstructure of the material



This phenomenon may be caused by the increase in temperature and by the strain-hardening induced by machining. It may be a matter of a change in phase or, more frequently, of surface recrystallization.

The immediate effect of this is to make the test invalid as the material tested is no longer the initial material. Every precaution should therefore be taken to avoid this risk.

#### **4.4.2 Surface condition of specimen**

The surface condition of specimens has an effect on the test results. This effect is generally associated with one or more of the following factors:

- the specimen surface roughness;
- the presence of residual stresses;
- alteration in the microstructure of the material;
- the introduction of contaminants

The recommendations below allow the influence of these factors to be reduced to a minimum. The surface condition is commonly quantified by the mean roughness or equivalent (e.g. 10 points roughness or maximum height of irregularities). The importance of this variable on the test results obtained depends largely on the test conditions, and its influence is reduced by surface corrosion of the specimen or plastic deformation.

It is preferable, whatever the test conditions, to specify a mean surface roughness  $R_z$  of less than  $0,2 \mu\text{m}$  (or equivalent).

#### **4.4.3 Dimensional check**

The dimensions shall be measured on completion of the final machining stage using a method which does not alter the surface condition.

#### **4.4.4 Procedure**

The test procedure is explained in the following way by the (ISO 12106 *Metallic materials – Fatigue testing – Axial-strain-controlled method*. P 17)

The low cycle fatigue test is reasonably complex and the quality of the results obtained depends on the methods employed as well as on the environment.

The tests shall be carried out under suitable environmental conditions:

- uniform ambient temperature and relative humidity
- minimum atmospheric pollution (dust, chemical vapours, etc.);
- no extraneous electrical signals that will affect machine control and data acquisition
- minimum extraneous mechanical vibrations.

#### **4.4.5 Test machine control**

The stability of the servo-control shall be such that the peak values of the applied strain are maintained throughout the test within  $\pm 1\%$  of the desired values.

#### **4.4.6 Mounting of the specimen**

Place the specimen in position such a way that any preliminary strain during mounting is avoided.

#### **4.4.7 Cycle shape – Strain rate or frequency of cycling**

The same cycle shape for the controlled parameter (strain) shall be retained throughout the whole test programme unless the aim of this programme is to study the effect of the cycle shape on the behaviour of the material. A triangular cycle shape is normally used for continuous cycling tests.

Low-cycle fatigue tests are generally carried out with an imposed constant strain rate.

The range frequency for low-cycle fatigue tests is more often between 0,01 Hz and 1 Hz. In terms of the total strain rate, the majority of tests are carried out within the interval ranging from  $5 * 10^{-4} s^{-1}$  to  $5 * 10^{-2} s^{-1}$  ( $0,05\% s^{-1}$  to  $5\% s^{-1}$ )

## **4.5 Start of test**

### **4.5.1 Preliminary measurements**

It is recommended that testing begin by cycling within the elastic range of the material at ambient temperature in order to measure the modulus of elasticity of the material and ensure the correct functioning of the measuring system (force and strain). The value of this modulus shall not deviate by more than  $\pm 5\%$  from the expected value.

### **4.5.2 Number of specimens**

A minimum of eight specimens is recommended to generate a fatigue strain-life curve covering at least three decade in numbers of cycles

### **4.5.3 Data recording**

The gathering of data from the testing will be done in accordance with ISO 12106 *Metallic material – Fatigue testing – Axial-strain-controlled method*.

At the start of the test, a continuous recording shall be made of the initial hysteresis loops – stress response as a function of the controlled strain. Then, during the course of the test, a periodic recording is sufficient. The frequency of these recordings shall be chosen as a function of the intended overall duration of the test. The option generally used consists of recording the first ten cycles and then applying a logarithmic increase (20, 50, 100, 200, 500, etc.)

In the case of automated data acquisition, the recording of loops may be programmed either with a predefined interval or as a function of the progression of each of the two parameters (stress and strain). In all cases, the sampling frequency shall be sufficient to allow clear definition of the hysteresis loop.

#### 4.5.4 Data acquisition

If test equipment permits, record stress, strain and temperature as functions of time. If this is not possible, at least record peak values of stress, strain and temperature so that the definition of failure may be invoked. Since the test in this thesis does not concern temperature, the temperature part will be excluded.

#### 4.5.5 Failure criteria

There are various ways of defining a failure, with total separation of the specimen being only one of these. It may depend on the interpretation of the fatigue test result and on the nature of the material being tested. The failure criteria under consideration are generally based on the appearance, presence of intensification of a phenomenon that has been observed or recorded that indicates severe damage or imminent failure of the specimen.

The number of cycles to failure,  $N_f$ , may be defined as the number of cycles corresponding to the following failure criteria:

- a) total separation of the specimen into two distinct parts;
- b) a certain percentage change in the maximum tensile stress in relation to the level determined during the test;
- c) a certain change in the ratio of the moduli of elasticity in the tensile and compressive part of the hysteresis loops; typically,  $E_T/E_C = 0,5$  is employed for defining failure;
- d) a certain percentage change in the maximum tensile stress in relation to the maximum compressive stress.

c), and d), will not be applicable for this test,

The use of criteria a) and b) is the most common. However, any of the above criteria can be used for failure. The specific failure criteria used for the test series shall be reported.

In all cases, the location of the failure in relation to the gauge length shall be identified and shall appear in the test results.

A post-test examination of the specimen shall be conducted in order to ensure the validity of the test. This means checking on the one hand for the correct location of the failure or main cracks and, on the other, ensuring the absence of faults or anomalies which could lead to

incipient and premature failure (surface faults, porosity, inclusions, excessively large imprints left by the extensometer or bending of the specimen related to an alignment problem).

#### **4.5.6 End of test**

The test is terminated when the conditions for the selected end-of-test criterion is fulfilled where the test machine is equipped with facilities allowing this criterion to be applied. If this is not the case, there shall be other possibilities for stopping the machine, either when a force threshold values is no longer reached (generally, a low fraction of full scale depending on the range) or, using the control signal, when the deviation between the command signal and the feedback signal reaches a certain value.

It is desirable that a test should not be automatically terminated by inappropriate preselection of stress limits, for example in the case of continuous cyclic softening. It is recommended in such cases that material response be observed prior to selection of stress limits and, in fact, a *post facto* determination of the number of cycles to failure may be necessary.

If the test terminates automatically prior to total failure of the specimen, the data shall be reviewed prior to specimen removal to ensure that the failure criterion has been achieved. If premature termination has occurred, then the test can be restarted. If the failure criterion has been met, then force control shall be re-established and zero force set for cool-down and specimen removal. If the specimen failure was “complete separation”, then the normal procedure would be to switch to “position-control” for cool-down and specimen removal.

## 5 Preparation of test specimens

Together with Rosenberg Worley Parson AS, the members were made using standard hot-rolled S355 carbon steel with yield strength of 355 MPa. Four plates were cut to the measurements 200mm x 90mm x 8mm.



*Figure 5-1 & Figure 5-2 Pre weld steel plates*

They were then welded together using Tungsten 141 weld. This was all done by the personnel at the welding school at Rosenberg. With high expertise a seamless weld was made. See the appendix A for the welding procedure. The plates were prepared for a double butt weld by making grooves with an angle grinder. A double butt weld was used to make sure that the weld was fully penetrated. During the welding the heat and the fact that the plates were welded from both sides caused some displacement.

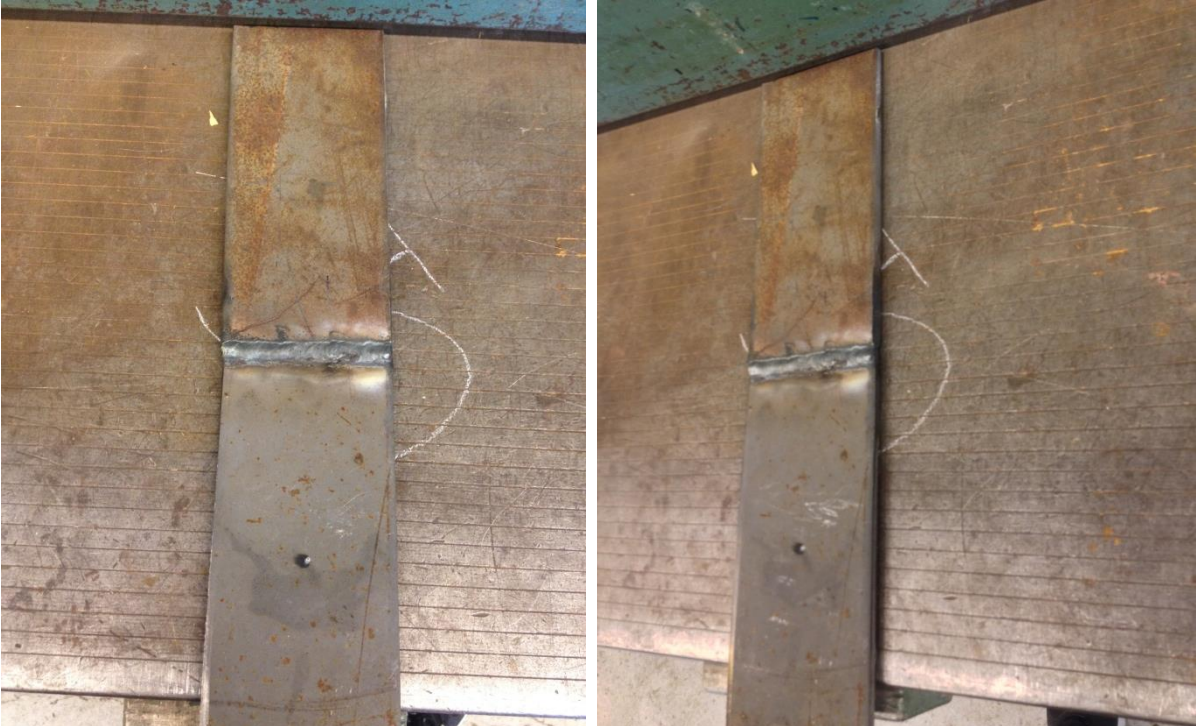


*Figure 5-3 & Figure 5-4 Post weld plates*

Using a clipping machine the welded plate was cut to more manageable length. From 400 mm (some reduction in the length happened due to the welding), the plate was now measured to be approximately 140 mm after the cut.

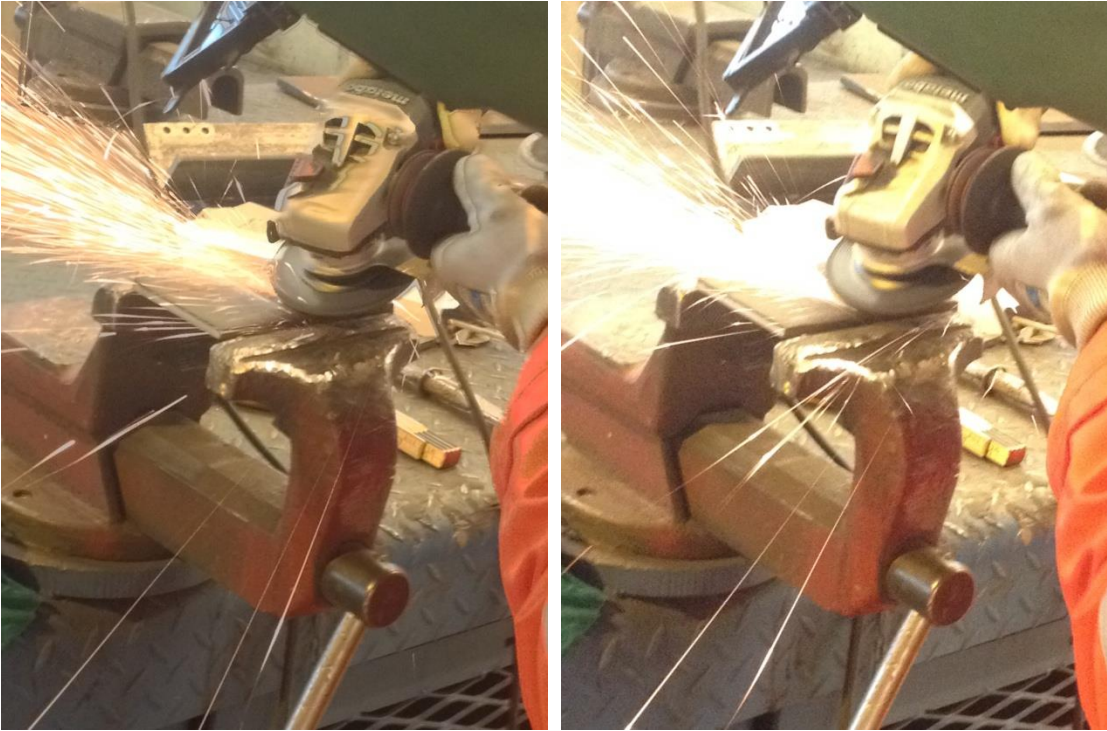




Figure 5-5, Figure 5-6 & Figure 5-7pre and post cut of welded plates



The weld needed to be grinded down and smoothed out, and this was done using a grinder. Because of the thickness of the plate and the width of the plate, machine cutting was not an option. The plates was divided into 15 members, and with the help of experienced personnel at Rosenberg the members were cut using an angle grinder.



*Figure 5-8 & Figure 5-9 Grinding of weld*

Precaution was necessary with regards to the cutting. The temperature rises quickly during the cutting process, and to avoid much change in the micro structure in the steel itself each member was cut in 10 minute intervals.



*Figure 5-10 & Figure 5-11 Cutting of specimens*

To avoid eccentricities with regards to the fatigue test, the mill in the machine laboratory at the University of Stavanger was used. The dimensions was corrected to approximately 8mm x 4.97 mm. The 15 members differs a small amount.



*Figure 5-12, Figure 5-13 & Figure 5-14 Pre milled specimen and milling of specimen*

# 6 Fatigue test

## 6.1 Background for fatigue test

It is desirable to study the effect of high strain levels on corroded and non-corroded standard off shore steel S355 with regards to LCF and ULCF. It is sought to follow ISO/DIS 12106 described above as well as reasonably practicable. It is desirable to check if this method can be used for tension-tension tests. The specimens have been subjected to six weeks corrosion, where the weld and parts of the base material has been left with no protection to simulate a breach in the coating of a welded steel joint. The aim is to see if the corroded specimens have a significant effect on the integrity of the welded joint, under the influence of high strain compared to non-corroded specimens.

The tests are conducted at the new laboratory at the University of Stavanger. pH measurements of the electrolyte (sea water) was measured weekly. During the course of 6 six weeks this was stable at approximately 8, meaning no change from start to finish of the corroding process. The specimens will be tested in ambient room temperature, in the Zwick Z020 tensile machine [Appendix A]. This machine is designed for tensile testing, but has certain master programs making it possible to test the specimens cyclically. An S-N curve will be presented for the strain levels, but again due to the limitations of the machine, this S-N curve will have limitations in its applicability. The curve will represent 3 individual test on 3 determined strain levels, with the test parameter of corrosion in either sea water or close to sea air. One non-corroded specimen, one corroded in sea water and one corroded in air close to the sea. So the number of tests for each parameter and strain level is not sufficient to present a valid S-N curve. Two extra sea water corroded, and two extra close to sea air specimens will be tested on the highest stress value. The highest stress values should correspond to the strain levels chosen. This is to recognize the difference of fatigue life due to the interaction effect of corrosive environment and uncertainties behind the process.



### 6.1.1 Material

As mentioned in chapter 5, the specimens are made using standard low-carbon steel. The steel is chosen as S355 since this is the most commonly used steel type for off shore constructions. From tensile tests done on low carbon steel, the average Young's modulus has been set to have the value 210 GPa. Obtained from NS-EN 1993-1-1:2005+NA:2008 (N. Standard, 2008)

#### Chemical composition of low-carbon steel

*Table 6-1 Chemical composition of low carbon steel*

Grade	C%	Mn%	P%	S%	Si%
S355	0.23 max	1.60 max	0.05 max	0.05 max	0.05 max

C – Carbon

Mn – Manganese

P – Phosphorus

S – Sulfur

Si – Silicon

Low-carbon steels contain up to 0,30 % Carbon. S355 steel usually has a maximum content of 0,23%. For steels containing 0,30% Carbon there is usually a Manganese content up to 1,5%. The usual application of these steels are stampings, forgings, seamless tubes and boiler plates. (Material, 2001)

## 6.1.2 Test machine

The test is conducted on the Zwick Z020 tensile machine.

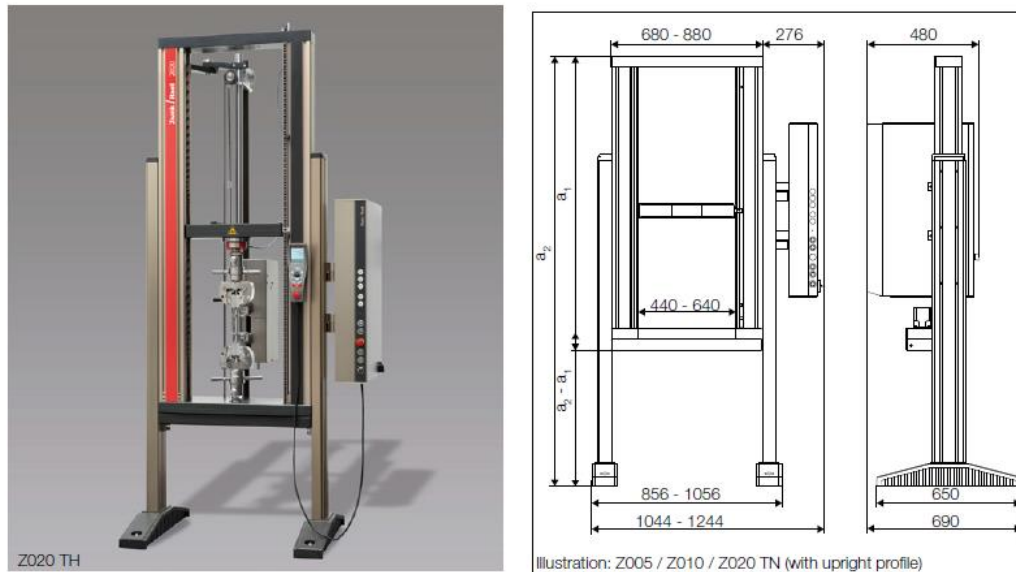


Figure 6-1 Illustration of test machine dimensions

## Machine specifications [Appendix C]

PI 284 2.1014\_sheet 2

Type	Z005 TH	Z005 TE	Z005 TNW	Z010 TH	Z010 TE	Z010 TNW	Z010 TH	Z010 TE	Z010 TNW	Z010 TH	Z010 TE	Z010 TNW
Item number	1000473	1000476	1000475	1000477	1000479	1000481	1000483	1000480	1000482	1000484	1000485	1000486
<b>Load frame</b>												
Test load $F_N$ in tensile / compression direction	5	5	5	5	5	10	10	10	10	10	10	10
Test area width	440	440	440	640	640	440	440	440	640	640	640	640
Height of the lower test area, without accessories	1030	1430	1785	1000	1400	1030	1430	1785	1000	1400	1755	
Height of the upper test area, without accessories /supplern. crosshead required	1015	1415	1785	1015	1415	1015	1415	1785	1015	1415	1785	
Height without leg profiles (a.)	1314	1714	2084	1324	1724	1314	1714	2084	1324	1724	2094	
Height with leg profiles (a.)	1528 ... 2108	1868 ... 2508	2238 ... 3078	1538 ... 2118	1878 ... 2518	1528 ... 2108	1868 ... 2508	2238 ... 3078	1538 ... 2118	1878 ... 2518	2248 ... 3088	
Width without leg profiles	680	680	680	880	880	680	680	680	880	880	880	
Width with leg profiles (and electronics console)	856 (1044)	856 (1044)	856 (1044)	1056 (1244)	1056 (1244)	856 (1044)	856 (1044)	856 (1044)	1056 (1244)	1056 (1244)	1056 (1244)	
Depth without leg profiles <sup>14</sup>	573	573	573	573	573	573	573	573	573	573	573	
Depth with leg profiles <sup>14</sup>	690	690	690	690	690	690	690	690	690	690	690	
Overall weight with electronics console, without leg profiles	161	183	205	208	230	163	185	207	210	232	254	
Noise level at maximum test speed	67	67	67	67	67	64	64	64	64	64	64	
<b>Drive system</b>												
Crosshead speed up to 110% of test load ( $V_{min} \dots V_{NOM}$ )	0.0005 ... 3000	0.0005 ... 3000	0.0005 ... 3000	0.0005 ... 3000	0.0005 ... 3000	0.0005 ... 2000	0.0005 ... 2000	0.0005 ... 2000	0.0005 ... 2000	0.0005 ... 2000	0.0005 ... 2000	
Increased crosshead return speed (at reduced force)	3000	3000	3000	3000	3000	3000	3000	3000	3000	3000	3000	
Drive system's travel resolution	0.95943	0.95493	0.95493	0.95943	0.95943	0.63663	0.63663	0.63663	0.63663	0.63663	0.63663	
<b>Power ratings</b>												
Electrical connections <sup>2</sup>	230	230	230	230	230	230	230	230	230	230	230	
Power rating	2	2	2	2	2	2	2	2	2	2	2	

<sup>1</sup> Leg profiles are included in the scope of supply of this materials testing machine.  
<sup>2</sup> Power supply: 230 V +/- 10% (1Ph, N, PE), 50/60 Hz.  
<sup>14</sup> Inclusive electronics console.  
<sup>14</sup> Inclusive base support (60 x 30 mm rectangular tube) with 210 mm front overhang.

Product Information  
Table-top machines Z005 up to Z020 of the Allroundline

Zwick / Roell

Zwick Materials Testing

Figure 6-2 Machine specifications

The machine is driven by an alternating current servo-motor with concentrated windings Hiperface® motor feedback system. The cross head has a repositioning accuracy of  $\pm 1 \mu m$ .

The machine is controlled by a software called TestXpert (Z. International, 2015). The software is user friendly, where the objective of the software is to reduce the training required to be able to do tests with the machine. The software provides a wide range of measurement methods, whether it be stress/strain, stress/number of cycles to failure etc.



*Figure 6-3 & Figure 6-4 Test machine's grips*

Tensile capacity of the machine is 20 kN. Clamps will be fastened to the load train, and the specimens are attached between both clamps.



*Figure 6-5 Specimen placed in machine's grips*

The available grips at the laboratory are shown in figure 5-4. These grips can be compared to a vice. This means that the grips need to be tightened by hand. These types of grips are not the best when it comes to fatigue testing. They are usually used for tensile test. Which means that the grips keep a tight grip while force is applied, but when this force is going down towards zero the grips tend to loosen their grip. It does not release its grip fully, but the amount it does could give problems with regards to the recording of strain and elongation. Grips that would be preferable in a tension-tension test would be hydraulic grips. This would ensure a tight grip in both directions of loading, from start of cycle to end of cycle.



### 6.1.3 Code guidelines for cyclic loading

DNV RP-C208 - *Determination of Structural Capacity by Non-linear FE analysis Methods.*

This document is intended to give guidance on how to establish the structural resistance by use of non-linear FE methods. The use of finite element methods (FE) is not applied in this thesis, but the standard supplies coefficients and exponents used for determining the stress and strain values that will be applied in the fatigue test.

DNV GL RP-0005 *Fatigue design of offshore steel structures.*

This Recommended Practice presents recommendations in relation to fatigue analyses based on fatigue tests and fracture mechanics. This standard will be used to obtain the details categories that needs to be determined in order to be able to decide if it is the weld or the base material that is most likely to suffer failure during the fatigue test.

Strain values will be estimated using equations from DNV RP C-208.

Due to the testing machine Zwick Z020's limitations the strain will be substituted with stress. This is done in the following way. Since one strain cycle takes on average 350 seconds ( 5,83 minutes), the peak stress value (maximum stress) in this cycle will be used as stress during the test. It is done this way to be able to complete the tests in a reasonable time period. This will give a constant strain amplitude with a strain accumulation. Since the strain cycle takes 350 seconds, it can reach the appointed strain value at relative low stress. When then applying this stress in a much shorter cycle the specimen will not receive the same amount of strain, but there will be a strain accumulation during the course of the tests. This accumulation will be shown with ever increasing increments of strain. This could result in significantly higher number of cycles to failure, but due to the limitations of the facilities at University of Stavanger, this is the way it has to be executed to obtain fatigue life for each specimen.

From table A1 in figure 5-6 in DNV GL RP-005 detail category B2 is chosen for the base material. The category for the weld was chosen as detail category E from table A-5 in figure 5-5.

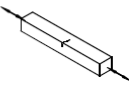
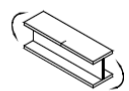
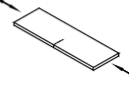
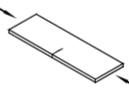
Table A-1 Non-welded details			
Notes on potential modes of failure			
In plain steel, fatigue cracks will initiate at the surface, usually either at surface irregularities or at corners of the cross-section. In welded construction, fatigue failure will rarely occur in a region of plain material since the fatigue strength of the welded joints will usually be much lower. In steel with bolt-holes or other stress concentrations arising from the shape of the member, failure will usually initiate at the stress concentration. The applied stress range shall include applicable stress concentration factors arising from the shape of the member.			
Reference is made to section 2.4.19 for non-welded components made of high strength steel with a surface finish $R_a = 3.2 \mu\text{m}$ or better.			
Detail category	Constructional detail	Description	Requirement
B1	1. 	1. Rolled or extruded plates and flats	1. to 2. — Sharp edges, surface and rolling flaws to be improved by grinding — For members that can acquire stress concentrations due to rust pitting etc. curve C is required.
	2. 	2. Rolled sections	
B2	3. 	3. Machine gas cut or sheared material with no drag lines	3. — All visible signs of edge discontinuities should be removed. — No repair by weld refill. — Re-entrant corners (slope $\geq 1:4$ ) or aperture should be improved by grinding for any visible defects. — At apertures the design stress area should be taken as the net cross-section area.
C	4. 	4. Manually gas cut material or material with machine gas cut edges with shallow and regular draglines.	4. — Subsequently dressed to remove all edge discontinuities — No repair by weld refill. — Re-entrant corners (slope $\geq 1:4$ ) or aperture should be improved by grinding for any visible defects. — At apertures the design stress area should be taken as the net cross-section area.

Figure 6-6 Table A-1 detail category of non-welded details (Veritas, 2014)

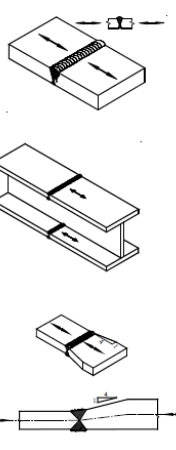
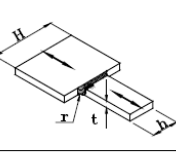
Table A-5 Transverse butt welds, welded from both sides (Continued)			
Detail category	Constructional detail	Description	Requirement
E	7. 	7. Transverse splices in plates, flats, rolled sections or plate girders made at site. (Detail category D may be used for welds made in flat position at site meeting the requirements under 4, 5, and 6 and 100% MPI of the weld is performed.)	7. — The height of the weld convexity not to be greater than 20% of the weld width. — Weld run-off pieces to be used and subsequently removed, plate edges to be ground flush in direction of stress.
	8. 	8. Transverse splice between plates of unequal width, with the weld ends ground to a radius.	
F1	$\frac{r}{h} \geq 0.16$		
F3	$\frac{r}{h} \geq 0.11$		

Figure 6-7 Table A-5 Detail category welded parts (Veritas, 2014)

From table A-5, it is indicated that the crack will form in the base material. This is due to the heat affected zone (HAZ) in relations with the welding process. The HAZ is the part of the base material that has been indirectly influenced by the weld. The temperature that has risen during the weld and has led to heating of the base material around the weld. This process alters the microstructure and properties of the material. Due to this it is the base material that will experience the stress concentration, and therefore will be likely point of fracture when the fatigue test is implemented on the specimens.

Also by milling the specimens, some small notches and other small imperfections has occurred. Since there is a significant larger portion of base material than weld, it is reasonable to expect them to have a bigger effect on the base material than the weld.

ISO 12106 *Metallic materials - fatigue testing - axial-strain-controlled method* explains LCF testing with equations given in Table 5-2 below. The coefficients and exponents are obtained from DNV RP-C208. For the purpose of the fatigue test in this thesis, the total strain (Eq. 5-1) is substituted with maximal principal strain range. Given as equation 5-2.

$$\frac{\Delta\varepsilon}{2} = \frac{\sigma'_f}{E} (2N_f)^b + \varepsilon'_f (2N_f)^c \quad \text{Eq. 6-1}$$

$$\text{Eq. 14 DNV} \quad \frac{\Delta\varepsilon_l}{2} = \frac{\sigma'_f}{E} (2N)^{-0,1} + \varepsilon'_f (2N)^{-0,43} \quad \text{Eq. 6-2}$$

$$\text{Eq. 13 DNV} \quad \frac{\Delta\varepsilon_{hs}}{2} = \frac{\sigma'_f}{E} (2N)^{-0,1} + \varepsilon'_f (2N)^{-0,5} \quad \text{Eq. 6-3}$$

## Low-cycle fatigue test - fatigue life

Table 6-2 Low cycle fatigue test – fatigue life

Property	Determination	Relation
$\sigma_f$ , fatigue ductility coefficient	Stress intercept at $2N_f = 1$ on $\lg \sigma_a - \lg 2N_f$ plot	$\sigma_a = \sigma'_f(2N_f)^b$ (Basquin equation)
$b$ , fatigue strength exponent	Slope of $\lg\left(\frac{\Delta \varepsilon_e}{2}\right) - \lg 2N_f$ plot (Specify $2N_f$ range)	
$\varepsilon_{f,p}$ , fatigue ductility coefficient	Plastic-strain intercept at $2N_f = 1$ on $\lg\left(\frac{\Delta \varepsilon_e}{2}\right) - \lg 2N_f$ plot	$\frac{\varepsilon_p}{2} = \varepsilon'_f(2N_f)^c$ (Coffin-Manson equation)
$c$ , fatigue ductility exponent	Slope of $\lg\left(\frac{\Delta \varepsilon_e}{2}\right) - \lg 2N_f$ plot (Specify $2N_f$ range)	
Total strain amplitude	$\frac{\Delta \varepsilon_t}{2} = \frac{\Delta \varepsilon_e}{2} + \frac{\Delta \varepsilon_p}{2}$ $\frac{\Delta \varepsilon_t}{2} = \left(\frac{\sigma'_f}{E}\right)(2N_f)^b + \varepsilon'_f(2N_f)^c$	

By this, the strain is chosen from Eq. 6-2 instead of Eq. 6-3 from the DNV RP-C208 standard which considers fatigue of weld. The Ramberg-Osgood relation gave the following strain values. The values of K is determined from Table 6-3 in DNV RP-C 208.

Table 6-3 Ramberg-osgood relation

Ramberg-Osgood relation parameters for base material	
Grade	K (MPa)
S235	410
S355	600
S420	690
S460	750

Ramberg-Osgood:

$$\varepsilon = \frac{\sigma}{E} + \left(\frac{\sigma}{K}\right)^{10}$$

Eq. 6-4

Table 6-4 Stress/strain values for test

stress	strain
<b>360</b>	<b>0,007761</b>
370	0,009714
380	0,012193
<b>390</b>	<b>0,01532</b>
400	0,019246
410	0,024151
420	0,030248
430	0,037789
440	0,047075
450	0,058456
460	0,072347
470	0,089227
402	0,020143
<b>405</b>	<b>0,021564</b>

This was compared to Eq. 6-2 from DNV RP-C208. This formula is a summation of elastic and plastic strain, and gives an estimation of half-strain cycle to failure on base materials in welded steel joints of common offshore steel. The formula predicts number of cycles to failure from a designated strain. The Ramberg-Osgood equation was implemented when choosing reasonable numbers of cycles to failure with regards to the time consuming tests on the Zwick Z020. It was also necessary to get a spectre of strain that can cover both LCF and ULCF.

The number of cycles to failure,  $N$ , for base material due to repeated yielding is estimated by solving the following equation. Newton-Raphson's method is used to estimate number of cycles to failure, where 1 cycle is the increment. Table 6-5 gives the following parameters for welded steel joints which is collected from DNV RP-C208.

Table 6-5 Parameters for Eq. 6-2

Data for low cycle fatigue analysis of welded steel joints
--

Environment	$\sigma'_f$	$\varepsilon'_f$
Air	175	0.095
Sea water with cathodic protection	160	0.060

As mentioned in the description of Table 6-3. The total strain amplitude is substituted. This is substituted with formula Eq. 6-2 from DNV RP-C208, and the  $\Delta\varepsilon_l$  represents the maximum principal strain range.

Results from Ramberg-Osgood implemented in Eq. 6-2 from DNV RP-C208

Table 6-6 Results from Ramberg-Osgood implemented in Eq.6-2

stress	strain		N	seawater	air
		VS	1	0,04302	0,068257
<b>360</b>	<b>0,007761</b>		<b>5</b>	<b>0,021783</b>	0,034415
370	0,009714		6	0,020175	0,031855
380	0,012193		7	0,01891	0,029841
<b>390</b>	<b>0,01532</b>		8	0,01788	0,0282
<b>402</b>	<b>0,021564</b>		9	0,017018	0,026829
410	0,024151		10	0,016284	0,02566
420	0,030248		11	0,015647	0,024647
430	0,037789		<b>12</b>	<b>0,015088</b>	0,023758
440	0,047075		13	0,014592	0,022968
450	0,058456		<b>15</b>	0,013746	<b>0,021623</b>
			<b>35</b>	0,009671	<b>0,015142</b>
			<b>60</b>	<b>0,007747</b>	0,012086
			<b>177</b>	0,004992	<b>0,007718</b>
			1200	0,002356	0,003553
			1300	0,002285	0,003442
			1400	0,002222	0,003342
			1500	0,002165	0,003252

Table 6-7 below represents the values that produces the S-N curve when applying the above equations from DNV and strain levels. It implies that the stress governs the number of cycles

required to impose a failure in a situation of high stress. The curves cover the low cycle fatigue spectrum of a whole S-N curve.

Estimated SN-Curve for corroded specimens in sea water and close to sea air based on the strain values calculated from Ramberg-Osgood and Eq. 6-2 from DNV RP-C208.

Table 6-7 Estimated number of cycles to failure on sea water corroded specimens from DNV

N	Stress
12	405
24	390
120	360
34	405
68	390
354	360

Red representing corroded in sea water and blue representing corroded in close to sea air

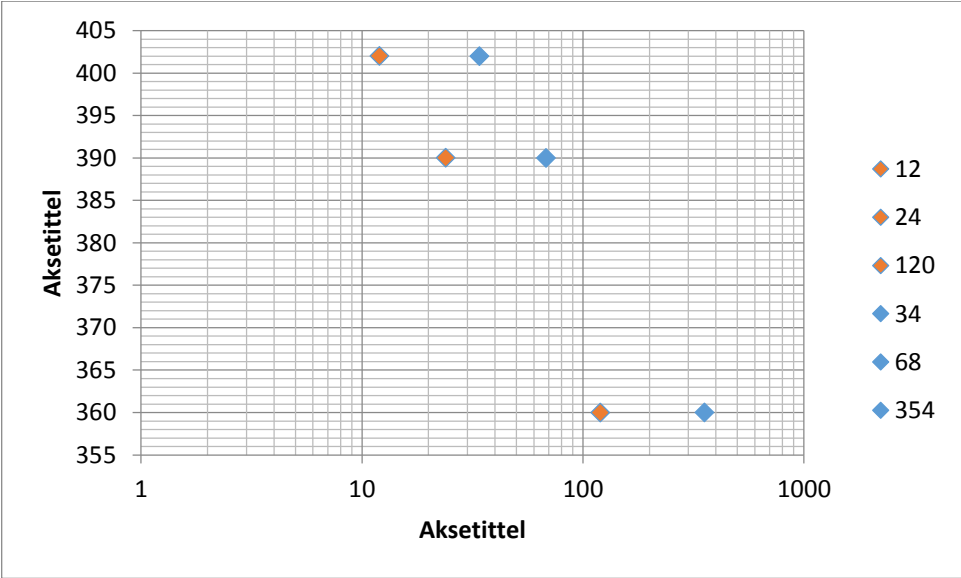
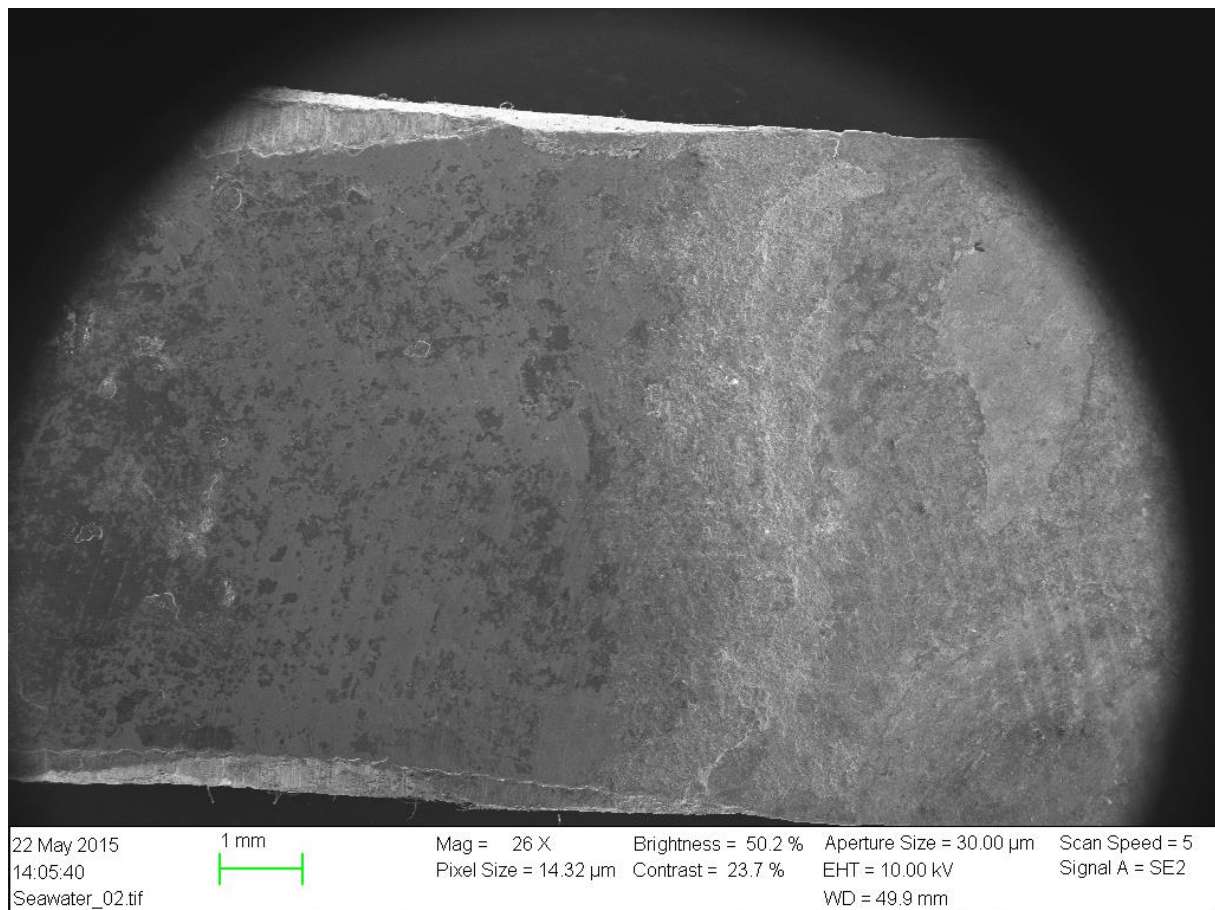


Figure 6-8 Calculated values from DNV sea water and close to sea air

## 6.2 Surface conditions of corroded specimens

Due to the fact that all the specimens were all made from the same material, the same weld was used, and the same procedure was followed on all the specimens with regards to milling one specimen was chosen to represent all the specimens exposed to sea water. It was also planned to check the surface condition of the specimens exposed to air, but the process of removing the oxide (rust) showed to be harmful to the surface condition. On these specimens, as opposed to the sea water corroded specimens, the oxide had dried. It proved to be impossible to remove the oxide by alcohol only. A finely grained sandpaper was tried, but started to make scratches in the surface. It was then decided to only use the SEM on the sea water exposed specimens, due to the fact that this, in theory, should be the most aggressive environment exposed to the specimens.



*Figure 6-9 Surface of sea water corroded specimen*



From this picture one can notice the marks left by the milling machine. The one thing that is odd by this is the fact that they seem to be going the opposite way of each other. The milling procedure was done with the milling head rotating in the same direction. In the process of shaping the specimens the specimen was moved around, but the marks left by the previous round of milling should be removed by the last milling round. Regardless of which way the marks go.

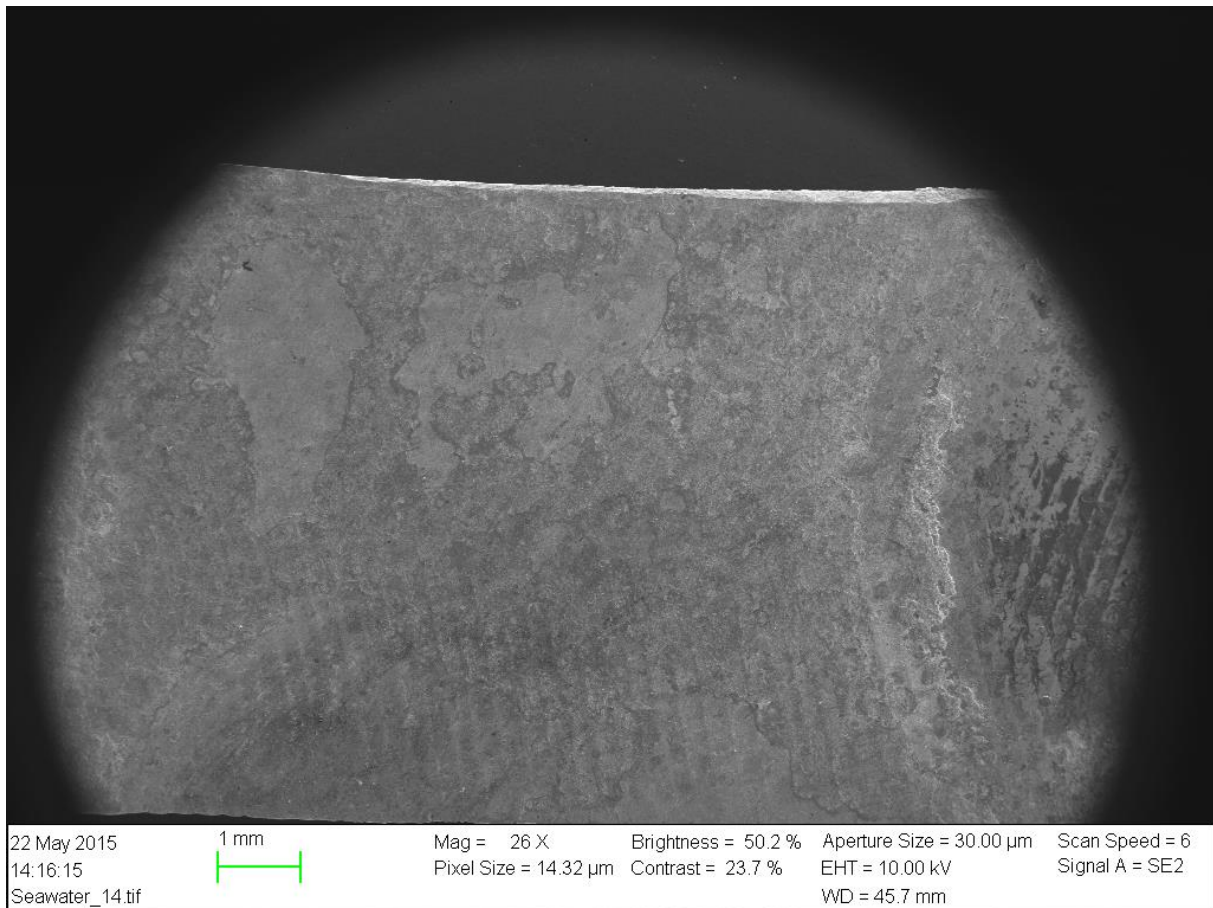


*Figure 6-10 Surface of sea water corroded specimens, milling marks*

One can also see this clearer on this picture. Some oxide can also be seen on this picture. Notice the section where the specimen gets darker, here one can clearly see that the scratches from the milling. The height of these scratches couldn't be determined by the examination of the specimens through the SEM. It was possible to determine the distance between the scratches using the SEM. This can be seen on the pictures below. The oxide on the left side of the dark area, is also the interface between the base material (S355) and the weld. This is where the oxide has had its most significant impact, as expected.

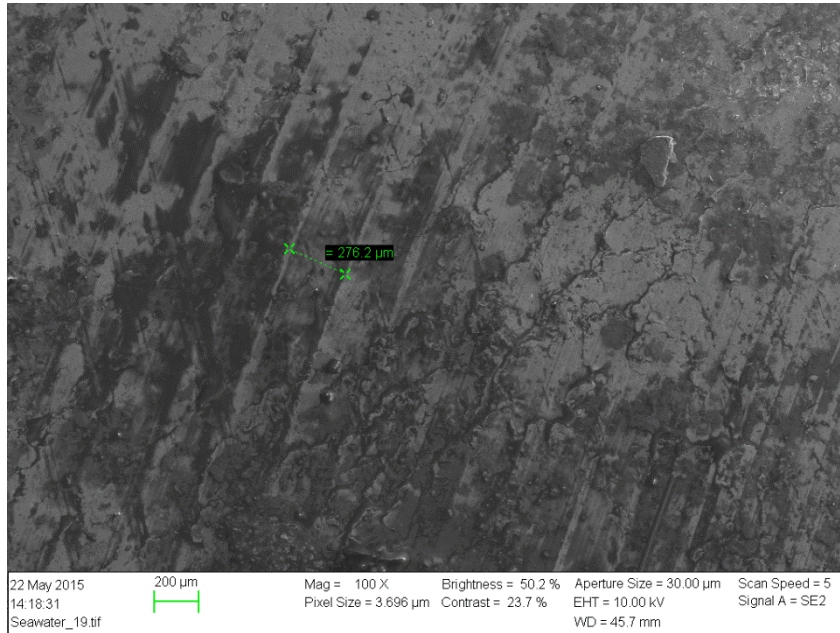


Figure 6-11 Higher magnification of longest milling marks

This picture shows the distance, measured in micro meters( $\mu m$ ). The scratches with the biggest distance had a distance of approximately 276.2  $\mu m$ .

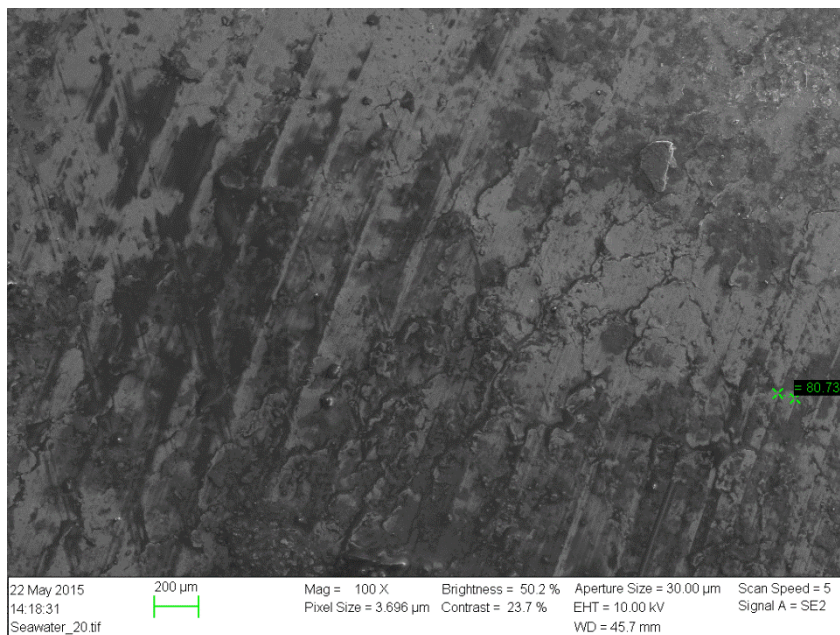


Figure 6-12 Higher magnification of shortest milling marks

The distance between the scratches with the shortest distance was measured to be approximately 60.73  $\mu m$ . The reason for this could originate from the milling process with regards to resistance in the material when milling. For instance more material would again cause more resistance,

and cause the milling head's advance to slow down. This would then make the mill head have rotations, but not the advance forward as it would have were the resistance was less.

Another reason could be the actual speed of the mill head, but this is unlikely since the speed was set at 340 rpm for the milling process of all the specimens.

An investigation of pitting corrosion was done by zooming in at different areas of the exposed surface. One particular area was of significant interest and is shown on the picture below.

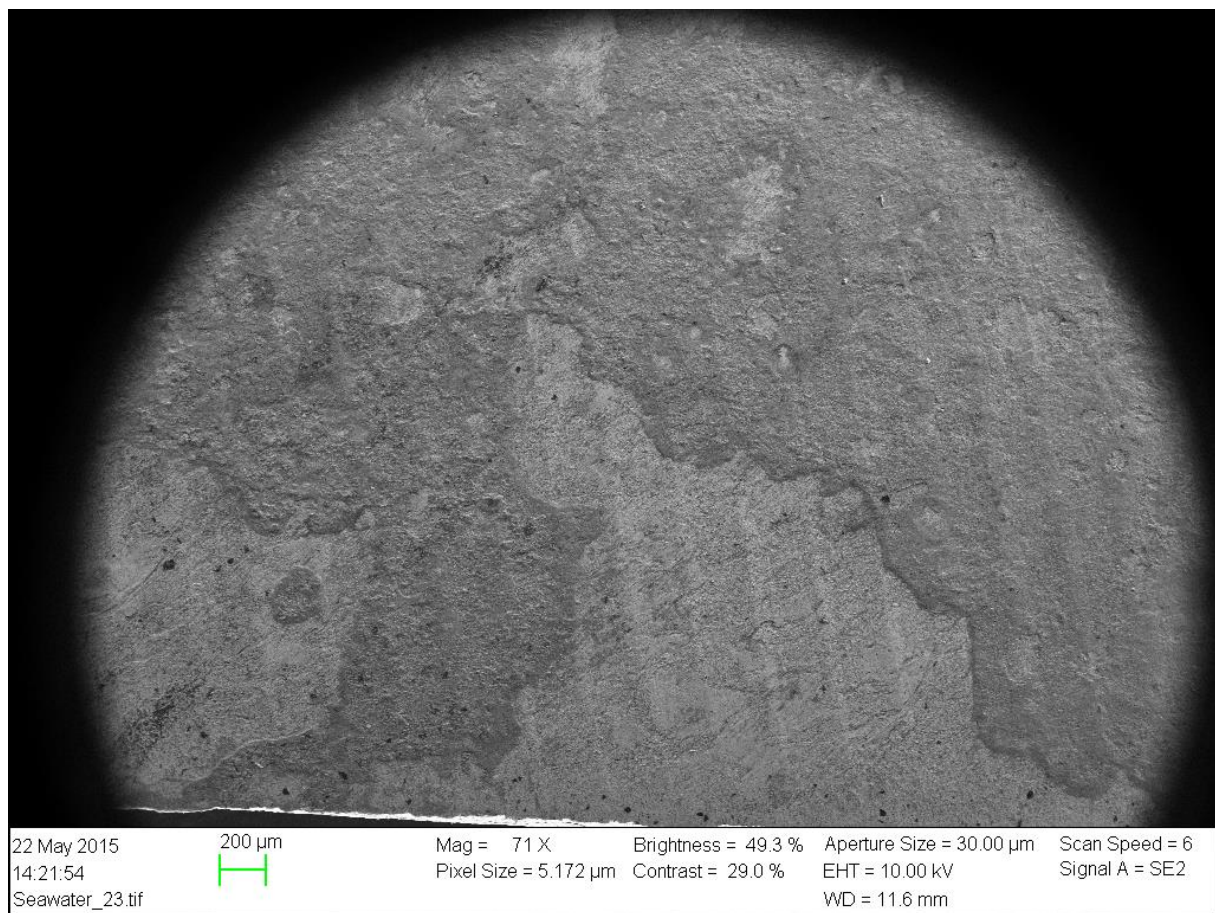


*Figure 6-13 Pitting corrosion*

On the bottom side of the specimen on this picture on can see darker circles in the surface. This could represent pitting corrosion. This is though difficult to determine, and actually present it as pits caused by pitting corrosion cannot be confirmed. By increasing the magnifying the laboratory technician was able to take a measurement of the pit's largest diameter.



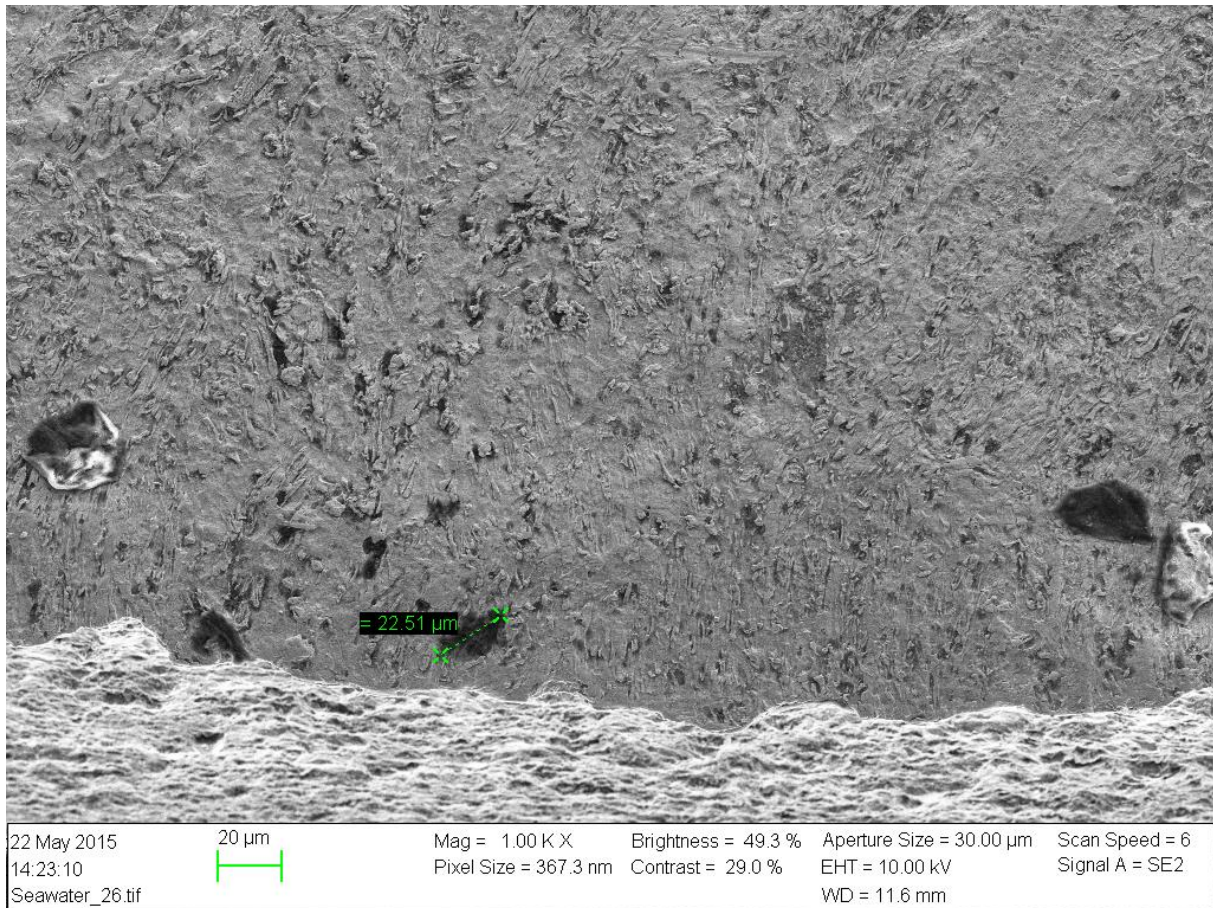
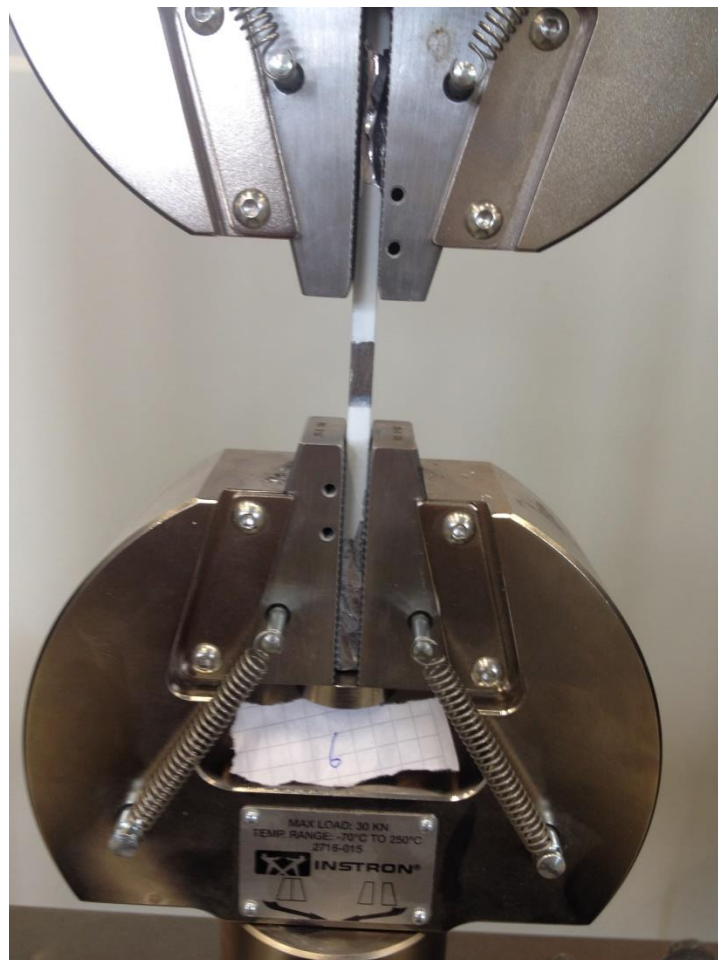


Figure 6-14 Higher magnification and measurement of pitting corrosion

As stated in chapter 2.2 the depth of a pit can be estimated to be as deep as the diameter. This is just the assumption. From this the largest depth of the alleged pit on the picture would be  $22.51 \mu m$ . If it is a pit, the depth can vary from 0 to  $22.51 \mu m$ . It can also vary in the direction of which it is going. Refer picture of types of pitting corrosion in chapter 2.6. Though it cannot be confirmed as a pit, if the assumption is made that this is a pit, it shows the danger of pitting corrosion. The specimen has only been subjected to the corrosive environment for 4 weeks at this point. One can only imagine the effect one year can have on this type of corrosion.

### 6.3 Fatigue test of specimens

The purpose of testing the specimens is to check if corrosion has any significant effect on the number of cycles to failure with the same stress levels. 3 Non-corroded specimens and 6 corroded specimens were tested on three specific stress levels. As mentioned above they were estimated from equations in DNV RP-C208. Usually an S-N curve is obtained by testing multiple specimens on the same stress or strain level. Reasoning for not testing several specimens on the same stress level has been explained earlier with regards to limitations of equipment available at the laboratory.



*Figure 6-15 Testing of specimen, pre necking*

Set up of the specimens in the testing machine. Shows that there is little, if any, misalignment of the specimen, assuring a tensile test where the stress will be uniformly distributed.

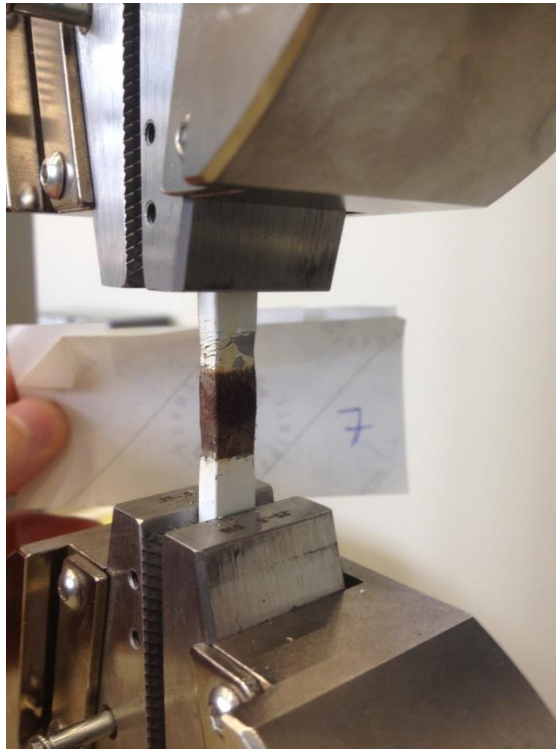


*Figure 6-16 Necking of specimen*

Necking of the specimen starts to occur, and as the cycles increase this becomes more and more visible. This indicates that the voids are starting to coalesce, and fracture is imminent.



*Figure 6-17 Fracture of specimen*

Fracture of specimen. Notice the necking on both sides of the weld. The base material as suspected has suffered the most loss of cross sectional area, and then suffered a total separation.

Real S-N curves compiled of the experimental data obtained from the fatigue test.

Table 6-8 Obtained number of cycles to failure from fatigue test

Sea water		Close to sea air	
N	Stress	N	Stress
93	397,83809	101	400,976816
613	375,201109	627	380,289577
995	358,528179	1234	361,159723

Two S-N curves. One for the sea water corroded specimens and one for the specimens whom has been subjected to humid air approximately 60 meters from the sea. Each curve represents the results of tests on the specified corrosive environment it was exposed to. Of important notice is the amount of cycles needed to produce failure in the true application of the principals stated in the DNV standards used. Reasons for the significant increase in number of cycles to failure could be:

- The frequency of which the cycles are tested in
- Stress instead of strain controlled
- Tension-tension test instead of tension-compression
- Uncertainties in the stress applied
- Little residual stresses

Tension-tension vs tension-compression will be estimated in the analysis of the results. Refer chapter 2.3.



Obtained N-curve for sea water corroded specimens.

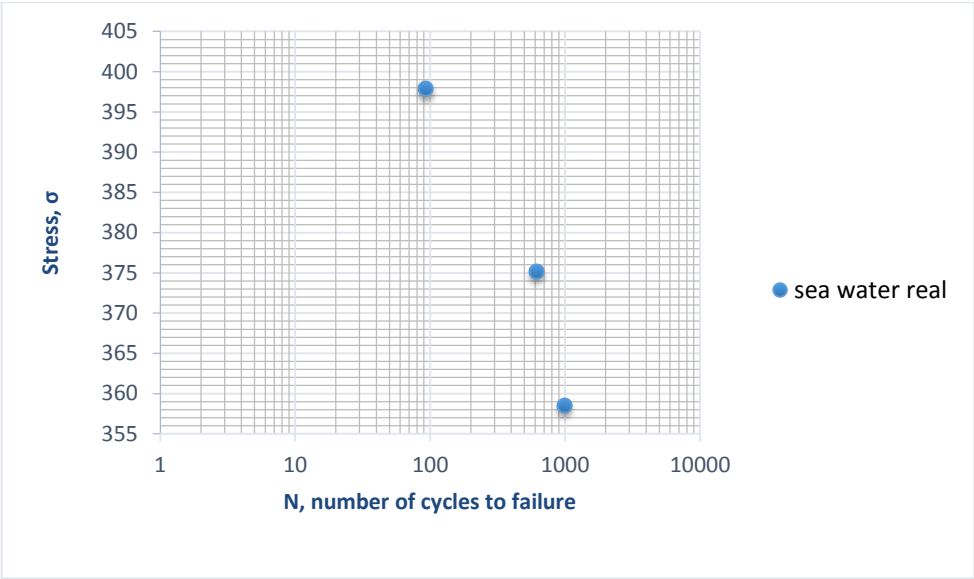


Figure 6-18 Obtained number of cycles to failure of sea water corroded specimens

Obtained SN-curve for air corroded specimens.

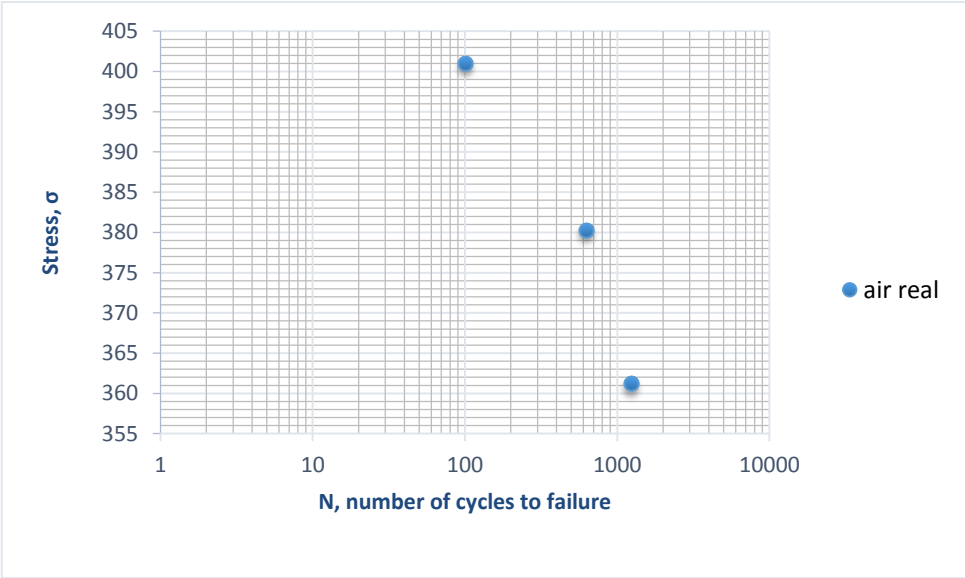


Figure 6-19 Obtained number of cycles to failure of close to sea air corroded specimens

A scatter diagram for the results of the whole fatigue test is presented in table 7-1 below.

## 6.4 Investigation of fracture

The following pictures show the fracture surface of one specimen. An inspection of all the specimens was not done, mainly due to the laboratory's tight schedule. It is reasonable to assume that the rest of the specimens will show similar results upon fracture. This assumption is based on that the specimens were made of the same material, and the same procedure was followed throughout the fabrication. They were also subjected to the same test where only the stress varied. An investigation of the fracture surface was conducted using the SEM machine that was used to investigate the surface conditions. The first picture shows surface of the crack of one of the two parts the specimen now has been divided into. One can clearly see the necking that has occurred. Necking is a phenomena that occurs when strain hardening is unable to keep up with the loss of cross sectional area. As opposed to a highly pure metal which often can form a sharp point with regards to ductile fracture, this has divided into a blunt tip.

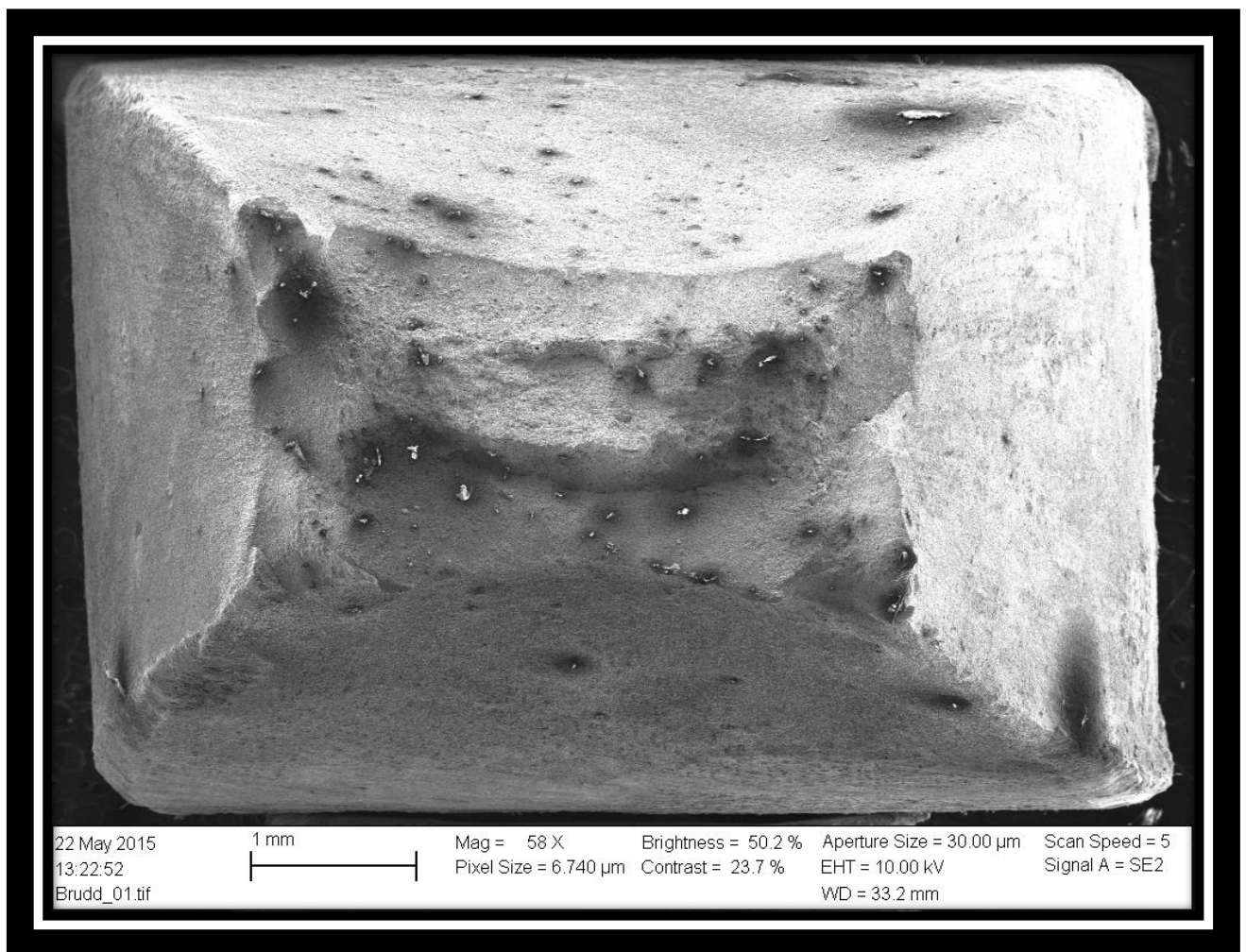


Figure 6-20 Fracture surface

The picture shows two distinct areas. Marked by red in the following pictures



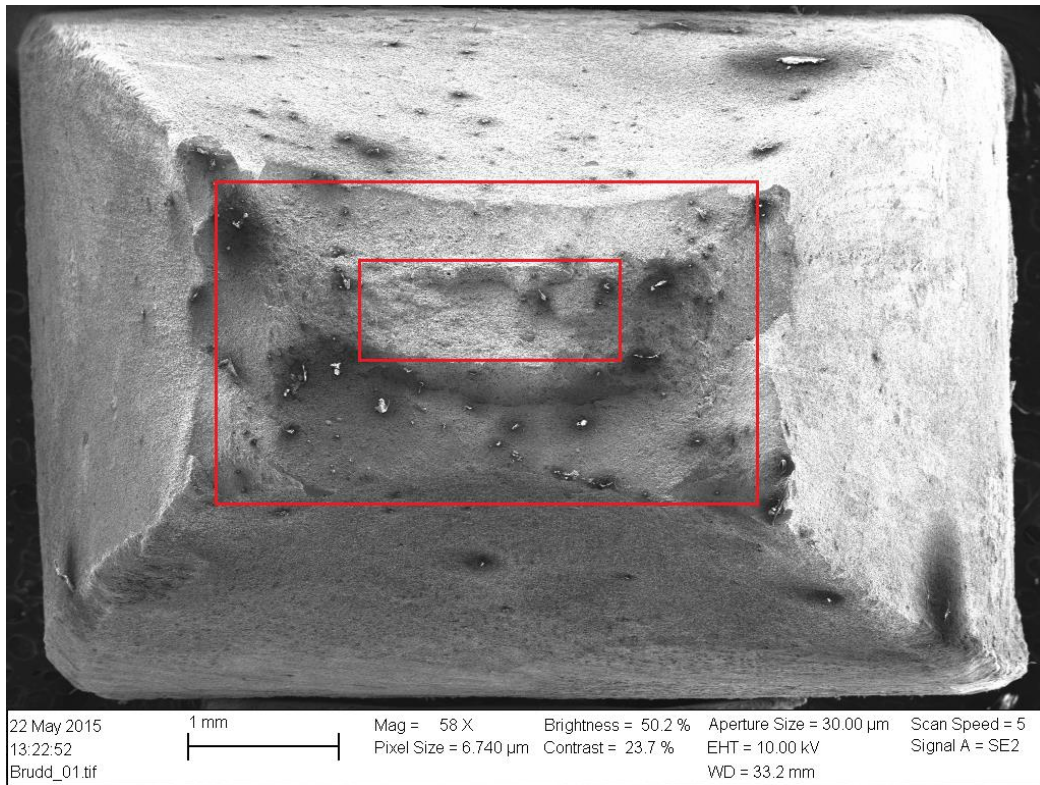


Figure 6-21 Two distinct areas of fracture

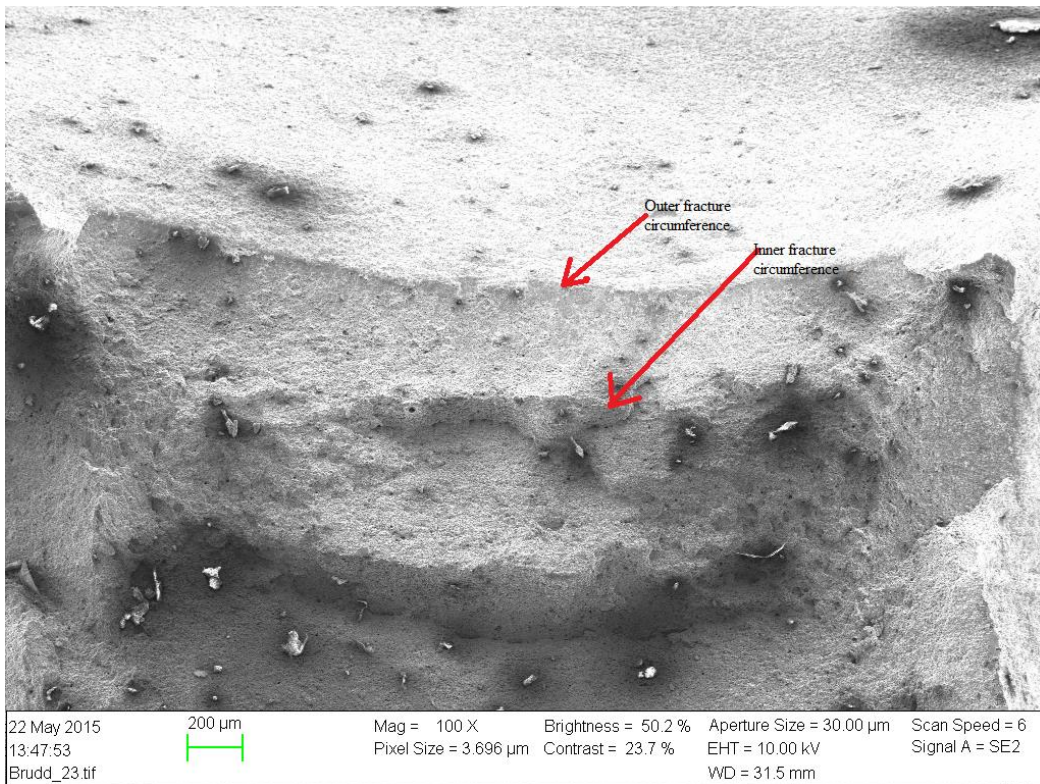
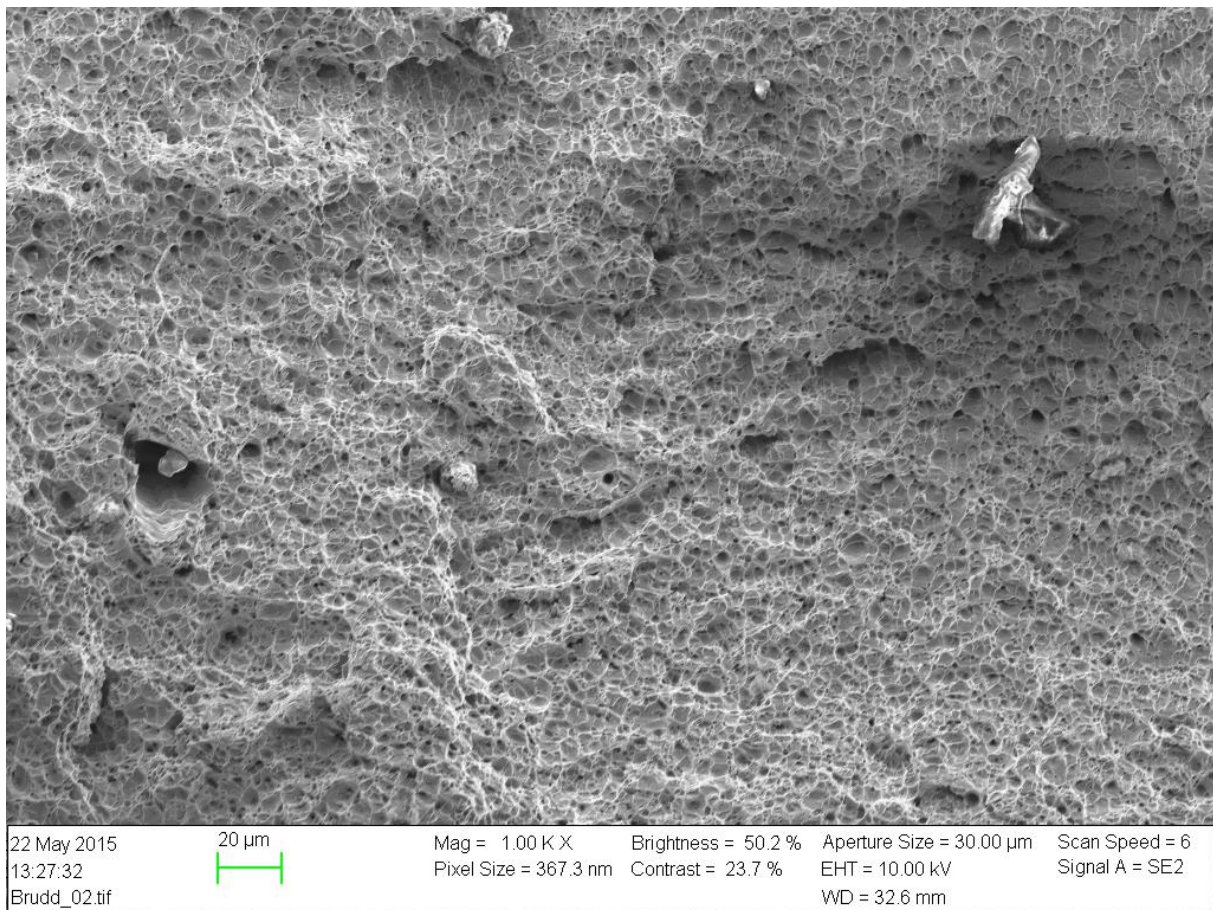


Figure 6-22 Two distinct areas of fracture

It is hard to determine where the fracture first occurred. There is no distinct mark that shows where the fracture first occurred. It is though reasonable to determine the outer circumference as where the fracture initiated. This is due to the formation of the necking, where it is the outer section of the cross section that reduces. Also at the moment where the specimen was divided in two, it was noticed that ones the necking had initiated, the specimen continued to get thinner all the way until the specimen was divided into to. As mentioned in the beginning of this chapter metal with impurities forms a blunt fracture tip. This indicates that the inner circumference was the last part of the specimen to fracture.

The whole surface was checked systematically. Started with the upper right corner and then proceeded clockwise. This was done to check if the fracture was ductile throughout.



*Figure 6-23 Upper right corner, ductile fracture*

One can see from this fractograph that the upper left corner is ductile. The next picture shows a better representation of this with a higher magnification.



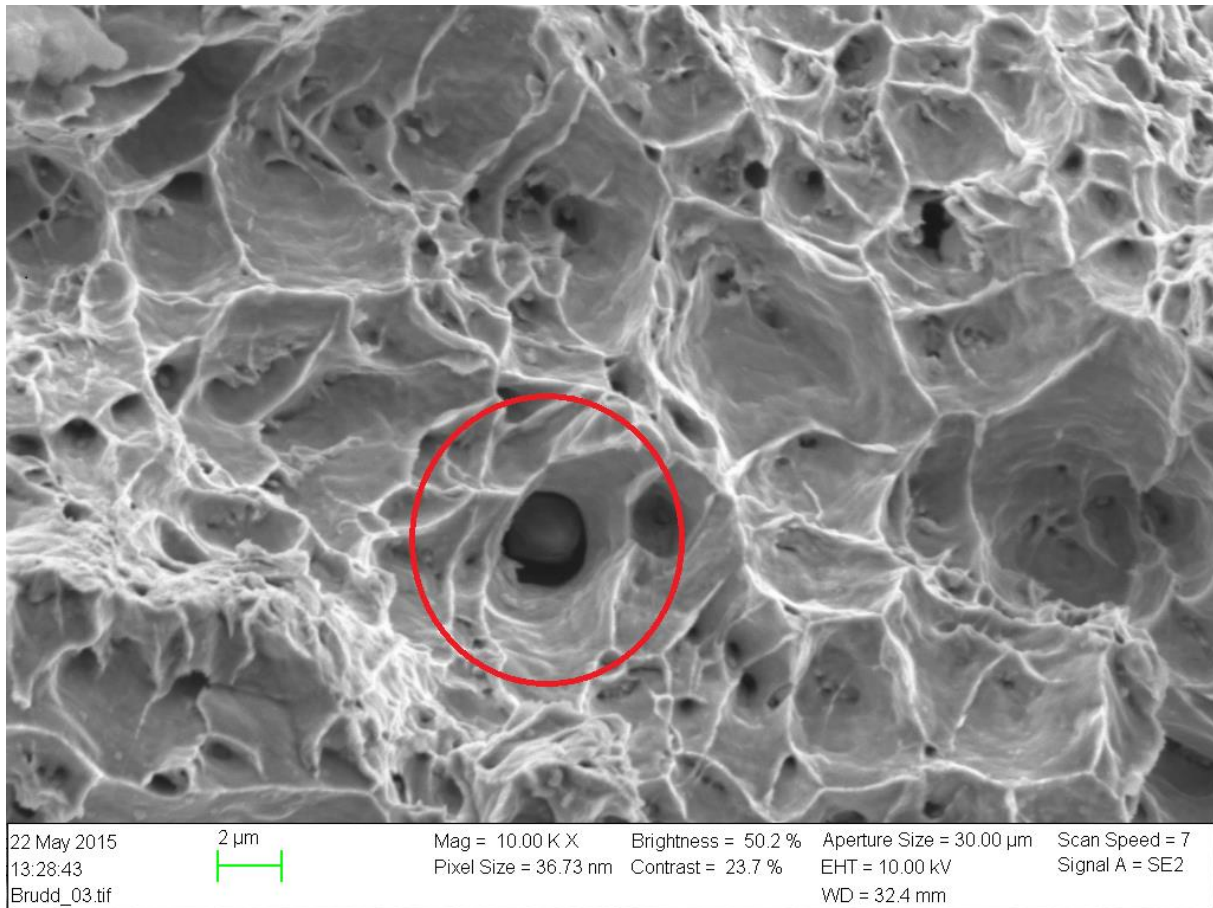
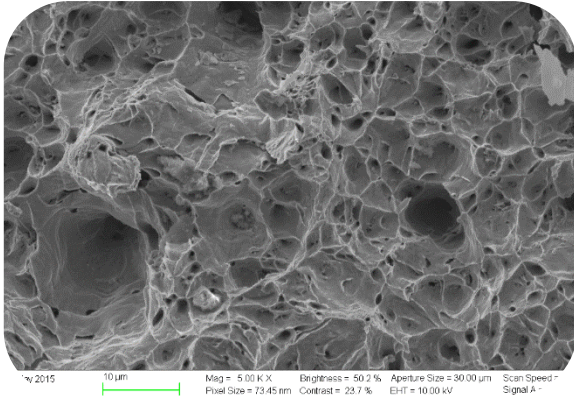


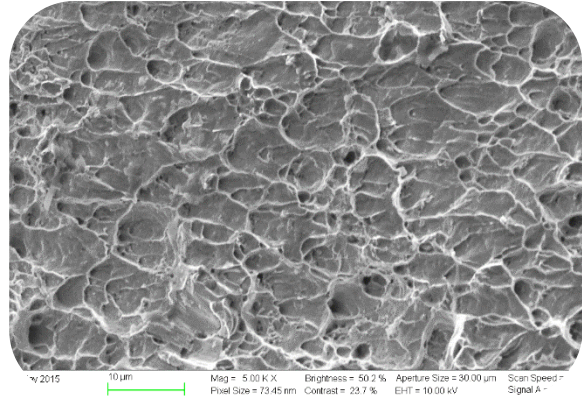
*Figure 6-24 Spherical inclusion which nucleated a microvoid*

From this high magnification fractograph one can see the spherical inclusion which nucleated a microvoid. The surface is covered in depressions caused by the repeated yielding and loading, the tips of these depressions who used to be the combined material, is now on the other part of the fractured specimen.

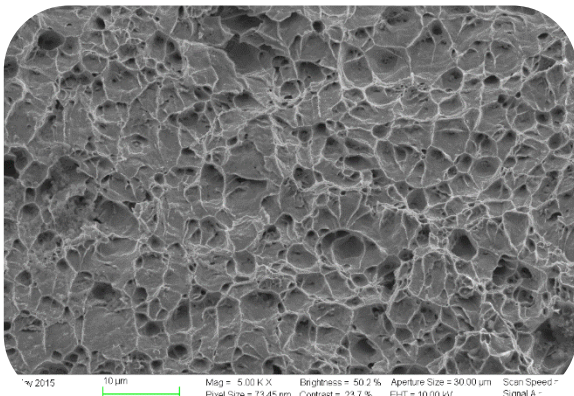
Further investigation over the whole fracture surface showed that the fracture was ductile overall. A representation of the whole surface is presented with the group of pictures below. It shows a clearly ductile fracture. There is no evidence that corrosion had any effect on the fracture and crack growth. This is mainly due to the fact that the specimens were only exposed to corrosive environment for six weeks.



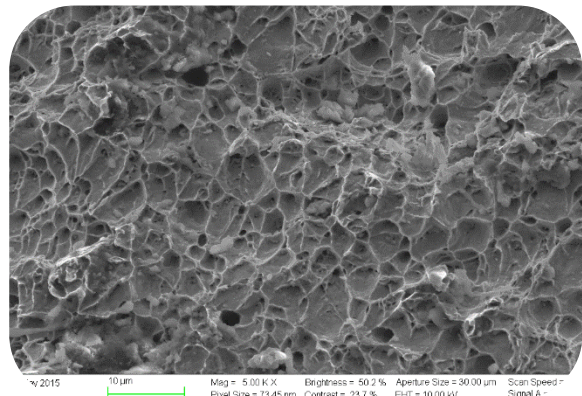
Upper right corner



Right side ridge



Bottom left corner



Bottom right corner

Figure 6-25 Overall inspection of ductile fracture

-

# 7 Interpretation of results

Modulus of elasticity could not be determined correctly in the absence of an extensometer or strain gauge. The elasticity modulus calculated from graphs from tests represents both elongation of specimens and the displacement of the test equipment. This ranged from 65 to 125 GPa. The correction for machine displacement could not be found in the testing machine manual. Also it was not possible to attach any strain gauge or extensometer to observe real elongation of the specimen. It was therefore determined in cooperation with associate professor S.A.S.C Siriwardane that the  $E_{1/4}$  should be set as the standard Young's modulus for mild steel. This is due to the fact that this thesis is more concerned with number of cycles to failure vs stress and strain.

$$E_{1/4} = 210\,000\text{ MPa}$$

With the problems regarding the correct measurements of strain, it was chosen to base the analysis on stress. Stress will give a better indication of the fatigue process due to the machines ability to measure the applied force on the specimen. The smallest cross section of every specimen is known. Also as mentioned earlier it was necessary to substitute strain with stress in the testing process.

Table 7-1 Smallest cross sectional area of the specimens

Member	Area mm <sup>2</sup>
1	37,503
2	37,9848
3	39,9784
4	37,0208
5	41,2228
6	36,9026
7	38,285
8	39,8028
9	32,8
10	39
11	40,095
12	40,089
13	39,7404
14	37,35
15	39,909

The obtained SN-curve for the non-corroded and corroded specimens is presented below.

Table 7-2 Overview of number of cycles to failure from all specimens

Environment	Specimen	Forve (N)	Stress
close to sea air	1	627	14262
sea water	3	613	15000
no corrosion	16	693	15120
sea water	5	93	16400
close to sea air	8	101	15960
no corrosion	10	102	15536
sea water	4	995	13273
no corrosion	6	1431	13283
close to sea air	7	1234	13827

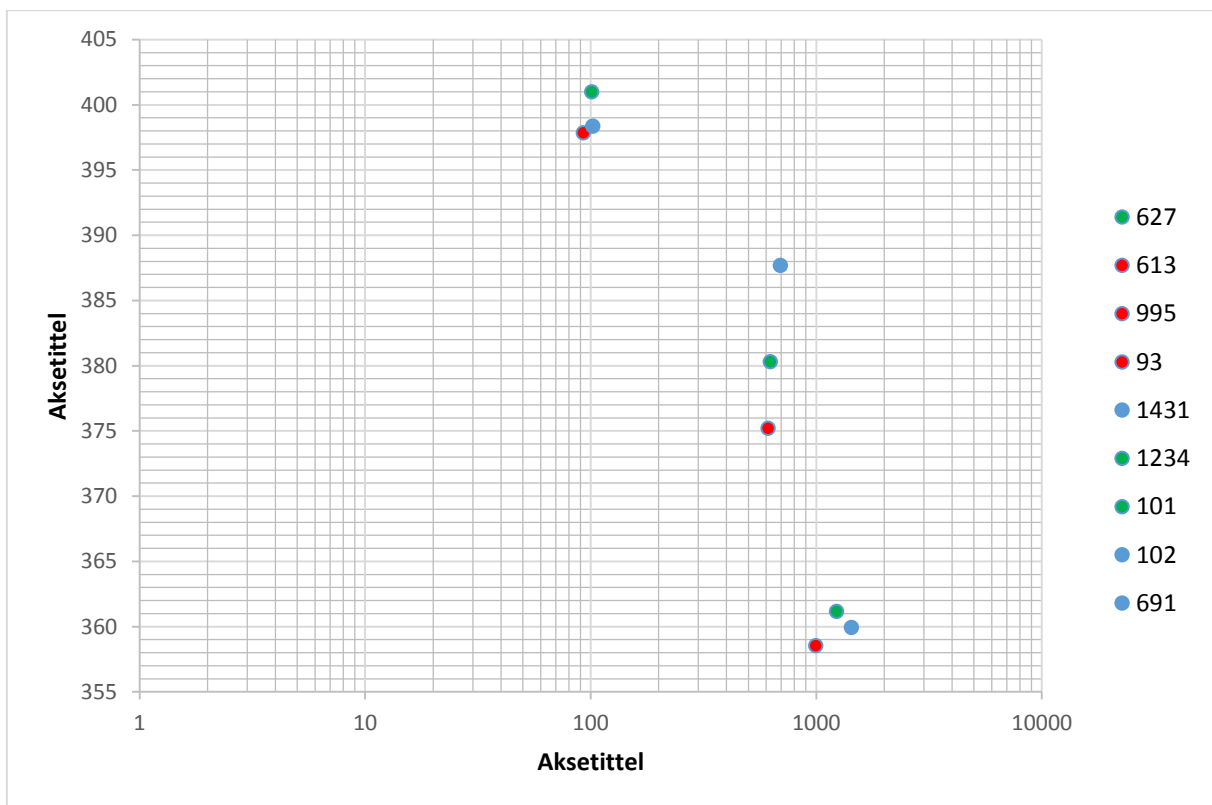


Figure 7-1 Obtained number of cycles to failure of all test specimens

It shows a significant higher number of cycles to failure than expected from the calculations of Ramberg-Osgood and eq.14. It also shows that the corroded specimens broke at lower number of cycles than the non-corroded. This on the other hand may be random since the difference is so insignificant. Four more specimens will be tested on the stress that should correspond to 0,021564 strain. Two specimens corroded in sea water and 2 specimens corroded in close to the sea air.



Tables below contains an overview of the tested specimens, and the parameters chosen to be the main focus of the test. They will contain stress ranges, the alternating stress and the mean stress. It will be shown by an logarithmic increase of cycles. The testing software had limitations of how many cells it was possible to export to excel, so the 200<sup>th</sup> cycle will be the latest cycles represented. The average mean stress, mean alternating stress and stress range will then be used to calculate the Goodman relation. Hysteresis loop for first and tenth cycle is presented. The first loop shows the so called conditioning cycle. The strain in the hysteresis loop cannot be taken as the true strain on the specimens. As explained above when establishing the Young's modulus, the machine records displacement of both the machine and the specimen.

Specimenn 1

Table 7-3 Results from fatigue test specimen 1

Cycle no	Stress Mpa			sigma_a	sigma_mean	Goodman relation
	max	min	range			
1	379,8571	-0,02702	379,8841	189,942	189,9150191	302,6397537
10	378,1418	0,015025	378,1268	189,0634	189,0784128	300,4544777
50	380,2536	0,026869	380,2268	190,1134	190,1402526	303,1260625
100	383,2166	0,01171	383,2048	191,6024	191,6141341	306,9144923
200	383,513	0,020609	383,4924	191,7462	191,7668082	307,2921501
Average	380,9964	0,009438	380,987	190,4935	190,5029254	304,0853873

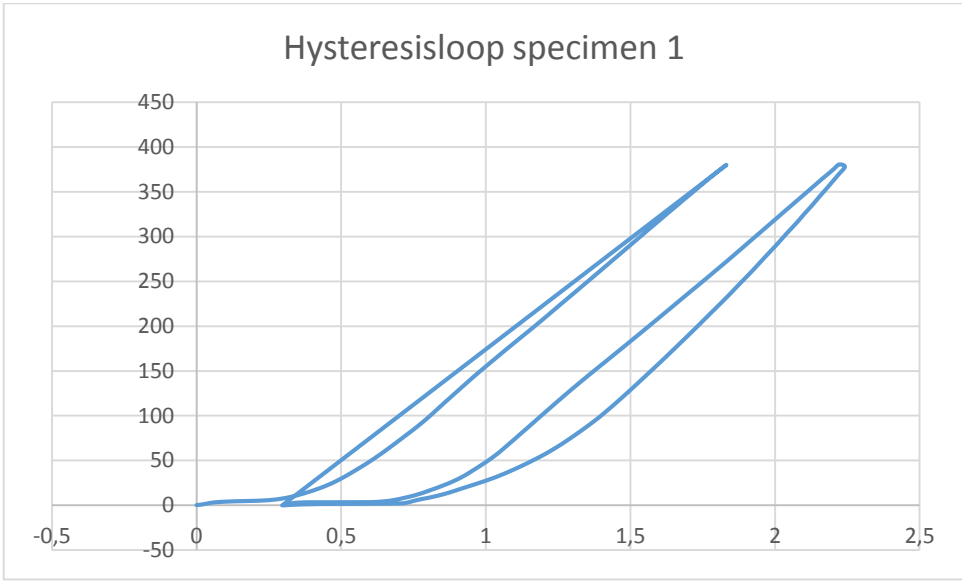


Figure 7-2 Hysteresis loop for specimen 1

When the calculated stress from the Goodman relation from table 7-2 is implemented in the equations from DNV, the corresponding theoretical strain applied to the specimens are  $\epsilon_1 = 0,002566029$ .

## Specimen 4

Table 7-4 Results from fatigue test specimen 4

Cycle	Stress Mpa			sigma_a	sigma_mean	Goodman relation
	max	min	range			
1	359,0555	0,011733	359,0437	179,5219	179,5336032	277,0513271
10	359,0948	0,003032	359,0917	179,5459	179,5488951	277,1011779
50	359,1345	0,064739	359,0698	179,5349	179,5996299	277,1267918
100	359,0345	0,049691	358,9849	179,4924	179,5421188	277,0130275
200	358,9633	0,084131	358,8791	179,4396	179,5237013	276,916019
Average	359,0565	0,042665	359,0138	179,5069	179,5495897	277,0416687

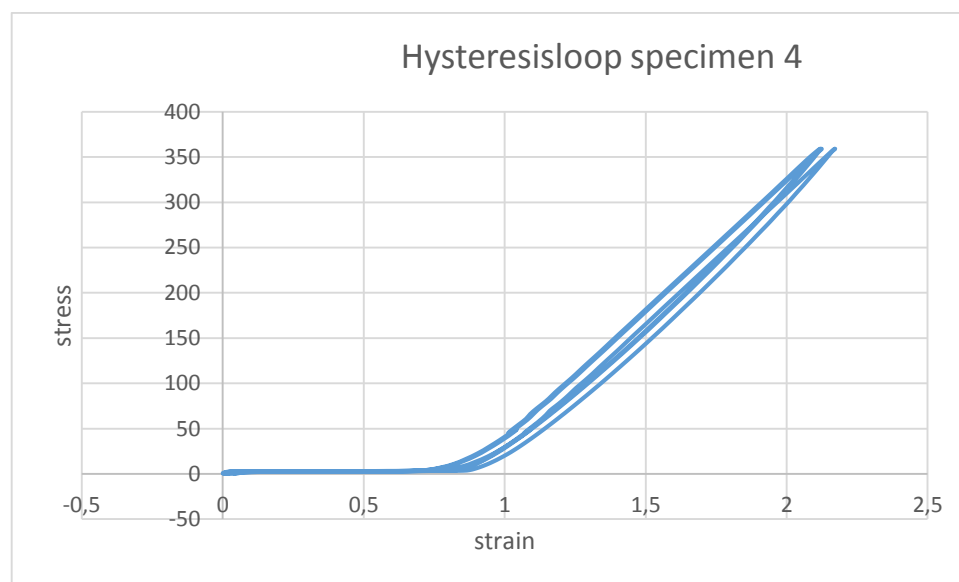


Figure 7-3 Hysteresis loop for specimen 4

Strain from Goodman relation calculated in table 7-3 stress level:  $\epsilon_4 = 0,001759738$

## Specimen 6

Table 7-5 Results from fatigue test specimen 6

Cycle	Stress Mpa			sigma_a	sigma_mean	Goodman relation
No	max	min	range			
1	364,8714	0,023789	364,8476	182,4238	182,4476084	284,0344022
10	364,8961	0,017727	364,8784	182,4392	182,4569103	284,0663918
50	362,5987	0,02498	362,5737	181,2869	181,31184	281,2888015
100	363,6891	0,01982	363,6693	181,8346	181,85446	282,6052928
200	364,5462	0,01568	364,5305	182,2653	182,28094	283,6431991
Average	364,1203	0,020399	364,0999	182,05	182,0703517	283,1276175

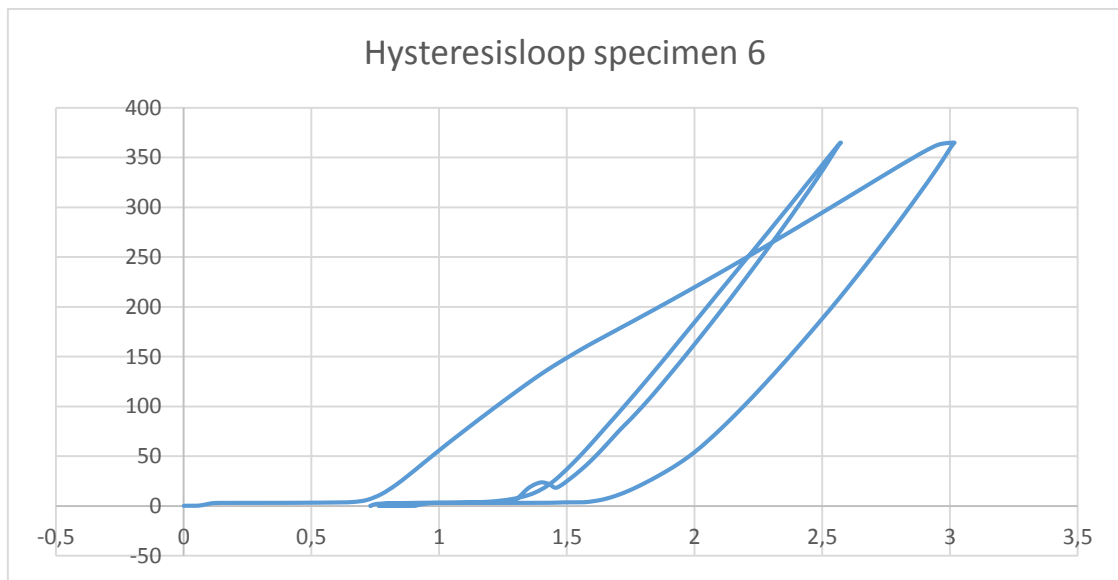


Figure 7-4 Hysteresis loop for specimen 6

Strain from Goodman relation calculated in table 7-4:  $\epsilon_6 = 0,001895633$

## Specimen 7

Table 7-6 Results from fatigue test specimen 7

Cycle	Stress Mpa			sigma_a	sigma_mean	Goodman relation
No	max	min	range			
1	362,8305	-0,03789	362,8684	181,4342	181,3962832	281,5897269
10	361,3436	-0,03884	361,3824	180,6912	180,6523865	279,8032239
50	363,4822	0,05952	363,4226	181,7113	181,77084	282,3416823
100	362,4851	0,02652	362,4586	181,2293	181,25581	281,151548
200	364,54	0,025489	364,5145	182,2573	182,2827447	283,6323041
Average	362,9363	0,006959	362,9293	181,4647	181,4716129	281,703697

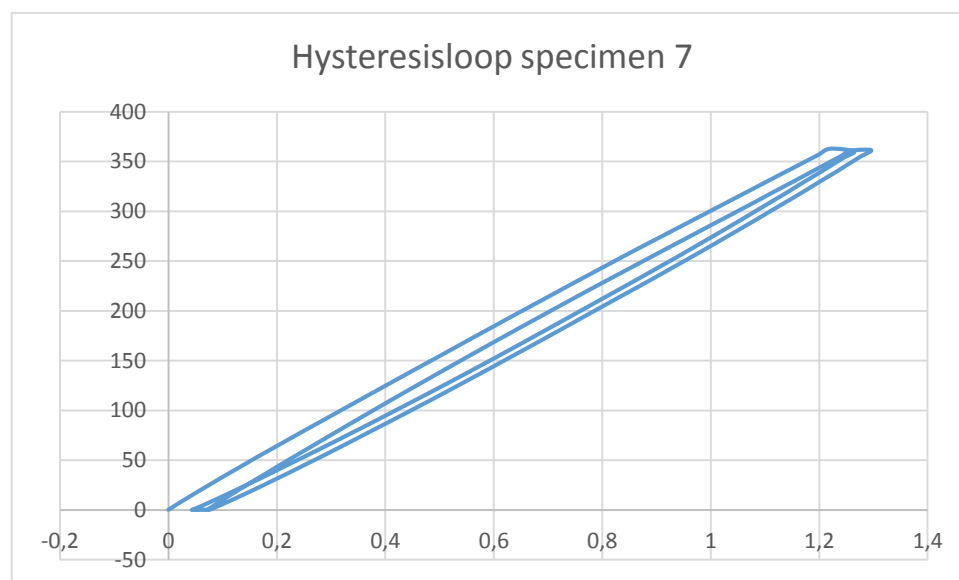


Figure 7-5 Hysteresis loop for specimen 7

Strain from Goodman relation calculated in table 7-5:  $\epsilon_7 = 0,001861937$

## Specimen 16

Table 7-7 Results from fatigue test specimen 16

Cycle	Stress Mpa			Sigma_a	Sigma_mean	Goodman relation
	Max	Min	Range			
1	387,7906	-3,68238	391,473	195,7365	192,0541269	313,9704771
10	390,471	-0,02662	390,4976	195,2488	195,2221646	316,3401929
50	390,8685	-0,03836	390,9069	195,4534	195,4150925	316,8659908
100	386,5542	-0,0469	386,6011	193,3006	193,2536608	311,2373358
200	389,7239	-0,03687	389,7607	194,8804	194,8434964	315,3639136
Average	389,0816	-0,76623	389,8479	194,9239	194,1577082	314,755582

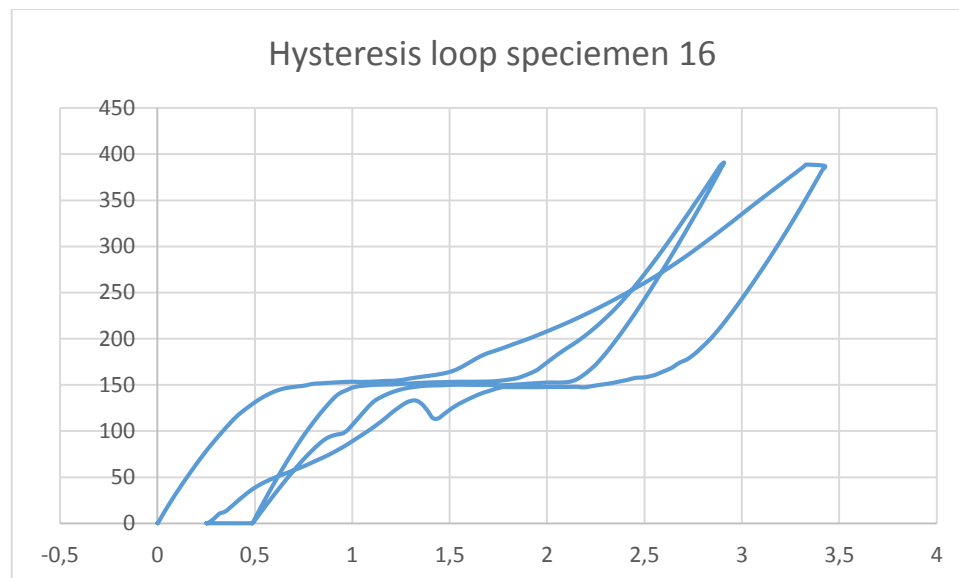


Figure 7-6 Hysteresis loop for specimen 16

Strain from Goodman relation calculated in table 7-6:  $\epsilon_{16} = 0,003077254$

## Specimen 5

Table 7-8 Results from fatigue test specimen 5

Cycle No	Stress Mpa			sigma_a	sigma_mean	Goodman relation
	max	min	range			
1	398,1564	1,1564	397,0000	198,5000	199,6564	326,2030
10	399,0022	1,1213	397,8809	198,9404	200,0617	327,3543
50	397,1564	0,0248	397,1316	198,5658	198,5906	325,1943
93	397,4565	0,054265	397,4022	198,7011	198,7554	325,5882
Average	397,9429	0,5892	397,3537	198,6768	199,2660	326,0849

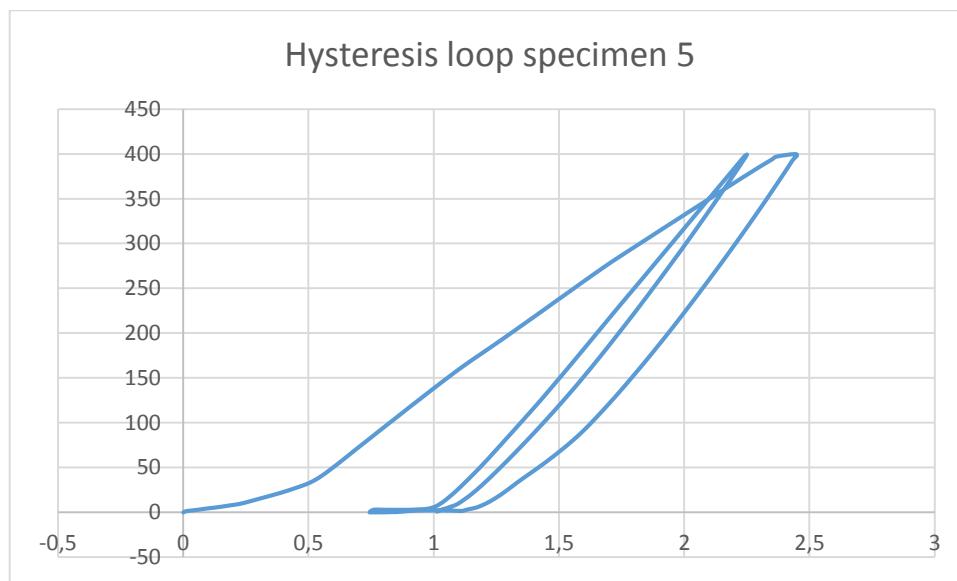


Figure 7-7 Hysteresis loop for specimen 5

Strain from Goodman relation calculated in table 7-7:  $\epsilon_5 = 0,003946562$

### Specimen 3

Table 7-9 Results from fatigue test specimen 3

Cycle No	Stress Mpa			sigma_a	sigma_mean	Goodman relation
	max	min	range			
1	374,4562	-0,0516	374,5078	187,2539	187,2023	295,8493
10	376,1540	0,1652	375,9888	187,9944	188,1596	297,9028
50	375,1265	0,2101	374,9165	187,4582	187,6683	296,6003
100	374,1532	0,0022	374,1511	187,0755	187,0777	295,4535
200	375,1865	0,1652	375,0213	187,5107	187,6759	296,6902
Average	375,0153	0,0982	374,9171	187,4585	187,5567	296,4982

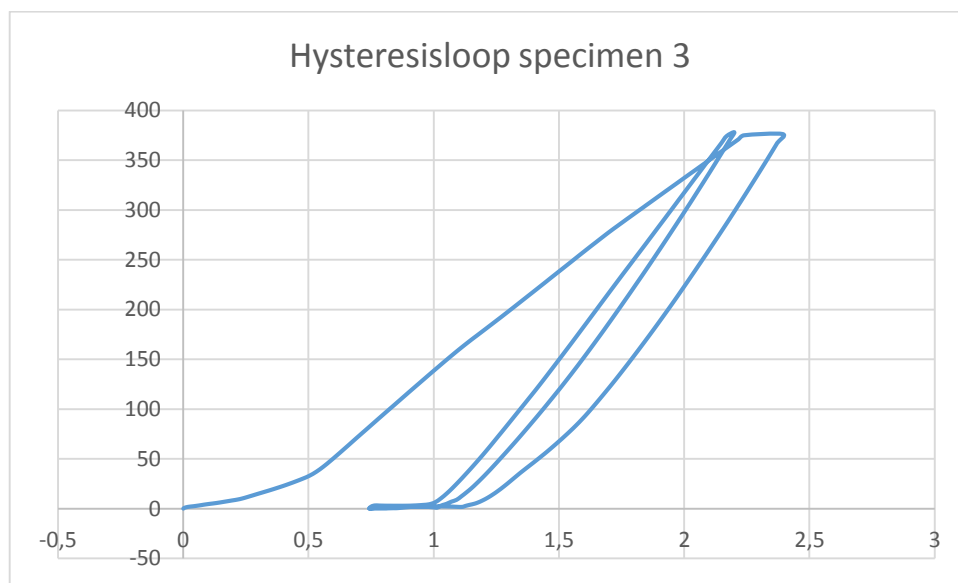


Figure 7-8 Hysteresis loop for specimen 3

Strain from Goodman relation calculated in table 7-8:  $\epsilon_3 = 0,002280273$



## Specimen 8

Table 7-10 Results from fatigue test specimen 8

Cycle No	Stress Mpa			sigma_a	sigma_mean	Goodman relation
	max	min	range			
1	401,5512	-0,0560	401,6072	200,8036	200,7476	331,1529
10	400,1517	-0,0655	400,2172	200,1086	200,0431	329,2566
50	401,1356	0,0651	401,0705	200,5352	200,6004	330,5530
100	400,9916	1,1566	399,8349	199,9175	201,0741	330,0400
102	402,0035	1,2654	400,7381	200,3691	201,6345	331,3866
Average	401,1667	0,4731	400,6936	200,3468	200,8199	330,4769

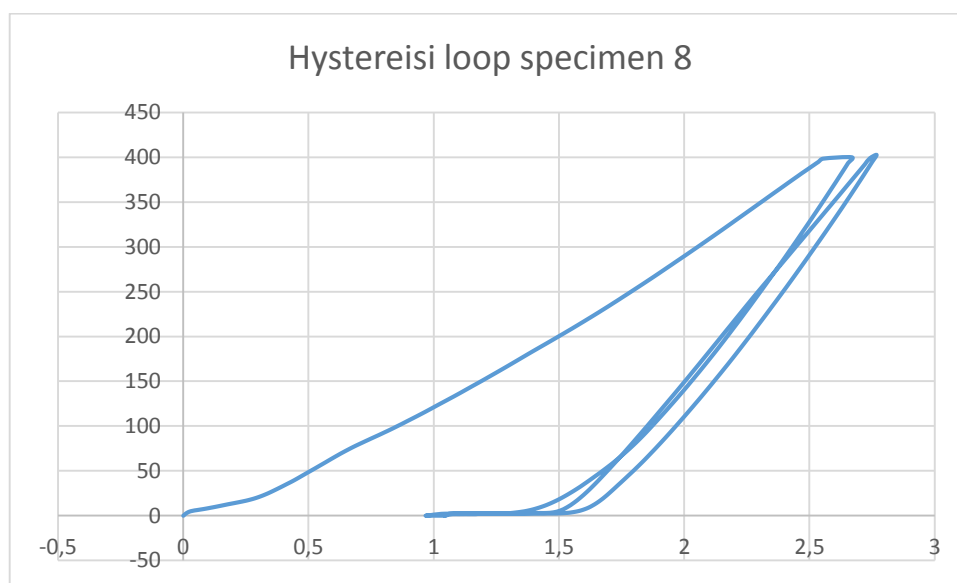


Figure 7-9 Hysteresis loop for specimen 8

Strain from Goodman relation calculated in table 7-9:  $\epsilon_8 = 0,004143495$

## Specimen 10

Table 7-11 Results from fatigue test specimen 10

Cycle No	Stress Mpa			sigma_a	sigma_mean	Goodman relation
	max	min	range			
1	398,1564	1,1564	397,0000	198,5000	199,6564	326,2030
10	399,0022	1,1213	397,8809	198,9404	200,0617	327,3543
50	397,1564	0,0248	397,1316	198,5658	198,5906	325,1943
100	397,5640	0,5121	397,0519	198,5260	199,0381	325,5969
101	399,0561	0,9853	398,0708	199,0354	200,0207	327,4672
Average	398,1870	0,7600	397,4270	198,7135	199,4735	326,3615

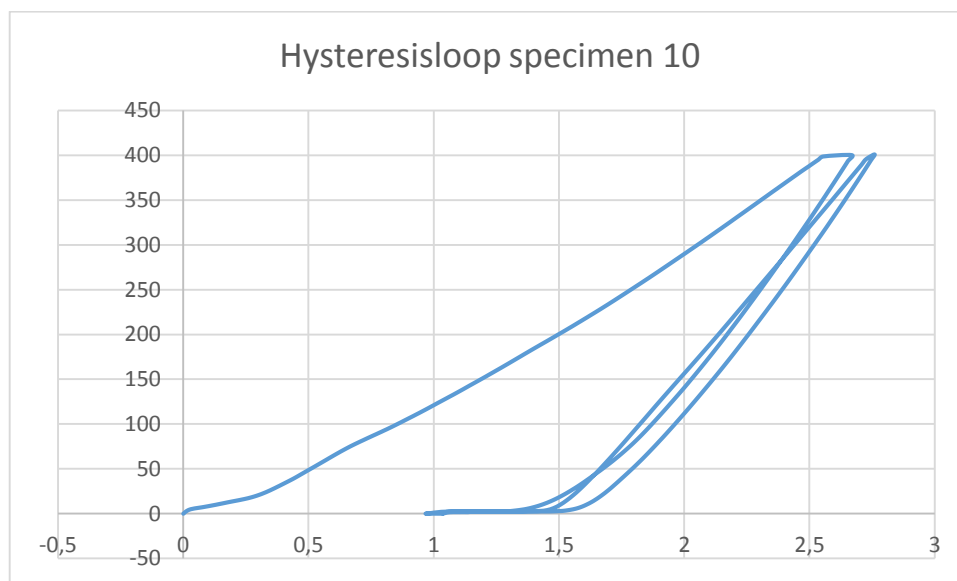


Figure 7-10 Hysteresis loop for specimen 10

Strain from Goodman relation calculated in table 7-10  $\epsilon_{10} = 0,003821234$

When testing three samples on the highest strain levels these results were obtained.

Table 7-12 Number of cycles to failure from test done on the highest stress levels

Environment	Specimen	N
sea water	Specimen 5	93
sea water	Specimen 14	189
sea water	Specimen9	157
air	Specimen 12	127
air	Specimen 13	193
air	Specimen 8	101

Notice from table 7-8 that there is a large span in required cycles to produce failure on strain level 0,021564. It also shows that the specimen which required the most cycles to failure was a specimen placed in air close to the sea for six weeks. It is then concluded that the effect of corrosion for only six weeks cannot be determined in terms of fatigue life. Therefore no difference between sea water corroded and close to sea corroded specimens in terms of needed cycles to failure from the test method used in this thesis.

The Goodman relation would imply a higher number of cycles were needed to produce failure than it actually took to produce failure. As one can see from the tables, all the specimens failed at lower numbers of cycles than the Goodman relation calculation would imply, but also at a higher number than the calculations from the equations in the DNV standards. It would seem that the tensile machine applies a greater stress on the specimen than the Goodman relation suggests. When testing, the machine applies tension force for a long duration. This happens when the machine is reaching the maximum force line. The result of this is that the material is kept in the yield point of the material for a long duration. This could mean that the voids expand more every cycle, which in return means fewer cycles to failure.

Table 7-13 Number of cycles to failure from extra specimens

Specimen	N	N
No	Expected from Goodman	Actual results
9	215	157
14	215	189
12	635	127
13	635	193

Table 6-9 shows the four specimens that were tested on the highest stress level after the S-N curve was established. It shows that there is no significant impact of corrosion after six weeks.

It can be interpreted as that the tension applied from the machine could be closer to the chosen tension than expected from the Goodman relation. From the Goodman relation  $\sigma = 405 \text{ MPa}$  would suggest a corresponding true fatigue stress  $\sigma_f = 335,8537 \text{ MPa}$ . When then applying these results to the equations from the DNV one would expect the members to fail similar to presented in table 6-9. This on the other hand has not happened.

The preliminary tests first indicated that the corroded specimens broke at lower number of cycles than the non-corroded specimens. At first it seemed that corrosion of only six weeks had an impact on the specimens. But as mentioned above, the tests performed later on the highest stress values seems to disprove this. This could also come from the fabrication and preparation of the specimens. Two and two plates were welded together. Although the same procedures were followed with regards to welding, cutting and milling, there could have been different alterations in the microstructure.

Of course this could also be operator mistakes. With little experience with laboratory work, and staff at the laboratory having little knowledge of the machine left the operator to figure it out for himself.

It seems that one of the most significant factors, besides the tension applied from the machine, for these tests has been the HAZ and the displacement caused when welding the two plates together. The corrosion has mainly distributed over the weld, which also had the most exposure. Nevertheless the fracture point of every specimen was in the borderline between the base material and the weld. Meaning that the HAZ and displacement were of importance with regards to the fatigue tests. This could imply that the residual stresses present in the material prior to the testing were present. The specimens were milled to specific dimensions, and were reduced with a substantial amount of the original cross sectional area. Usually the HAZ is removed with milling or grinding. But since this was a fully penetrated double butt weld, it can be reasonably assumed that the residual stresses and HAZ was still present within the material. The specimens went through three different heating stages in the fabrication stages. First it was welded. Then they were cut using an angle grinder, and lastly milled. The milling process can most certainly be ruled out as having a major influence on the altering of the microstructure. This is assumed as the author himself did the milling, and could by just touching the specimens recognize that there was not any mentionable temperature rise in the specimens. When it comes to the cutting of the specimens, although it was cut in intervals, the temperature rose to the point that it would vaporize water.

Also as mentioned in chapter 4, the heat in the welding process caused some displacement of the plates.



*Figure 7-11 Displaced specimen after weld*

This displacement was milled straight, but the misalignment caused by the welding will still be present in the intersection between the weld and the base material, see figure 6-7. This causes eccentricities which could play a role in the results achieved in the tests.

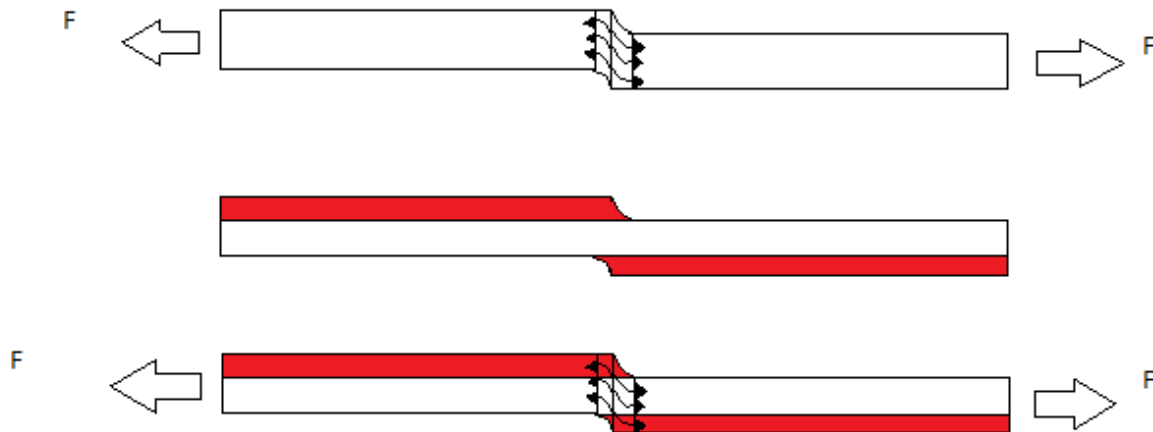


*Figure 7-12 Illustration of residual stresses in specimens*

Red shows the part of the specimens that has been milled. From the third specimen on Figure 7-12 one can see the curvature of the load in the intersection between the two welded parts. This came into play during the welding process. The plates were placed flat against each other, but the melting process when welding has caused the plates to push away from one another. This causes residual stress in the orientation shown on figure -712 Although the displacement has been milled away, there is bound to be residual stresses in this orientation caused by the misalignment.

Although this is considered a factor with regards to the result. The stress caused by this should not have an impact in the degree the number of cycles would imply. The main reason for the number of cycles to failure deviation has to be the machine and operator mistakes.

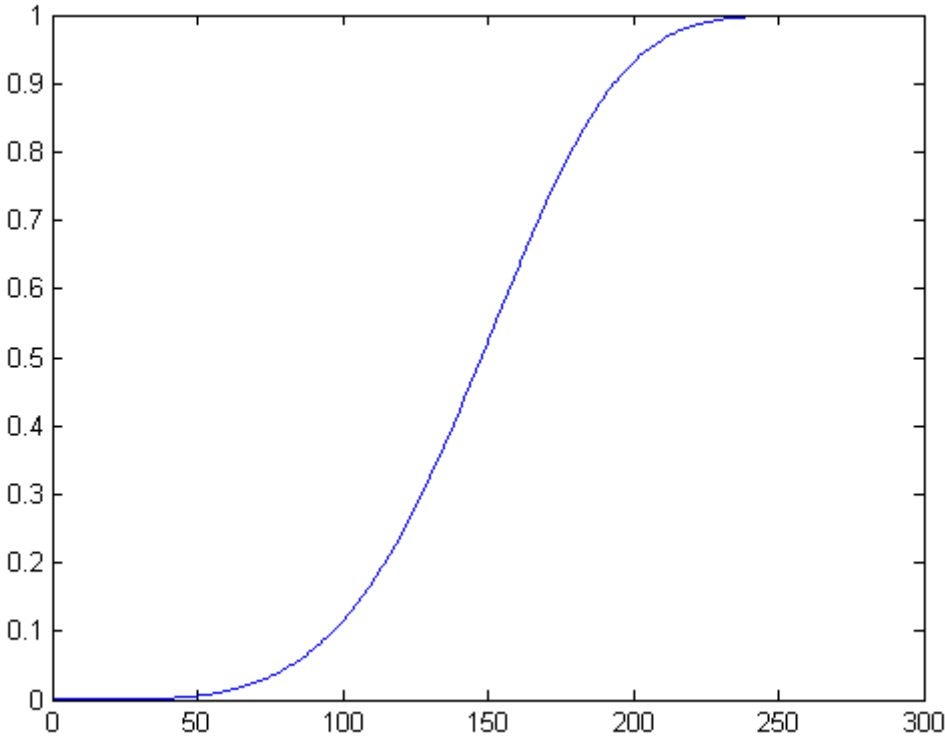
With light cast on these implications, one should nevertheless be able to determine an effect of corrosion on the specimens. If there were an effect after just six weeks of corrosion, the number of cycles would reveal this.

# 8 Probability

Cumulative distribution function (CDF) of a Weibull distribution of sea water corroded specimens. The Weibull distribution shown below represents three specimens tested on these parameters:

- Stress = 405 MPa
- Test machine Zwick Z020
- Sea water corroded for six weeks

[93, 157, 189]



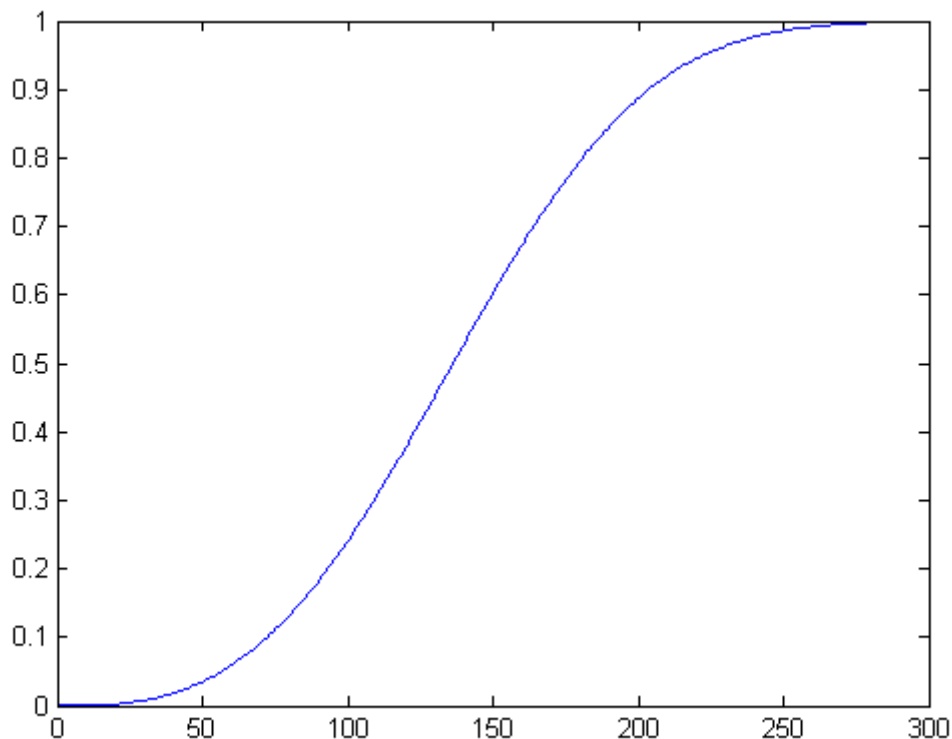
Figur 8-1 Probability curve for sea water corroded specimens

The distribution shows the probability of number of cycles needed to produce failure.  $P_{90} \approx 200$ , meaning that the probability of failure to occur below 200 cycles is 90 %  $P_{10} \approx 100$ , showing that there is approximately 10 % chance for a specimen to fail below 100 cycles.

CDF of a Weibull distribution of close to sea air corroded specimens. The distribution below represents the three specimens tested in close to sea air. It was tested on the following parameters:

- 405 MPa
- Test machine Zwick Z020
- Close to sea air corroded for six weeks

[101, 127, 193]



*Figur 8-2 Probability curve for close to sea air corroded specimens*

The distribution shows a small difference in the distribution when compared to the sea water corroded specimens. Since only three specimens has been tested, there is not enough data to say that the probability of failure in specimens corroded in sea water occur on lower number of cycles than close to sea air. But the tests that was done showed on average a larger number of cycles was needed for the close to sea air specimens to fail.

It has to be said that only three values to produce this probability curve is not sufficient. But with regards to the time consuming test, more specimens would be unreasonable with regards to other work throughout the thesis.



## 9 Discussion

During the course of the thesis several changes have been made with regards to the original idea. From the original idea of testing in the high cycle fatigue area, it was discovered that the equipment available at the University of Stavanger could not support this type of testing. The main reason for this is that the machine used, is designed for tensile test. It was then agreed to test in low cycle fatigue and ultra-low cycle fatigue area. This meant time consuming reshaping of the specimens. As a result of this, there were only six weeks was available to let the specimens corrode. As the work progressed unforeseen problems was discovered. A lot of time was used to familiarize with the test equipment. The machine had a problem where it used to stop at 200 cycles. This problem was later eliminated, but because of this each test was initiated with only 500 cycles as test duration. When, and if, a test reached 500 cycles a new test had to be initiated on the specimen.

The specimens showed every sign to corrode in the proper manner explained in previous chapters, but it is necessary to emphasize that six weeks had little to no effect on the testing, with regards to number of cycles to failure.

ISO 12106 *Metallic materials - fatigue testing - axial-strain-controlled method*, has certain criteria's when it comes to procedures that needs to be followed when conducting a low cycle fatigue test. These were followed to best possible measure when doing it on the test machine available. Certain exclusions were necessary. These exclusion should not have any significant impact on the test results themselves as the exclusions did not regard the parameters and test method.

The testing was done in the new laboratory at the University of Stavanger. The members were placed in the machine and the given parameters were implemented. It was early noticed that the number of cycles did not correspond to expected values. But even though they did not fail at expected values, some rulings could be made with regards to the effect of corrosion on number of cycles to failure. The selected stress values for the test was set as 360 MPa, 390 MPa and 405 MPa. The reason for the low stress values was that a trial specimen broke during the first cycle on 450 MPa. To avoid invalidation of the specimens, lower values were chosen.

Although the fatigue testing itself did not give any concluding answers with regards to the effect of pitting corrosion. The inspection of the surface of the sea water corroded specimens was of significant interest to this subject. From figure 5-13 and 5-14 one can see what seems

to be pits. There are more than 20 individual pits over the welded surface. Keep in mind that this is only after 4 weeks of corrosion. If this corrosion growth keeps the same rate over the course of years, the impact of the pits with regards to fatigue life can be significant.

Especially if this takes form in an otherwise ignored part of a structure where inspections rarely occurs due to safety and accessibility.

Pits implies cracks in an otherwise uniform surface. If no corrective actions are implemented to the exposed surface the pits will continue to grow from both the imposed corrosion and the cyclic loading on the structure.

Preventive actions that can be done once pitting has initiated can be:

- Grinding the surface, meaning removing parts of the material where pitting has occurred. Once this is done a new layer of protective coating must be applied. This implies a loss of cross sectional area, and should only be considered where there is enough material redundancy.
- Use an alloy which is less susceptible to corrosion. Economic interests limits this to smaller structures and surfaces
- Cathodic protection should be considered before installing a structure in corrosive environments. The way to do this is to limit the loss of electrons, refer chapter 2.1.4. It is normal to apply the principal of sacrificial anode, meaning placing a metal which has a lower nobility causing it to oxidize instead of the material.

# 10 Conclusion

Specimens representing a welded joint has been exposed to two different corrosive environments for six weeks, and has then been subjected to low cycle fatigue tests. The stress levels determined for the test has been 360, 390 and 405 MPa. To assure corrosion on the specimens a small area has been left unprotected to simulate a breach in the coating of a steel joint. Number of cycles to failure obtained from tests has been compared to estimated number of cycles to failure obtained by calculations of given equations in DNV RP C-208. The results did not give any indications of any effect of corrosion with regards to number of cycles to failure. The results obtained deviated from the expected values calculated from the Ramberg-Osgood relation and equation of low cycle fatigue of base material in welded joints from DNV RP C-208. Also the specimen which required most cycles to failure was a specimen corroded in air close to the sea.

A scanning electron microscope was used to investigate the surface of a specimen subjected to corrosion for four weeks. The magnification showed promising results regarding pit formation on the surface. It showed the rapid formation of pitting corrosion in common environments surrounding off shore structures.

## 10.1 Recommendations for future work

Given the results of the surface inspection, recommendations for future work would be to a similar study with correct testing equipment. Meaning a suitable oscillating machine, specimens where a correct measurement of strain is possible. It would also be wise to let the specimens corrode for a much greater time period than six weeks.

# References

- Anderson, T. L. (2005). *Fracture mechanics : fundamentals and applications* (3rd ed. ed.). Boca Raton, Fla: Taylor & Francis.
- Anijs, M. A. (2013). *Low Cycle fatigue in the North sea environment*.
- Board, N. T. S. (2015). Collapse of a Suspended Span of Inter- state Route 95 Highway Bridge over the Mianus River
- Center, N. R. (2015). Stress and Strain. from <https://www.nde-ed.org/EducationResources/CommunityCollege/Materials/Mechanical/StressStrain.htm>
- Doctors, C. (2015). Fouling and Biofouling. from <http://corrosion-doctors.org/Seawater/Fouling.htm>
- Dong, Y., & Frangopol, D. M. (2015). from <http://www.scopus.com/record/display.url?eid=2-s2.0-84928747096&origin=resultslist&sort=plf-f&src=s&st1=corrosion%2c+fatigue%2c+probability&sid=1357DE88512354455338651D0C884826.fM4vPBipdL1BpirDq5Cw%3a610&sot=b&sdt=b&sl=46&s=TITLE-ABS-KEY%28corrosion%2c+fatigue%2c+probability%29&relpos=0&relpos=0&citeCnt=0&searchTerm=TITLE-ABS-KEY%28corrosion%2C+fatigue%2C+probability%29>
- EPIInc. (2012). What is fatigue loading.
- ETBX. (2001-2008). Stress-life fatigue analysis. from [http://www.fea-optimization.com/ETBX/stresslife\\_help.htm](http://www.fea-optimization.com/ETBX/stresslife_help.htm)
- Fontana, M. G., & Greene, N. D. (1978). *Corrosion engineering* (2nd ed. ed.). New York: McGraw-Hill.
- Garnham, C. (2006). Redox Halves. from [http://commons.wikimedia.org/wiki/File:Redox\\_Halves.png](http://commons.wikimedia.org/wiki/File:Redox_Halves.png)
- Greene, F. (1967). Eight forms of corrosion. from <http://corrosion-doctors.org/Corrosion-History/Eight.htm>
- International, N. (2002). Corrosion cost and preventive strategies in the United States. from <https://www.nace.org/uploadedFiles/Publications/ccsupp.pdf>
- International, N. (2015a). from <https://www.nace.org/Pitting-Corrosion/>
- International, N. (2015c). Pitting Corrosion. from <https://www.nace.org/Pitting-Corrosion/>
- International, Z. (2015). testXpert II is the testing software for all testing machines and instruments.
- Jiang, Y., & Zhang, J. (2008). Benchmark experiments and characteristic cyclic plasticity deformation. *International Journal of Plasticity*, 24(9), 1481-1515. doi: <http://dx.doi.org/10.1016/j.ijplas.2007.10.003>
- Material, T. (2001). Classification of Carbon and Low-Alloy Steels. from <http://www.totalmateria.com/articles/Art62.htm>
- Moan, T. Fatigue Reliability of Marine Structures, From the Alexander Kielland Accident to Life Cycle Assessment.
- Moan, T. (2010). Alexander Kielland accident, 30 years later. from <http://www.psa.no/getfile.php/PDF/Konstruksjonsseminar%20aug2010/Alexander%20L.%20Kielland%20ulykken%20%E2%80%93%2030%20%C3%A5r%20etter%20-%20Torgeir%20Moan%20%28NTNU%29.pdf>
- NORSOK. (2010). Integrity of offshore structures.
- Smith, R. A. (2007). Railways and materials: synergetic progress. from [http://www.sheffield.ac.uk/polopoly\\_fs/1.395281!/file/55th\\_slides.pdf](http://www.sheffield.ac.uk/polopoly_fs/1.395281!/file/55th_slides.pdf)
- Speller, F. N. (1935). *Corrosion: causes and Prevention - An Engineering Problem*.
- standard, I. (2003). ISO 120106 Metallic materials - Fatigue testing - Axial-strain-controlled method.
- Standard, N. (2008). Eurocode 3: Design of steel structures - Part 1-1: General rules and rules for buildings

- Trethewey, K. R., & Chamberlain, J. (1995). *Corrosion for science and engineering* (2nd ed. ed.). London: Longman.
- University, I. S. (2011). Fatigue Life Evaluation. from [http://www.public.iastate.edu/~e\\_m.424/Fatigue.pdf](http://www.public.iastate.edu/~e_m.424/Fatigue.pdf)
- University, I. S. (2015). Palmgren-Miner rule.
- Veritas, D. N. (2013). Determination of Structural Capacity by Non-linear FE analysis Methods.
- Veritas, D. N. (2014). DNVGL-RP-0005.
- Vervoort, D.-I. S., & Wurmman, D.-I. G. (2015 ). History of fatigue. from <http://www.atzonline.com/index.php;do=show/site=a4e/sid=GWV/alloc=38/id=61/special=Special+Simulation>
- Weck, A., Wilkinson, D. S., Maire, E., Toda, H., & Embury, D. (2015). Ductile fracture. from <http://www.weck.ca/index.php?mode=7>

# Appendix A

<b>ROSENBERG</b> WorleyParsons Group		<b>WELDING PROCEDURE SPECIFICATION (WPS)</b>			WPS No.: P150-05						
					Ref.:						
					Date: 01.03.13 Rev.: 04						
Prod. by: <b>Rosenberg</b>		Client: <b>ALL</b>		Ref. stand: <b>EN-ISO-15614-1</b>							
Project: <b>BASIS</b>		Ref. spec.: <b>NORSOK M-601, Rev. 5</b>		Exam. body:							
Location: <b>Rosenberg WorleyParsons</b>		Ref. WPQR: <b>KVI-P-795.6T RVP-TO-151.6T</b>		RP120H05.1/2.5							
Welding process	1 141		2	3							
Shielding gas type	1 ARGON 4.6 I1		2	3							
Weaving (yes/no)	YES max.: 10 mm		2	max.: mm		max.: mm					
Purging gas type	NA l/min										
Welding positions	ALL -PG										
Joint type	SEE SKETCH										
Joint preparation	MACHIN./GRIND										
Cleaning method	GRIND / BRUSH										
Backing	NO										
Single/Double	SEE SKETCH										
Back gouging	GRINDING										
Flux designation	NA										
Flux handling	NA										
Tungsten electrode	2.4 mm										
Torch angle	NA °										
Stand off distance	NA mm										
Nozzle diameter(s)	NA										
Tack welding proc.	COL750-R Rev.:										
<b>Identification of parent metal</b> I C max: CE max: 0, 43 PCM max: II C max: CE max: 0, 43 PCM max:											
	Name/Grade	Standard	Group	Delivery cond.	Thickness range [mm]	Diameter range [mm]					
I	API 5L X52 and lower		1, 2		3, 00 - 17, 40	21, 30 - 99999					
II	API 5L X52 and lower		1, 2		3, 00 - 17, 40	21, 30 - 99999					
<b>Identification of filler metal</b>											
Index	Trade name	Classification	Group	Filler handling							
1	ESAB OK Tigrod 13.26	AWS A5.28 / ER80S-G		CO2767-R							
2											
3											
<b>Welding Parameters</b> Equipment:											
Pass no.	Index	Dia. [mm]	Welding process	Wire feed speed [m/min]	Current [A]	Volt [V]	Current / Polarity	Welding speed [mm/min]	Run Out Length [mm]	Gas [l/min]	Heat input [kJ/mm]
1*	1	2,00	141	-	85 - 97	8 - 10	DC-	28,0 - 40,0	NA	15 - 20	1,0 - 2,1
Fill		2,00	141	-	97 - 114	10 - 12	DC-	45,0 - 85,0	NA	15 - 20	0,7 - 1,8
OR											
1	1	2,40	141	-	100 - 130	10 - 12	DC-	56,0 - 74,0	NA	15 - 20	0,8 - 1,7
2	1	2,40	141	-	135 - 185	11 - 13	DC-	65,0 - 120	NA	15 - 20	0,7 - 2,2
Fill	1	2,40	141	-	145 - 200	11 - 13	DC-	75,0 - 140	NA	15 - 20	0,7 - 2,1
<b>Heat treatment</b> Method: *PROPAN											
Preheat min: 50 °C		Interpass temp. max: 245 °C		Heat treatment proc.:			Temp. control: TEMP.STICKS/DIGITAL				
PWHT min: °C		max: °C		Soaking: min/mm		Heating rate: °C/h		Cooling rate: °C/h			
Remarks:							Additional info enclosed (Yes/No):				
For systems without the "sour service" requirements pre-heat can be reduced to room temperature (10C deg).							Date/Signature: 01.03.13 CT				
Repair welding: Preheating to be increased by 50C deg.							Constantinos Tesfay				
* Small bore pipes preheat only 20C deg.							Approved: 01.03.13 CT				
							Constantinos Tesfay				

Index: 7902943

Page 1 of 1

Produced by WeldEye®

# Appendix B

## Palmgren-Miner Rule

Suppose a body can tolerate only a certain amount of damage,  $D$ . If that body experiences damages  $D_i$  ( $i = 1, \dots, N$ ) from  $N$  sources, then we might expect that failure will occur if

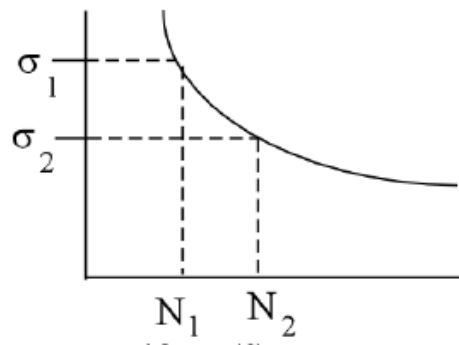
$$\sum_{i=1}^N D_i = D$$

or, equivalently

$$\sum_{i=1}^N \frac{D_i}{D} = 1$$

defines failure, where  $D_i / D$  is the fractional damage received from the  $i$ th source.

We can use this linear damage concept in a fatigue setting by considering the situation where a component is subjected to  $n_1$  cycles at alternating stress  $\sigma_1$ ,  $n_2$  cycles at stress  $\sigma_2$ , ...,  $n_N$  cycles at  $\sigma_N$ . From the S-N curve for this material, then we can find the number of cycles to failure,  $N_1$  at  $\sigma_1$ ,  $N_2$  at  $\sigma_2$ , ...,  $N_N$  at  $\sigma_N$ .



It is reasonable in this case to let the fractional damage at stress level  $\sigma_i$  be simply  $n_i / N_i$ , so that the Palmgren-Miner rule would say that fatigue failure occurs when

$$\sum_{i=1}^N \frac{n_i}{N_i} = 1$$

Example:

A part is subjected to a fatigue environment where 10% of its life is spent at an alternating stress level,  $\sigma_1$ , 30% is spent at a level  $\sigma_2$ , and 60% at a level  $\sigma_3$ . How many cycles,  $n$ , can the part undergo before failure?

If, from the S-N diagram for this material the number of cycles to failure at  $\sigma_i$  is  $N_i$  ( $i=1,2,3$ ), then from the Palmgren-Miner rule failure occurs when:

$$\frac{0.1n}{N_1} + \frac{0.3n}{N_2} + \frac{0.6n}{N_3} = 1$$

so solving for  $n$  gives

$$n = \frac{1}{\left(\frac{0.1}{N_1} + \frac{0.3}{N_2} + \frac{0.6}{N_3}\right)}$$

Remarks

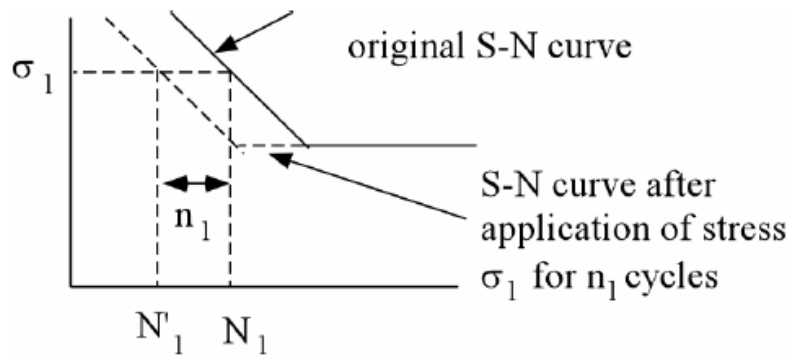
1. "High-low" fatigue tests where testing occurs sequentially at two stress levels ( $\sigma_1, \sigma_2$ ) where  $\sigma_1 > \sigma_2$  generally shows that failure occurs when

$$\sum_{i=1}^2 \frac{n_i}{N_i} = c$$

where  $c$  normally is  $< 1$ , i.e the Palmgren-Miner rule is non-conservative for these tests. For "low-high" tests,  $c$  values are typically  $> 1$ .

2. For tests with random loading histories at several stress levels, correlation with the Palmgren-Miner rule is generally very good.
3. The Palmgren-Miner rule can be interpreted graphically as a "shift" of the S-N curve. For example, if  $n_1$  cycles are applied at stress level  $\sigma_1$  (where the life is  $N_1$  cycles), the S-N curve is shifted so that goes through a new life value,  $N_1'$ :



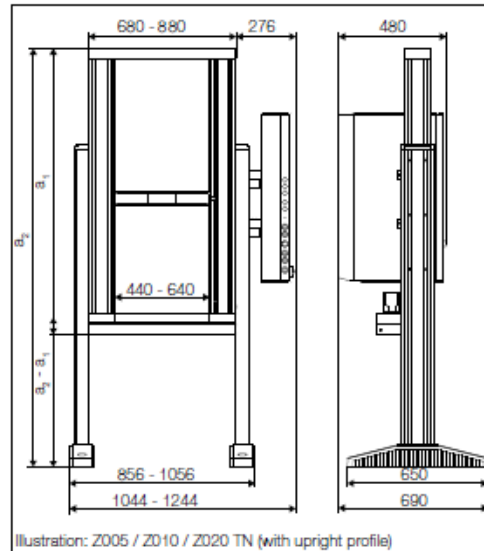


4. A major limitation of the Palmgren-Miner rule is that it does not consider sequence effects, i.e. the order of the loading makes no difference in this rule. Sequence effects are definitely observed in many cases. A second limitation is that the Palmgren-Miner rule says that the damage accumulation is independent of stress level. This can be seen from the modified S-N diagram above where the entire curve is shifted the same amount, regardless of stress amplitude.

# Appendix C

## Product Information

Table-top machines Z005 up to Z020 of the AllroundLine



### General advantages of AllroundLine with Zwick testControl II electronics

#### Modern load-frame design

- Drive is via maintenance-free, digitally controlled AC drive technology, which in combination with the innovative motor feedback system ensures excellent constant velocity properties, even at very low speeds.
- The materials testing machines are equipped with a patented, flexurally stiff hollow profile with guide cylinder, while long crosshead guides with a large surface area provide extremely precise guidance. This combination minimizes undesirable mechanical influences on the specimen.
- Integral T-slots in the profile ensure flexible mounting options.

#### High level of operator convenience

- Ergonomics are top priority when it comes to operating the new AllroundLine machine.
- Adjustable for optimum ergonomic configuration; modular design allows adaptation as and when required.
- Adjustable upright profiles plus low base-height enable flexible adjustment of the working area, facilitating wheelchair-friendly operation.

### Innovative electronics

The new testControl II measurement and control electronics provide the ideal basis for precise, reproducible test results. Impressive features include new drive technology, high measured-value acquisition-rates and a high level of modularity (full details on Page 2).

### Highest safety standards

The statutory safety requirements of the EC Machinery Directive are implemented in all AllroundLine machines, which then receive the EC Declaration of Conformity. Only the latest safety technologies and proven industrial components are used. A very high level of safety is guaranteed for user, test results, specimen material and testing system.

### Future-proof

Modular design means that the testing system can be re-equipped or upgraded whenever required. Moreover, the testControl II control electronics are compatible with the future generation of Zwick software, with spare parts available for a minimum of ten years after the product has been discontinued.

**Product Information**

Table-top machines Z005 up to Z020 of the AllroundLine

Data	Value
<b>Load frame</b>	
Finish	RAL 7021 black grey and RAL 7038 agate grey
Ambient temperature	+10 ... +35 °C
Air humidity (non-condensing)	20 ... 90 %
<b>Drive system</b>	
Motor	AC servo-motor with concentrated windings Hiperface® motor feedback system
Motor holding brake	yes
Input signal, set-value preset	digital (real-time Ethernet, EtherCAT®)
Controller / Cycle time	adaptive / 1000 Hz
Positioning, repetition accuracy on the crosshead	± 2 µm
<b>Measurement and control electronics</b>	
Number of slots available for measurement and control modules	2 synchronized module bus slots (expandable to 5)* 1 synchronised PCIe slot
Force measurement	grade 0.5 / 1 see load cell, to DIN EN ISO 7500-1, ASTM E4,
Calculated resolution (for example in tensile / compression direction)	24 bits
Data acquisition rate, internal	400 kHz
Test data transmission rate to the PC	500 Hz (optional 2000 Hz)
Zero-point correction	automatically at measurement begin
Measurement signal runtime correction for all channels	yes
Interface for PC	Ethernet
Eco Mode	yes, power section automatically switched off (time adjustable)
CE conformity	yes, according to machine guidelines 2006/42/EG
<b>Power ratings</b>	
Mains frequency	50/60 Hz

\* A high-quality DCSC measurement module for a load cell is included in delivery (occupies one module bus slot).

**testControl II - options, e.g.**

Description	Item number
Option testControl II plus: Expansion of electronics to 6 slots	<b>1008208</b>
2000 Hz Online test data transmission: Increasing the test data transmission from 500 Hz (standard) to 2000 Hz. The test data is transmitted to testXpert II and is processed in real-time.	<b>057860</b>
Display remote control for testControl II for effective, ergonomic operation of the materials testing machine	<b>057984</b>

**Options on request, e.g.**

- Supplementary crossheads for the additional second test area
- CE-compliant electrically lockable safety device
- Mounting platforms
- Leg profiles

All data at ambient temperature.

All rights reserved.

**Product Information**

Table-top machines Z005 up to Z020 of the AllroundLine

Type Item number	Test load $F_N$ in tensile / compression direction	Test area width	Height of the lower test area, without accessories	Height of the upper test area, without accessories /supplern. crosshead required)	Height without leg profiles (a <sub>1</sub> )	Height with leg profiles (a <sub>2</sub> )	Width without leg profiles	Width with leg profiles (and electronics console)	Depth without leg profiles <sup>1,4</sup>	Depth with leg profiles <sup>1,4</sup>	Overall weight with electronics console, without leg profiles	Noise level at maximum test speed	Crosshead speed up to 110% of test load ( $v_{min}$ ... $v_{max}$ )	Increased crosshead return speed (at reduced force)	Drive system's travel resolution	Electrical connections <sup>2</sup>	Power rating
Z010 TEW 1004484 <sup>1,4</sup>	10	640	1755	1785	1324	2248 ...	880	1056	573	690	254	64	0.0005 ... 2000	3000	0.63663	230	2
Z010 THW 1004482	10	640	1400	1415	1724	1878 ...	880	1056	573	690	232	64	0.0005 ... 2000	3000	0.63663	230	2
Z010 TNW 1004480	10	640	1000	1015	1324	1538 ...	880	1056	573	690	210	64	0.0005 ... 2000	3000	0.63663	230	2
Z010 TE 1004483 <sup>1,4</sup>	10	440	1785	1785	2084	2238 ...	680	856	573	690	207	64	0.0005 ... 2000	3000	0.63663	230	2
Z010 TH 1004481	10	440	1430	1415	1714	1868 ...	680	856	573	690	185	64	0.0005 ... 2000	3000	0.63663	230	2
Z010 TN 1004479	10	440	1030	1015	1314	1528 ...	680	856	573	690	163	64	0.0005 ... 2000	3000	0.63663	230	2
Z005 THW 1004477	5	640	1400	1415	1724	1878 ...	880	1056	573	690	230	67	0.0005 ... 3000	3000	0.95943	230	2
Z005 TNW 1004475	5	640	1000	1015	1324	1538 ...	880	1056	573	690	208	67	0.0005 ... 3000	3000	0.95943	230	2
Z005 TE 1004478 <sup>1,4</sup>	5	440	1785	1785	2084	2238 ...	680	856	573	690	205	67	0.0005 ... 3000	3000	0.95493	230	2
Z005 TH 1004476	5	440	1430	1415	1714	1868 ...	680	856	573	690	183	67	0.0005 ... 3000	3000	0.95493	230	2
Z005 TN 1004473	5	440	1030	1015	1314	1528 ...	680	856	573	690	161	67	0.0005 ... 3000	3000	0.95493	230	2

PI 28/4.2.1014\_sheet 2

<sup>1</sup> Leg profiles are included in the scope of supply of this materials testing machine.  
<sup>2</sup> Power supply: 230 V +/- 10% (1Ph, N, PE), 50/60 Hz.  
<sup>3</sup> Inclusive electronics console.  
<sup>4</sup> Inclusive base support (60 x 30 mm rectangular tube) with 210 mm front overhang.

All data at ambient temperature.

All rights reserved.

**Product Information**

Table-top machines Z005 up to Z020 of the AllroundLine

Type	Z020 TN	Z020 TH	Z020 TE	Z020 TNW	Z020 THW	Z020 TEW	
Item number	1004485	1004487	1004489 <sup>1)</sup>	1004486	1004488	1004490 <sup>1)</sup>	
<b>Load frame</b>							
Test load $F_N$ in tensile / compression direction	20	20	20	20	20	20	kN
Test area width	440	440	440	640	640	640	mm
Height of the lower test area, without accessories	1030	1430	1785	1000	1400	1755	mm
Height of the upper test area, without accessories /supplem. crosshead required)	1015	1415	1785	1015	1415	1785	mm
Height without leg profiles $a_1$	1314	1714	2084	1324	1724	2094	mm
Height with leg profiles $a_2$	1528 ... 2108	1868 ... 2508	2238 ... 3078	1538 ... 2118	1878 ... 2518	2248 ... 3088	mm
Width without leg profiles	680	680	680	880	880	880	mm
Width with leg profiles (and electronics console)	856 (1044)	856 (1044)	856 (1044)	1056 (1244)	1056 (1244)	1056 (1244)	mm
Depth without leg profiles <sup>2)</sup> <sup>4)</sup>	552	552	552	552	552	552	mm
Depth with leg profiles <sup>3)</sup>	690	690	690	690	690	690	mm
Overall weight with electronics console, without leg profiles	165	187	209	212	234	256	kg
Noise level at maximum speed	61	61	61	61	61	61	dB(A)
<b>Drive system</b>							
Crosshead speed up to 110% of test load ( $v_{min}$ ... $v_{Nom}$ )	0.0005 ... 1000	0.0005 ... 1000	0.0005 ... 1000	0.0005 ... 1000	0.0005 ... 1000	0.0005 ... 1000	mm/min
Increased crosshead return speed (at reduced force)	1500	1500	1500	1500	1500	1500	mm/min
Drive system's travel resolution	0.32495	0.32495	0.32495	0.32495	0.32495	0.32495	nm
<b>Power ratings</b>							
Electrical connections <sup>2)</sup>	230	230	230	230	230	230	V
Power rating	2	2	2	2	2	2	kVA

<sup>1)</sup> Leg profiles are included in the scope of supply of this materials testing machine.

<sup>2)</sup> Power supply: 230 V +/- 10% (1Ph, N, PE), 50/60 Hz.

<sup>3)</sup> Inclusive electronics console.

<sup>4)</sup> Inclusive base support (60 x 30 mm rectangular tube) with 210 mm front overhang.